High Resolution study of NF-kB - DNA Interactions

Imtiaz Nisar Lone

THÈSE

En vue d'obtention du grade de

Docteur de l'Ecole Normale Supérieure de Lyon-Université de Lyon

Discipline: Biologie

Laboratoire de Biologie Moléculaire de la Cellule, LBMC

Ecole Doctorale de Biologie Moléculaire Intégrative et Cellulaire, BMIC

Présentée et soutenue publiquement le 14 Fevrier 2013

par **Imtiaz Nisar LONE**

High Resolution study of NF-kB – DNA Interactions

Directeur de thèse: Dr. Dimitar ANGUELOV

Apres l'avis de: Dr. Marco BIANCHI

Dr. Malcolm BUCKLE

Devant la commission d'examen formée de:

Dr. Dimitar ANGUELOV	Directeur de thèse, ENS de Lyon
Dr. Marco BIANCHI	Rapporteur, San Rafael, Milan
Dr. Malcolm BUCKLE	Rapporteur, ENS Cachan
Dr. Stefan DIMITROV	Examinateur, UJF/IAB, Grenoble
Dr. Ali HAMICHE	Examinateur, IGBMC, Strasbourg
Dr. Gael YVERT	Président, ENS de Lyon

Thèse préparée au sein du

Laboratoire de Biologie Moléculaire de la Cellule

École Normale Supérieure

46 allée d'Italie

69364 Lyon cedex 07, FRANCE

To my parents

Acknowledgements

″Man cannot discover new oceans unless he has the courage to lose sight of the shore. (Andre Gide). This odyssey to discover new oceans requires guidance, support and assistance of others. There are a number of people who I would like to acknowledge for their kind support and encouragement throughout my studies.

First and foremost, I would like to thank my supervisor Dr. Dimitar Angelov for providing me an opportunity and space to work in the lab. Dimitar deserves a special recognition because of his wholehearted support to this project and his precious advices. Most critical to the overall effort was the enormous infusion of guidance, encouragement and inspiration contributed by him. I would also like to thank Dr. Stefan Dimitrove for introducing me to Dimitar Angelov and for encouraging and guiding me time to time.

I would like to thank my thesis committee members Prof. Hans Geiselman and Dr. Marie Josephe for monitoring my work and for helpful discussions.

I would like to extend my gratitude to all the members of Angelov group, past and present. In particular, I would like to thank Dr. Charles Richard for making my stay in Lyon so wonderful. My special thanks to Lama Soueidan - “The Stress buster” for making the lab environment wonderful and also for all the translations she had to do for me. My thanks to Ogi, Ram and Elsa for all the help and for the wonderful time we shared in Angelov team.

One of the special advantages I have had is my access to the extraordinary community of research scholars at ENS, Lyon. More often than not, the help I needed to tie down a loose end was right at hand. In this regard, I am especially indebted to Dr. Maria Sirakov for her help and positive criticism and also for giving me an opportunity to collaborate with her. You have been an amazing friend, a constant source of encouragement and of course a wonderful cook.

My special thanks to all my best buddies -Dane Georgess, Esber, Mubarak, Jeelani, Faiyaz and Bilal for their friendship. I would specially like to thank “Page layout artist” Mubarak for helping me with the final editing of the manuscript.

For chiseling and carving my overall personality my family, especially my parents, my sister and my brother deserve the special mention. They are the special people of my life. My deepest gratitude goes to them as they have always been concerned about me and wished me success and happiness forever in my enterprises. I am particularly thankful to them for patiently putting up with my long absence and for their buoyancy.

Imtiaz Nisar

Contents

Table of figures: Introduction

Manuscript 1: Tables and figures

Table of figures: Manuscript 2

Table of figures: Manuscript 2 supplementary figures

List of abbreviations

1D	One dimension
3C	Chromosome conformation capture
3D	Three dimensional
aa	Amino acid
ACF	ATP-utilizing chromatin assembly and remodeling factor
ADP	Adenosine diphosphate
ATP	Adenosine triphosphate
bp	Base pair
CH	Carboxy terminal helix
CHRAC	Chromatin accessibility complex
CIA	Constitutive and Immediate Accessibility
DBD	DNA binding domain
DBP	DNA binding protein
DCs	Dendritic cells
DNA	Deoxyribonucleic acid
FCS	Fluorescence correlation spectroscopy

FRAP	Fluorescence recovery after photobleaching
GD	Globular domain
GR	Glucocorticoid receptor
H1	Histone H1
H2A	Histone H2A
H2B	Histone H2B
H3	Histone H3
H4	Histone H4
HATs	Histone acetyl transferases
HDCs	Histone deacetylases
HIV	Human immunodeficiency virus
HLH	Helix-loop-helix
HTH	Helix-turn-helix
IKK	IκB kinase
IN080	Inositol requiring 8
ISWI	Imitation switch
K	Lysine
K_d	Dissociation constant
kDa	Kilo Dalton
LPS	Lippopolysachride
mH	median Helix
MITOMI	Mechanically induced trapping of molecular interactions
MMTv	Mouse mammary tumor virus
MNase	Micrococcal nuclease
NCP	Nucleosome core particle
NDRs	Nucleosome depleted regions
NF1	Nuclear factor 1
NF-kB	Nuclear factor kappa B
nm	Nanometer
NTD	N- terminal domain
NURF	Nucleosome remodeling factor

PBMs	Protein binding microarrays
PKAc	Protein kinase A catalytic subunit
PTMs	Poet translational modifications
R	Arginine
RHD	Rel homology domain
RHH	Ribbon – helix-helix
RSC	Chromatin structure remodeling
SDR	Specificity determining region
SELEX	Systematic evolution of ligands by exponential enrichment
SNPs	Single nucleotide polymorphisms
SPR	Surface Plasmon Resonance
SWI/SNF	Switch/Sucrose Non Fermentable
TAD	Transactivation domain
TBE	Tris-borate-EDTA
TF	Transcription factor
Tr	Translocation domain
TSS	Transcription start site
UV	Ultraviolet
kB	kappaB

Summary of the thesis

In this thesis we have attempted to study four basic aspects of DNA-protein interactions: Affinity, specificity, accessibility and kinetics. With NF-κB as our model transcription factor, we wanted to investigate how a particular dimer recognizes a specific binding sequence? How fast are these interactions? And finally, how does the NF-κB interact with it binding site in the chromatin context? Specificity of NF-κB-DNA interactions has recently come into focus after it was shown that these dimers can bind to the sequences which do not fall into the NF-kB general consensus motif. We studied seven such sequences for their specificity for four NF-κB dimers. Our results show that p50 homodimers are least discriminative and can bind specifically to all these sequences. While as, RelA homodimers were highly discriminative and did not bind to most of these nontraditional sequences. We used two different methods to measure binding affinities: traditional gel mobility shift assay (EMSA) and a novel technique called as UV laser footprinting. Our results show that UV laser footprinting is the better method to determine the binding constants.

For studying the dynamics of NF-κB-DNA binding, we combined UV laser footprinting with stopped flow device. This combination, not only give us one base pair resolution but also milli second time resolution. Using p50 homodimers as a model transcription factor, we showed that the binding of this factor follows a two step mechanism. First step involves the fast recognition of the sequence and second step follows a slower kinetics most likely for the stabilization of the complex. Our experiments suggest that flanking sequences play a role in the recognition and stabilization process of the complex formation.

Finally, we also studied the accessibility of nucleosomes to NF-κB. Our *in vitro* data sheds light on the *in vivo* requirements for the alterations in chromatin structure necessary for the productive binding of NF-κB. These include either a removal of H2A-H2B dimers from the nucleosome and/or chromatin remodeler induced relocation of the histone octamer.

Our data sheds light on the *in vivo* requirements for the alterations in chromatin structure necessary for the productive binding of NF-κB. We hypothesize that some factors like PU.1 might be able to target the chromatin remodeling/dimer eviction machinery to particular nucleosomes and lead to productive binding of NF-κB.

INTRODUCTION

DNA is the information center of the cell. The information stored in DNA will be useless if it cannot be properly retrieved. The cells have evolved an extensive system to read this information and to translate it. This requires the recognition of the information units on DNA by the proteins. A central question in protein-DNA recognition is the origin of specificity that allows the binding to the correct site in the presence of excess, non-specific DNA. Proteins, such as transcription factors (TF) that bind to specific DNA sequences are vital for the proper regulation of gene expression.

How do these sequence specific proteins recognize the DNA sequences? From a physic-chemical perspective, two reactants will react and form a stable product only if there is a decrease in Gibbs free energy. Applying this principal to Protein-DNA interactions, proteins and DNA molecules will interact if there is a loss of Gibbs free energy on the formation of a complex. Change in free energy (ΔG) during complex formation depends upon the change in both enthalpy (ΔH) and entropy (ΔS) such that $\Delta G = (\Delta H) - (T \times \Delta S)$. For a protein-DNA complex, the enthalpy arises from several very short range non-covalent interactions between protein and DNA. The entropy depends on the nature of the solvent and on the interacting surfaces of protein and DNA, before and after complex formation. To make a favorable contribution to ΔG, both the enthalpy and entropy terms require the protein to have a surface shape that is highly complementary to that of its DNA target. However, the complimentary shapes alone will not lead to the formation of the complex. In addition to a complementary shape, the chemistry of the interacting surfaces must also be complementary. The nature and the three-dimensional arrangement of the functional groups on the protein must match precisely those of the DNA target site. Thus, the recognition process can be conceptually divided into two steps: (I) recognition of complimentary molecular shapes and (II) chemical recognition at atomic level [1]. This would mean that both, DNA and proteins need to have not only complimentary shapes but also suitable functional groups exposed for the successful interaction. Proteins have evolved a wide range of DNA-binding structural motifs to recognize the binding sites on the DNA. For example, helix-turn-helix (HTH) motif is one of the most frequently represented motifs in DNA-binding proteins and proteins bearing HTH motif mostly bind to major groove [2]. Other DNA binding motifs include helix-loop-helix (HLH), immunoglobulin like β-sandwich, β-trefol, zinc finger, ribbon-helix-helix (RHH). Apart from having special DNA-binding motifs, TFs employ many

strategies to enhance the binding recognition in order to bind more specifically. The first strategy is to add on arms or tails that recognize additional features of the DNA, particularly in the minor groove [3, 4]. The second strategy is to double up the recognition by forming either homo or heterodimers. This helps to specify a longer DNA sequence and to increase recognition possibilities through a combinatorial approach [5, 6]. Third strategy is to employ multiple DNA binding domains, either by using tandem repeats of the same type of DNA-binding motif [7] or by linking together different types of motifs [8]. Similarly, DNA sequence can also influence its interaction with protein as DNA structure varies in a sequence dependent manner [9]. For example, in B-DNA the major groove is wider and better suited to accommodate protein secondary structure than minor groove. Furthermore, in major grooves the pattern of hydrogen bond donors and acceptors is unique for each base pair, whereas in minor groove it is impossible to distinguish between AT from TA base pairs, and between GC and CG base pairs [1].

There are four major aspects of sequence specific TF-DNA interactions: affinity and specificity of binding, kinetics of these interactions and accessibility of the binding sites in the context of chromatin.

1.1 Specificity of protein-DNA interactions

Specificity of a transcription factor could be defined as its ability to distinguish between different DNA sequences in the absence of any other cooperative or competitive interaction. This is very important for gene regulation as a transcription factor can activate or repress the transcription only if it binds to the correct site. Specificity of a TF can be better described by understanding a relatively simpler term “affinity”. Considering the binding of the protein to DNA as a bimolecular reaction in which transcription factor (TF) binds to a DNA sequence (S), at equilibrium such a reaction is governed by two rate constants k_{on} (for the formation of the complex) and k_{off} (for the dissociation of the complex). The affinity of the TF for sequence S is usually defined as the ratio of k_{off}/k_{on}. This ratio is represented by another constant called as dissociation constant (K_d) [10]. In simpler terms, K_d is the concentration of the TF at which half of the binding sites are occupied. In a broader sense, specificity is related to affinity by the fact that higher the affinity of the TF towards a binding site, greater is its specificity for that site. However, *in vivo* the affinity of the TF is not as crucial as its specificity. Inside a bacterial cell or a

eukaryotic nucleus, the concentration of DNA is so high (typically millimolar for potential binding sites) that transcription factors will essentially always bind to DNA, even if there are no high affinity sites. For the regulatory network to function properly, the TF must be able to distinguish its functional or regulatory binding sites from the vast majority of the non-functional potential sites. This ability of the TF to distinguish between the affinities of the potential binding sites reflects its specificity.

Several recent studies have demonstrated that many of the binding sites within the genome do not affect the gene expression and it is still not clear whether these sites perform any other function [11, 12]. So it becomes imperative to understand how TFs are screening these sites and how they chose to bind only to the ones with regulatory roles. Knowing the intrinsic specificity of the TF, together with the binding locations provides a wealth of information about gene regulatory system. For example, if binding sites with high affinity are not bound, it could imply that those regions are not accessible to the factor possibly owing to the local chromatin structure. Conversely, if the TF binds to the regions of genome that lack the strong binding sites could imply that the TF is either binding indirectly or is binding to a weak binding site that requires the co-operativity with other factors [13].

1.2 Tools for determining the specificity of protein-DNA interactions

Several recent technological advancements have made it feasible to determine the intrinsic specificity of transcription factors. These advances include both *in vivo* and *in vitro* experimental methods and the development of new computational analyses *(In silico)*. The *in vivo* approaches like ChIp-on-chip and ChIp-seq are used for indirect affinity measurements. These techniques determine the location of putative TF binding site within the genome and provide candidate genes that they are likely to regulate [14, 15]. The advantage of these techniques is that they are high-throughput and can be used for different cell types, under different environmental condition to assess the regulatory changes that are associated with changes in the cell physiology [11]. However, their resolution is not sufficient to identify the binding site; rather they give a binding region roughly about 100 base pair (bp) long. MITOMI (mechanically induced trapping of molecular interactions) and SPR (surface Plasmon resonance) are relatively low throughput techniques but can determine binding affinities directly. They also require

specialized equipment. Protein binding microarrays (PBMs) is another large scale and high throughput technique for assessing the binding specificities of TFs and requires purified proteins. SELEX (Systematic Evolution of Ligands by Exponential Enrichment) in its various forms uses purified proteins to select high affinity binding sites from random libraries. This *in vitro* technique is high throughput and was applied for studies using cellular extracts [10]. Bacterial one-hybrid selection system is a very powerful approach. It requires the cloning of the transcription factor and its expression in *E. coli.* Randomized binding sites are placed upstream of a weak promoter that drives the expression of the selectable gene [16]. Stronger the binding site, higher the expression of the selectable gene.

1.3 Kinetics of DNA-protein interactions

Another important aspect of DNA-TF interactions is the kinetics with which TFs recognize and bind their cognate binding sites. TFs factors have to search locate and bind to the specific site to function properly. It is important for these proteins to bind to their DNA target site with an appropriate affinity and specificity, as well as binding to and releasing from their DNA targets with appropriate kinetics. To search for a binding site on a large molecule of DNA, TF have to diffuse through the nucleoplasm. The diffusion rate through the nucleoplasm could set the maximum limit for the rate of TF binding. However, Riggs *et al.* showed that *in vitro* the *lac* repressor (LacI) finds its operator apparently faster than the rate limit for three-dimensional (3D) diffusion [17]. The logical explanation to this unexpected observation was provided by Von Hippel and coworkers through facilitated diffusion theory, which states that TFs search for their binding sites through a combination of 3D diffusion in the nucleoplasm and 1D diffusion (sliding) along DNA [18]. This theory has been recently supported by Johan Elf and coworkers [19]. Using single molecule imaging technique, they demonstrated that lac repressor displays facilitated diffusion in living cells. In addition to these two search mechanisms, a protein can search the DNA *via* hopping or *via* intersegmental transfer. The facilitative diffusion reduces the chances of non-productive events and hence increases the actual rate of the reaction.

Sliding plays a key role in localization of the target site by DNA-binding proteins [20]. To slide along the contour of DNA, the DBP encounters the DNA, scans for the

nonspecific sites. During this process, electrostatic forces attract the protein to DNA. Structural studies of proteins bound to semi-specific DNA sequences have demonstrated that nonspecific interactions are mostly dominated by electrostatic interactions between the positively charged protein side chains and the negatively charged DNA backbone [21-23]. This notion is further supported by a greater dependence of the nonspecific interactions on salt concentration in comparison with specific protein–DNA complexes [24-26]. As the protein reaches its target DNA site, it switches from purely electrostatic binding to a specific set of interactions with the DNA bases that also involves formation of hydrogen bonds between donors and acceptors from protein side chains and DNA bases [2, 26], stabilization by van der Waals and hydrophobic forces, electrostatics and water mediated interactions between polar groups [20, 27]. The transition from the encounter complex (stabilized by nonspecific interactions) to the specific protein–DNA complex may also involve conformational changes to one or both biomolecules [20].

In order to understand the mechanism of specific DNA-proteins recognition and binding, it is imperative to probe the transition from nonspecific to specific interaction during this process. However, transitory nature of the nonspecific interactions makes it quite difficult to probe this transition. Recent technological advancements have made it possible for us to undertake such endeavors. Individual events such as protein-protein or protein-DNA interactions and rate-limiting conformational changes often occur in the millisecond timescale, and can be measured directly by stopped-flow and chemical-quench flow methods [28]. The stopped-flow apparatus is a rapid mixing device used to study the chemical kinetics of a reaction in solution. After two or more solutions containing the reagents are mixed, they are studied by whatever experimental methods are deemed suitable. Typically fresh reactants in the observation cell are illuminated by a light source and the change in many optical properties such as absorbance, fluorescence [29], light scattering [30], turbidity and fluorescence anisotropy [31] can be measured as a function of time. The measurement of these optical properties is performed by the system's detectors. Although these methods provide an excellent temporal resolution, they do not offer a sufficient spatial resolution. To overcome this problem, footprinting experiments have been combined with stopped-flow [32-34]. For example, Scalvi et al. used time resolved hydroxyl radical footprinting to characterize the RNA polymerase intermediates during the open complex formation [35]. The main advantage of hydroxyl

radical footprints is its high structural resolution of the protection pattern. However, hydroxyl radical footprinting is not suitable to sequence specific DNA-protein interactions. For studying the sequence specific DNA-protein interactions we have combined rapid mixing of stopped-flow with UV laser footprinting. This dynamic UV laser footprinting provides millisecond time resolution and one base pair space resolution simultaneously. In this thesis, I will highlight the application of dynamic UV laser footprinting for probing the kinetics of binding of NF-κB to its canonical binding site.

The current understanding about the search mechanisms is based on either the bacterial system or pure *in vitro* system using naked DNA. However, in eukaryotes all the DNA templated processes take place in the context of chromatin. This imparts another level of complexity not only to the search mechanisms but also the accessibility of the binding sites to TFs.

1.4 Accessibility of binding sites

The packaging of DNA into chromatin inherently restricts the access to underlying DNA by TFs. The chromatin organization and the strategies to make it accessible are discussed in detail in the following sections of this thesis.

1.5 Chromatin: The beginning

The field of chromatin started in 1880, when W. Flemming coined the term "chromatin" owing to its affinity to stains [36]. During that time F. Miescher and A. Kossel had laid the crucial groundwork for the characterization of chromatin components. Miescher in 1871 described "nuclein", a phosphorous rich acid (nucleic acids) as a component of the chromatin [37]. Later, he also described a basic component of chromatin which he named as "protamine". H. Zacharia in 1881 performed the microscopy study of the protease digested isolated nuclei and observed that "nuclein" is resistant to degradation. This prompted W. Flemming to write, *"In view of its refractile nature, its reactions, and above all its affinity to dyes, is a substance which I have named chromatin. Possibly chromatin is identical with nuclein, but if not, it follows from Zacharias work that one carries the other. The word chromatin may stand until its chemical nature is known, and meanwhile stands for that substance in the cell nucleus which is readily stained"[37].* So the name chromatin stands until now.

1.6 DNA packing and nuclear architecture

In humans, a single DNA double helix contains about $1.5x10^8$ nucleotide pairs. Stretched out, such a molecule would be about 4cm long, thousands of times the diameter of a cell nucleus. That's just a tip of an iceberg, considering that the haploid human genome contains approximately 3 billion base pairs of DNA packaged into 23 chromosomes. Of course, most cells in the body (except for female ova and male sperm) are diploid, with 23 pairs of chromosomes. That makes a total of 6 billion base pairs of DNA per cell. Since each base pair is around 0.34 nanometers long, each diploid cell therefore contains about 2 meters of DNA $[(0.34 \times 10^{-9}) \times (6 \times 10^9)]$. Now the question is how 2 meters of DNA is kept in micron size nucleus? The nature has come up with a very efficient way to solve this problem; hierarchically packaging the genomic DNA of eukaryotes into chromatin by histones. The fundamental subunit of chromatin is the nucleosome core particle, which consists of 146bp of DNA wrapped 1.7 times around a protein octamer composed of two copies of each of the four core histones (H3, H4, H2A and H2B). The wrapping of DNA around the histone octamer to form nucleosomes shortens the fiber length about sevenfold. In other words, a piece of DNA that is 2 meter long will become a "string-of-beads" chromatin fiber just 28 centimeters long. Despite this shortening, chromatin is still much too long to fit into the nucleus, which is typically only 10 to 20 microns in diameter. Clearly, wrapping of the DNA around the histone octamer is not sufficient to accommodate the DNA within the nucleus, hence further folding and compaction is needed. This is achieved by another histone called as "Linker histone" such as H1, which binds to the linker DNA between the nucleosomes. The addition of linker histone protein wraps another 20 base pairs, resulting in two full turns around the octamer leading to the formation of even shorter and thicker fiber, termed the "30-nanometer fiber", as it is approximately 30 nanometers in diameter **(Figure1)**. However, great variety is achieved by a complex system of accessory proteins, which modify, bind and reorganize histone complexes to produce different functional domains within the eukaryotic nucleus.

Traditionally, chromatin was classified into euchromatin and heterochromatin domains by Emil Heitz, which reflect different patterns of histone modification and are associated with different modes of nucleosome packaging [38]; presumably this is

reflected in differences in higher order packaging [39] and nuclear organization. Euchromatin or “active” chromatin is decondensed chromatin, consisting largely of coding sequences with the potential for transcriptional activity. This chromatin state undergoes many modifications through the action of many different proteins. For example, chromatin remodeling proteins utilize ATP to move a nucleosome along the DNA. In other cases, histone-modifying enzymes can introduce covalent modifications to specific histone residues. On the other hand heterochromatin is highly compact and silenced chromatin. It includes among other regions the centromeric and telomeric chromosomal domains and covers 96% of the mammalian genome. Recently, a finer classification of chromatin was proposed on the basis of integrative analysis of genome-wide binding maps of 53 broadly selected chromatin components in Drosophila cells [40] [41]. This study identified and color-coded five distinct states of chromatin BLACK, GREEN, BLUE, RED and YELLOW.

The RED and YELLOW chromatin correspond to active chromatin. The RED chromatin contains many tissue-specific genes and hotspots where many seemingly unrelated proteins co-localize. The YELLOW chromatin contains a majority of ubiquitously expressed housekeeping genes. The BLUE chromatin is characterized by the binding of Polycomb group proteins, which repress transcription. The BLACK chromatin is the most prevalent repressive chromatin type and contains two thirds of all silent genes. Finally, the GREEN chromatin is marked by the heterochromatin protein 1 (HP1) and SU[44]3-9, with several HP1-associated proteins and covers large domains in pericentric regions. However this state does not correspond to the repressive state usually attributed to the term heterochromatin but rather to a neutral

alternative [45].

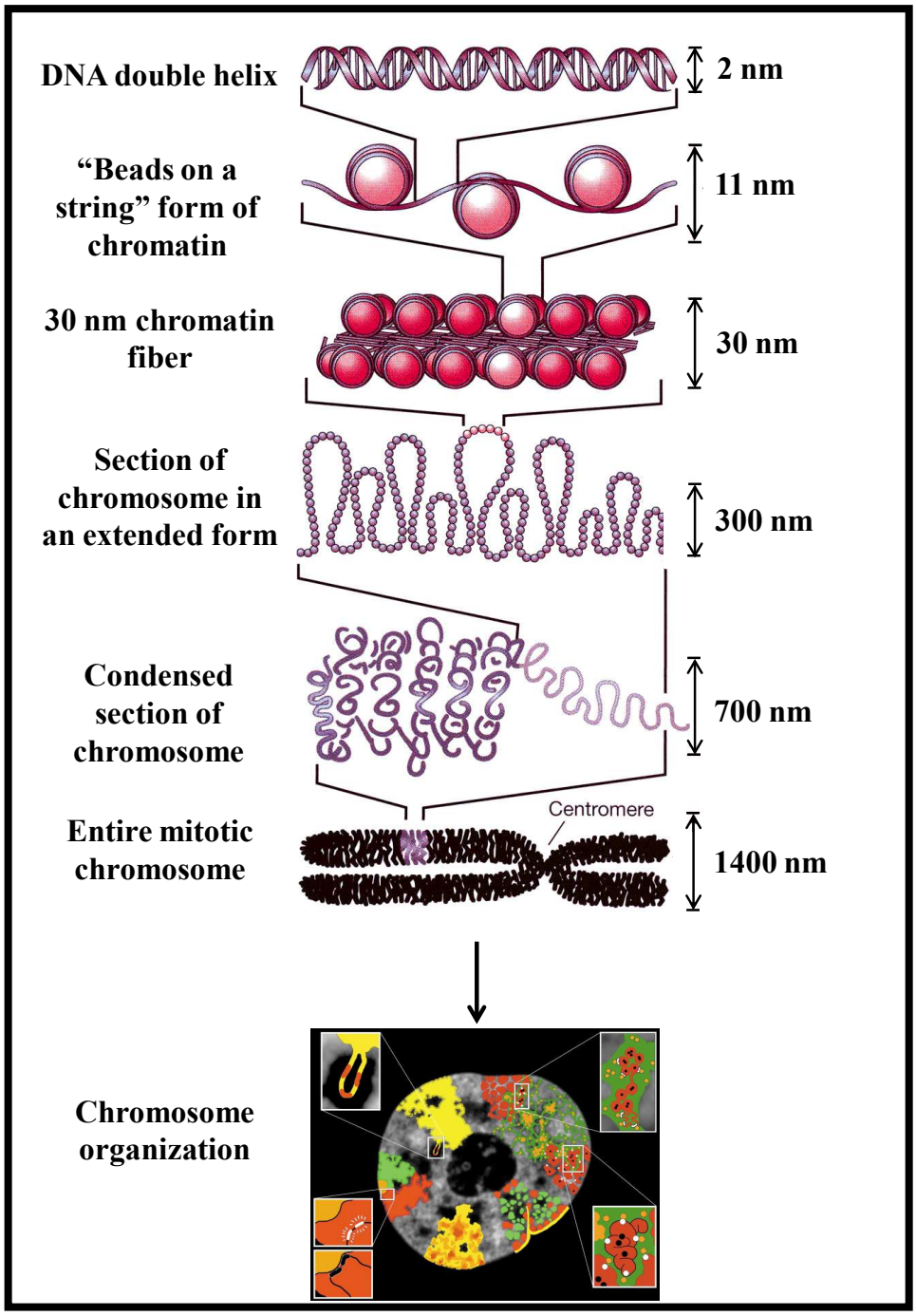

Figure 1: The organization of DNA within the chromatin. DNA is wrapped around histone octamer leading to lowest level of organized structures, the nucleosomes. At the next level of organization the string of nucleosomes is folded into a 30 nm fiber, and these fibers are then further folded into higher-order structures such as mitotic chromosomes. The chromosomes are further organized into chromatin territories. Figure adopted and modified from [42] and [43].

Beyond the fine scale arrangement of chromatin, what is the higher order structure of chromosomes? The current view is that chromosomes are compartmentalized and occupy distinct, non-overlapping, sub-nuclear regions named chromosome territories [43]. This

has been supported by genome wide chromosome conformation capture (3C) in budding yeast [47]. The location of a gene within the chromosome territory seems to influence its access to DNA template machineries.

1.6.1 Nucleosome

Nucleosome is the fundamental unit of chromatin and is composed of DNA and Histones. It provides the first level of compaction of the DNA in the nucleus. Historically, the periodic nature of chromatin was revealed by its biochemical and microscopic studies. The partial digestion of the chromatin isolated from rat liver nuclei, generated 180-200 bp fragments, which were separated and resolved by electrophoretic migration [48, 49]. This regularity of chromatin structure was later confirmed by electron microscopy that showed chromatin is composed of regularly spaced particles and is arranged as "beads on a string" [50, 51]. The stoichiometry of DNA and histones was determined to be 1/1 using chemical cross linking [52]. All these observations led to the proposal that nucleosome is the fundamental unit of chromatin. The nucleosome core comprises 147 bp of DNA and a histone octamer containing a pair of each of the core histone proteins H2A, H2B, H3 and H4. The histone octamer is composed of central $(H3\text{-}H4)_2$ tetramer flanked by two H2A-H2B dimers. The neighboring nucleosomes are separated from each other by 10-50 bp long stretches of unwrapped linker DNA, thus 75-90% of genomic DNA is wrapped in nucleosomes. The linker DNA is of variable length, depending on the cell type and species. The nucleosome core, linker DNA and Histone H1 make up the complete nucleosome.

1.6.2 Core Histones

Based on the composition and sequence, histone proteins are classified into 5 classes- H1, H2A, H2B, H3 and H4 [53]. Each of them includes some gene variants or subtypes which are likely to provide tissue specific and developmental stage dependent variations of chromatin structure [54]. H2A, H2B, H3 and H4 are small basic proteins (11- 16 kDa) and are known as "core histone" since they supercoil DNA around them to form the nucleosome core particle (NCP). These histones induce structural bending in the major and minor grooves of DNA, compressing and narrowing the ones facing octamer and

expanding the ones facing outside [55]. The core histones have three distinct types of structural domains, a central region (approximately 70 aa) called as “histone fold”. N-terminally from the histone fold domains of H3 and H4 and C-terminally from the Histone fold domains of H2A and H2B are the “Histon fold extensions”. Finally, N-termini of all core histones are the random-coil elements, from 16 (H2A) to 44 (H3) amino acids in length, known as flexible “tails”. These tails contain the sites of post translational modifications like acetylation, methylation, phosphorylation, ubiquitination, sumolation, biotinylation, glucosylation and ADP-ribosylation.

1.6.3 The histone octamer

On looking straight into the dyad axis, histone octamer looks like a tripartite assembly of a central V-shaped $(H3\text{-}H4)_2$ tetramer flanked by two H2A-H2B dimers. Individual core histones have a symmetrically duplicated helix-turn-helix motif called as “histone fold” motif. This motif consists of three helices: a short helix on the N-terminal side of the symmetry center of the fold, the long median helix (mH) and a short C-terminal helix (CH) [56]. The helices are joined by NL loop between NH helix and mH helix, and CL loop between mH helix and CH helix [57]. The histone fold domains of the core histones combine to form crescent-shaped H2A/H2B and H3/H4 heterodimers in which the two monomers are intimately associated in a head to tail manner in a so called “handshake motif” [58, 59]. In the absence of DNA or salt, the stable histone oligomers are the dimers of H2A/H2B and tetramers of H3/H4 dimers. However, in the presence of DNA or in high salt conditions (more than 1.2M NaCl), one H3/H4 tetramer and two H2A/H2B dimers combine to form an octamer **(Figure 2)**.

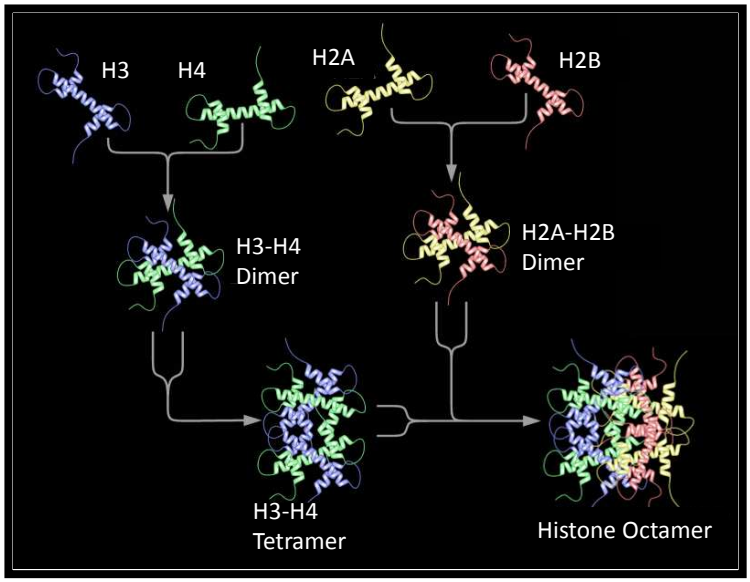

Figure 2: Formation of histone octamer.

1.6.4 Nucleosome Core particle

The nucleosome core particle (NCP) is the crystalizable substructure of the canonical nucleosome, defined by the DNA protection pattern of histone octamer in nuclease digestion of chromatin **(Figure 3)**. A number of crystal structures of the NCPs and variants have been determined [57, 58, 60-63]. It consists of 147 bp of DNA wrapped 1.65 turns around the histone octamer. The histone fold domains of the octamer organize the central 129 bp of DNA in 1.59 left handed super helical turns with a diameter only fourfold that of the double helix [64]. Two types of DNA binding sites occur in histone-fold heterodimer: Two L1L2 loop sites and one α1α1 site. Each site binds to DNA centered on one of the three adjacent minor grooves, bending it through 140^{o}. The relatively straight 9 bp segments at the DNA termini are weakly bound by the H3 αN helices and contributes little to the curvature of the complete 1.65 turn super helix [58]. There are three types of interactions by which the histones bind to the nucleosome core DNA: charge neutralization of acidic DNA phosphate groups, hydrophobic interactions and hydrogen bonds, especially between main chain amide groups and phosphate oxygen atoms. The flexible tails of the histones reach out between and around the gyres of the DNA super helix. The N-terminal tails of both H2B and H3 have random-coil segments that pass through a channel in the super helix formed by the minor grooves of two juxtaposed DNA gyres [58]. The two H4 N-terminal tails have divergent structures; only one is well localized and was found to make extensive contact with a region of extreme acidity on an H2A/H2B dimer of an adjacent particle [58, 63].

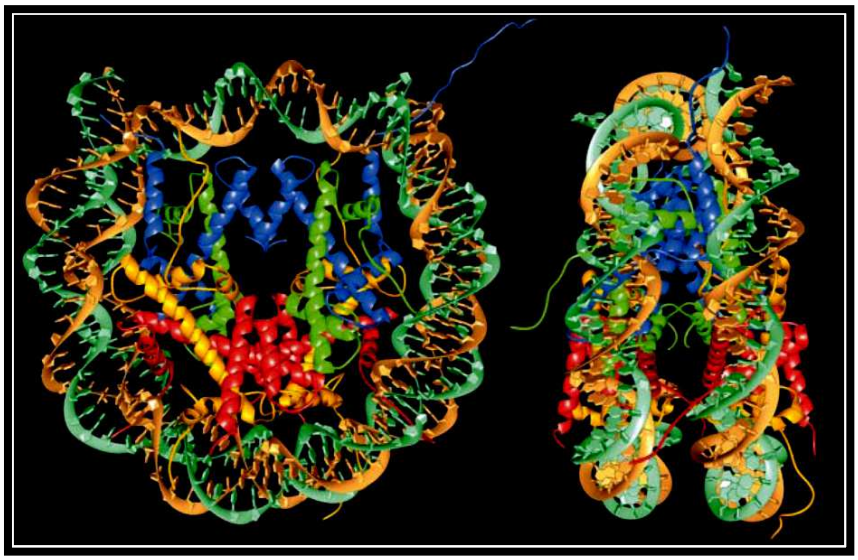

Figure 3: Ribbon structure of nucleosome core particle. 146 bp of DNA (brown and turquoise) wrapped around the histone octamer (H3: Blue, H4: Green, H2A: Yellow and H2B: Red). The views are down the DNA super helix axis for the left particle and perpendicular to it for the right particle. Image adopted from [58].

1.6.5 Linker Histone

Linker histones are a diverse class of histones that lack the histone fold domain and are rich in lysine and arginine. Unlike the core histones, they have a tripartite structure, with unstructured N-terminal domain (NTD, 13-40 amino acids in length) and C-terminal domain (CTD, ~100 amino acids) flanking a well-folded 'globular domain' (GD) of ~80 amino acids [65]. The linker histone family is highly diverse exhibiting stage and species-specific variants [66-68], which differ in molecular weight, amino acid sequence, biochemical/biophysical and immunochemical properties [69]. The nature of NTD is ambiguous as no specific function has been observed for it. The central, globular domain [70, 71] contains at least two separate DNA-binding sites: the first involves a classical winged helix motif and the second a cluster of conserved basic residues on the opposite face of that domain [71]. These two DNA-binding domains allow the linker histone globular domain to bridge different DNA molecules and form tram-track structures [72], and explain the preferential binding of linker histone to DNA crossovers [73] and four-way junctions [44]. The unstructured C-terminal domain (rich in lysines) is essential for chromatin compaction *in vitro* [74-76] and its absence leads to greatly reduced chromatin binding *in vivo* [77, 78].

1.6.6 Binding of linker histone to nucleosomes

Linker histones such as H1 histones are involved in chromatin condensation and in limiting the access for regulatory proteins to nucleosomal components [79, 80]. They binds to the nucleosomes of chromatin fibers at the nucleosomal DNA entry and exit sites [81-83] and increase the micrococcal nuclease protection of nucleosomes from 146 to ~168 bp [84]. Several models have been postulated to decipher the exact location of the globular domain on either native or reconstituted nucleosomal substrate **(Figure 4)**. The first such model was proposed in 1986 and states that GD binds 10 bps entering and 10 bps exiting DNA (linker DNA) of the nucleosome in such a way that it is placed near dyad axis in a symmetrical manner [74]. This model was supported by the GD specific DNaseI footprint on the nucleosomal dyad [85]. However, Zlatanova and coworkers challenged this model by proposing asymmetrical GD binding model [82]. Asymmetrical model proposes that GD protects 20 bp of either entering or exiting DNA. Zhou et al. came up with another model, called as "bridging model". According to this model linker histone interacts with the dyad and with only one free DNA arm (either entering or exiting). This model was supported by *in vivo* photobleaching experiments and subsequent modeling [86].

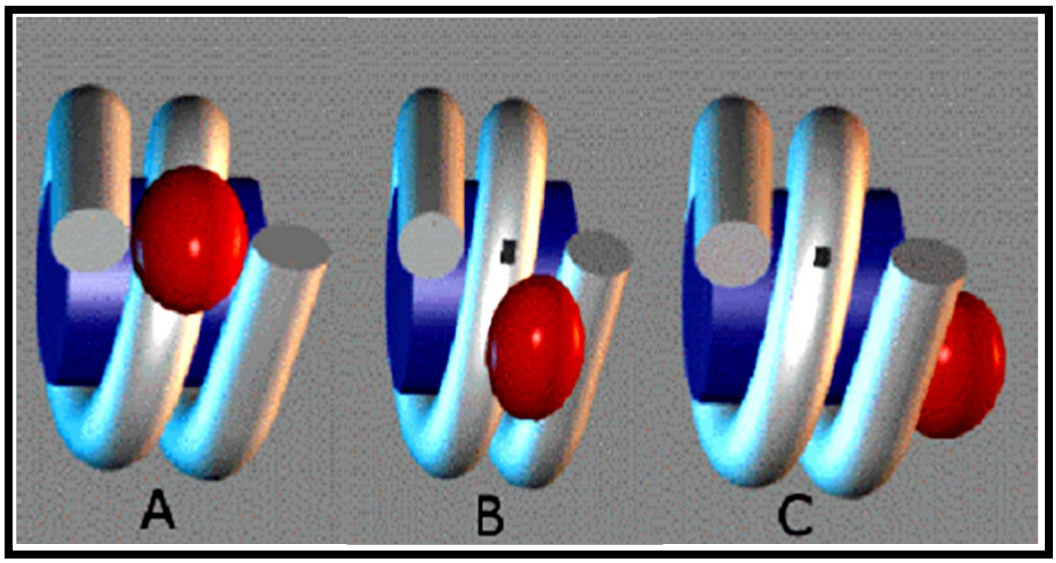

Figure 4: Three major models showing the binding of globular domain to nucleosome.
(A) Symmetrical model (B) Bridging model (C) Asymmetrical model.

Fluorescence recovery after photobleaching (FRAP) studies suggested the presence of only two DNA binding sites in globular domain. One of the two binding sites fits within major groove close to the dyad axis and the other within minor groove on the linker DNA close to NCP [86]. However, Fan and Roberts [87] suggested three binding site model based on extensive rigid molecular docking programs. This model proposed asymmetrical binding of GH5, in which one of the three binding sites contacts the nucleosome at the dyad and two others bind symmetrically to the entering and exiting linker DNA.

The reasons for the controversial models could be partly attributed to the way H1 is deposited on the nucleosomes. The above mentioned *in vitro* studies used salt dialysis to deposit H1 on the nucleosomes. However, this method leads to improper assembly of the H1 [88]. Another reason that could contribute to the controversy is the positioning of the nucleosome. To determine the exact location of the binding of globular domain on the nucleosome, it is important that nucleosomes themselves are properly positioned on the sequence. Previously, the nucleosomes were mostly reconstituted on 5S DNA. However, 5S DNA has been shown to exhibit several translational positioning, which in turn would interfere with the mapping of histone H1: nucleosomal DNA contacts [89].

1.7 Chromatin structure:

Controlled micrococcal nuclease (MNase) treatment of chromatin generates mononucleosomes, dinucleosomes, trinucleosomes (connected by linker DNA), and so forth [49]. When DNA from MNase-treated chromatin is separated on a gel, a number of bands will appear, each having a length that is a multiple of mononucleosomal DNA [90]. The simplest explanation for this observation is that chromatin possesses a fundamental repeating structure. This observation, together with data from electron microscopy and chemical cross-linking of histones gave birth to "subunit theory" of chromatin [91, 92]. The subunits were later named nucleosomes [51] and were eventually crystallized [58]. Chromatin structural hierarchies can be classified into primary, secondary and tertiary structures [93]

1.7.1 Primary structure:

This is the basic organizational level of the chromatin and under low ionic strength conditions chromatin is arranged as 11 nm "beads on a string" [51] which confers 5-10 fold compaction of the genomic template.

1.7.2 Secondary Structure:

Specific interactions between nucleosomes lead to the formation of 30 nm condensed fiber which induces 50-fold compaction. How nucleosomes interact with each other inside the 30 nm fiber is not completely understood [94, 95]. Finch and Klug proposed the first post-nucleosomal model of the chromatin fiber - a one start solenoid model. According to this model there are approximately 6 nucleosomes per turn (~11 nm), bent DNA linkers continue the helical trajectory established in the nucleosome core and each nucleosome makes close contact with its immediate neighbor in the array [96]. A few years later, Worcel et al. [97] and Woodcock et al. [98] proposed alternative zigzag structures consisting of a two-start helical ribbon with straight DNA linkers **(Figure 5)**. Several other topologies besides the basic zigzag and solenoid models have been proposed: for example the interdigitated solenoid [99] where planes of nucleosomes coming from the adjacent turns of the solenoid crisscross one another.

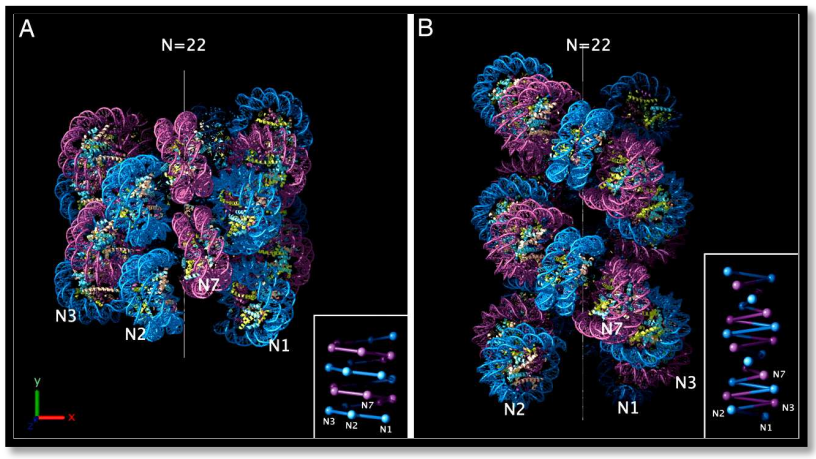

Figure 5: Currently accepted models of 30nm chromatin fiber. (A) Interdigital one–start model (B) Two-start helical cross linker model. The helix in both the cases contains 22 nucleosomes. Alternate nucleosome pairs are colored marine and magenta. The positions of the first, second, third, and seventh

nucleosomes in the linear DNA sequence are marked on both models with N1, N2, N3, and N7. Image adopted from [100]

1.7.3 Tertiary structure

These are the structures formed by the interaction of the secondary structures leading to the interphase and metaphase chromosomes. Several models have been proposed over the years. According to radial loop model [101] DNA of interphase chromatin is negatively super coiled into independent domains of ~85kb. This model suggests a form of organization of mitotic chromosomes in which loops of DNA are anchored in a central proteinacious scaffold. Loops can be seen directly when majority of the proteins are stripped from the mitotic chromosomes. The protein depleted chromosomes take the form of a central scaffold surrounded by a halo of DNA **(Figure 6)**. Belmont and Bruce proposed chromonema model in which fibers with diameter of 60-80 nm are coiled into 100-130 nm fibers, which in turn coil into 200-300 nm fibers that constitute the metaphase chromosome [102].

Figure 6: Electron micrograph of a histone depleted metaphase chromosome from HeLa. The chromosome consists of a central, densely staining scaffold or core surrounded by a halo of DNA extending 6-9 μm outward from the scaffold. Image adopted from [101].

1.8 Chromatin dynamics and its regulation

In eukaryotes, all DNA-templated reactions occur in the context of chromatin. Nucleosomes, as shown by crystal structure, exhibit multiple interactions between DNA and core histones and are highly stable but dynamic structures. The packaging of DNA around the histone octamer not only restricts DNA accessibility for regulatory proteins but also provides an opportunity to regulate DNA based processes through modulating nucleosome positions and local chromatin structure. Chromatin accessibility, as mentioned before, reflects the availability of DNA sequences for molecular interactions, typically by DNA binding factors. Nucleosomes are major determinants of local DNA accessibility: a DNA sequence tightly wrapped around a nucleosome is less easily bound by a DNA binding factor then the same sequence in a nucleosome free stretch of DNA. This model is supported by experimental data [103-105]. Chromatin, at all levels of the organization, is not static but very dynamic. This dynamicity and plasticity is crucial to ensure proper functioning of the cell. Modification of chromatin structures is the prime step in regulation of all the DNA templated processes like transcription, replication, repair and recombination. These processes require quick changes in the chromatin organization and structure. The dynamic control of genome accessibility is governed by contributions from DNA sequence, ATP dependent chromatin remodeling, histone variant incorporation and post translational modification of histones [106].

1.8.1 Sequence determinants of chromatin accessibility

Nucleosomes are the primary determinant of DNA accessibility [107, 108]; it is crucial to understand the rules underlying nucleosome positioning *in vivo*. As the DNA has to bend sharply around the surface of the histone octamer, nucleosome formation is favored by flexible or intrinsically curved sequences, whereas more rigid, less flexible sequences are unfavorable for histone-octamer incorporation. Indeed nucleosomal DNA is sharply bent to achieve tight wrapping around the histone octamer [64]. This bending occurs at every 10 -11 bp DNA helical repeat, where the major groove of the DNA faces inwards towards the histone octamer, and again ~5 bp away, with the opposite direction, when the major groove faces outwards. The bends of each direction are facilitated by specific dinucleotides [109, 110]. For example periodic A/T dinucleotide spacing has

been suggested to bend the DNA, creating a consistent curvature that gives rise to an intrinsically stable nucleosome **(Figure 7)**. Such nucleosome-positioning sequences appear to contribute to the rotational setting of the DNA helix on the surface of the histone octamer.

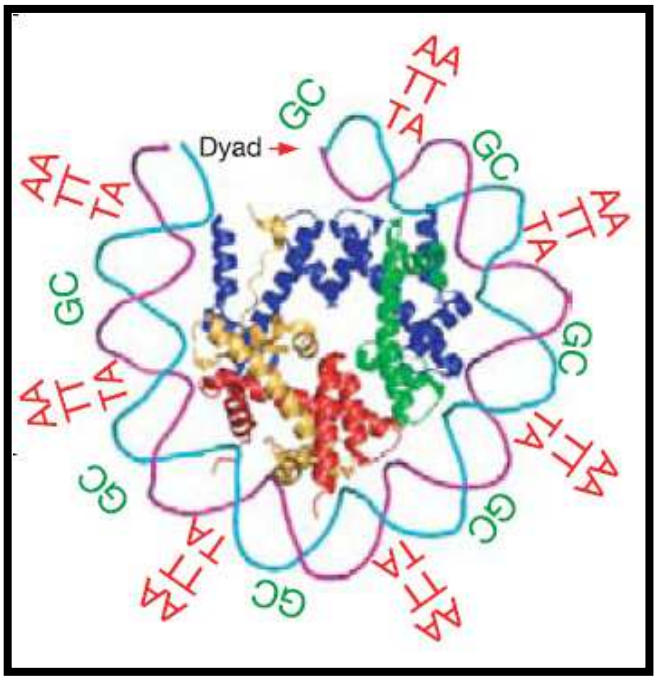

Figure 7: Effect of sequence on DNA bendability. Key dinucleotides inferred from the alignments are shown relative to the three-dimensional structure of one-half of the symmetric nucleosome. AA/TT/AT- lead to expansion of major groove while as GC- leads to contraction of major groove. Figure adopted from [111].

DNA sequences differ greatly in their ability to bend sharply [109, 110, 112] and form nucleosoms. *In vitro* studies show that the range of histones-DNA binding affinities is at least thousand fold [113]. Given these facts, it is reasonable to assume that *in vitro* nucleosome positions are determined purely by intrinsic sequence preferences and by steric exclusion between neighboring nucleosomes. Do the genomes use these sequence preferences to control the distribution of nucleosomes *in vivo* is still not very clear as nucleosomes compete with non histone DNA binding factors for access to genomic DNA which may result in overriding the intrinsic sequence preferences. For example, nucleosome positioning might be regulated in cells in *trans* by abundant [114] ATP dependent nucleosome remodeling complexes [115] which might override the sequence preference of the nucleosomes. The relative importance of the intrinsic sequence

preferences, chromatin remodeling complexes, competition with the other factors and the formation of higher order structures for shaping and maintaining *in vivo* chromatin is still debatable.

Nucleosomes have been mapped genome wide in *Saccharomyces cerevisiae* [116-118] *Drosophila melanogaster* [119], *Caenorhabditis elegans* [120, 121] and *Homo sapiens* [122]. Earlier studies showed a general depletion of nucleosomes from promoter regions [116, 117]. This important observation was refined in a pioneering study by Yuan et al. [118], who used microarrays to map nucleosome positions across 482 κB of budding yeast genome, spanning almost entire chromosome III and 223 additional regulatory regions. This study confirmed the earlier low-resolution reports that intergenic DNA in yeast was nucleosome-depleted relative to the coding DNA, and found Nucleosome-Depleted Regions (NDRs) of 150bp immediately upstream of many annotated coding sequences. Although the microarray resolution was insufficient for mapping individual nucleosomes with a bp-level precision, the authors were able to carry out a limited study of the sequence determinants of nucleosome positioning, and found that the nucleosome-free regions were enriched in poly-A and poly-T motifs. These motifs tend to occur in promoters, suggesting a causal role of poly (dA-dT) tracts in establishing NDRs.

In 2008, Maverich et al established a "canonical" picture of nucleosome organization in which well positioned -1 and +1 nucleosomes bracket an NDR upstream of *S. cerevisiae* genes [123]. The authors argue that positioning of bulk nucleosomes is largely a consequence of steric exclusion: +1 and to a certain extent -1 nucleosomes form a barrier against which other nucleosomes are "phased". This suggests that sequence specificity would be important only for a small fraction of nucleosomes, which is consistent with the observation that nucleosomal dinucleotide patterns are more pronounced in the -1 and +1 nucleosomes then in the bulk ones [123]. Later, Eran Segal and coworkers made a comparison between nucleosome positions *in vitro* and *in vivo* [124]. The results showed a striking similarity suggesting that nucleosome positions are largely encoded by intrinsic DNA sequence signals, because a purely sequence dependent model fit on the *in vitro* data was able to predict *in vivo* nucleosome locations with reasonably high accuracy. It was also observed that 5-mers with the lowest average nucleosome occupancy were AAAAA and ATATA. In addition, 10-11 bp periodic

dinucleotide signal caused by DNA bending, with AA/AT/TA/TT frequencies out of phase with CC/CG/GC/GG frequencies was also observed. The interesting observation of this study was that 5' NDR is much shallower for *in vitro* chromatin and there are no characteristic oscillations in the flanking regions. The absence of these oscillations indicates that nucleosomes are not positioned as precisely, and suggests that the intrinsic sequence signals are not the sole contributors to the *in vivo* anchoring of the nucleosomes. This observation was further strengthened by Kevin Struhl and coworkers [125] who showed that ACF (chromatin remodeler) is capable of overriding intrinsic sequence specificities of nucleosome core particle. They hypothesized that some component of the transcriptional machinery interacts with a nucleosome remodeling complex and/or histones to position the +1 nucleosome. Once in place, +1 nucleosome positions the +2 and +3 nucleosomes and so on by steric exclusion **(Figure 8)**. This is supported by the observation that *in vivo* +2 and +3 nucleosomes are much better positioned than their -2 and -3 counterparts. These results highlight our limited ability to predict nucleosome positioning from DNA sequence alone, but they do suggest that *trans*-acting proteins have a major role in determining the precise nucleosome positioning and occupancy *in vivo*. In particular, there is a dynamic competition between the nucleosomes and the transcription factors for important *cis*-regulatory sequences in gene promoters. This competition is influenced by the chromatin modifiers and the chromatin remodelers [60, 126-128].

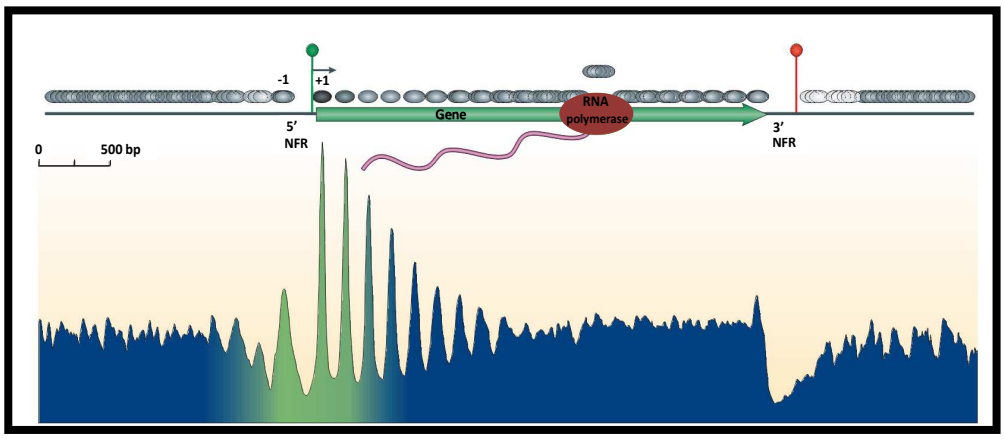

Figure 8: Nucleosome (grey ovals) distribution around all yeast genes. The nucleosomes are well positioned around the transcription start site (TSS) as shown by the peaks and the positioning is lost a few nucleosomes from the TSS represented by green circle. The green-blue shading in the plot represents the transitions observed in nucleosome composition and phasing (green represents high levels of H2A.Z,

acetylation, H3K4 methylation and phasing, whereas blue represents low levels of these modifications). The red circle indicates transcriptional termination within the 3' NFR. Figure adopted from [129].

1.8.2 Chromatin remodeling and DNA accessibility

Chromatin remodeling is an enzyme-assisted and ATP dependent histone or nucleosome mobilization, which influences local chromatin structure to facilitate or prevent protein accessibility which is required to initiate DNA-templated reactions. These enzymes are called as chromatin remodelers and they play an important role in maintaining the promoters either in permissive state or in non permissive state [128]. Accordingly, remodelers have been shown to modulate transcription, replication and DNA repair [60, 130]. The different outcomes of the remodeling are shown in the **(Figure 9)**.

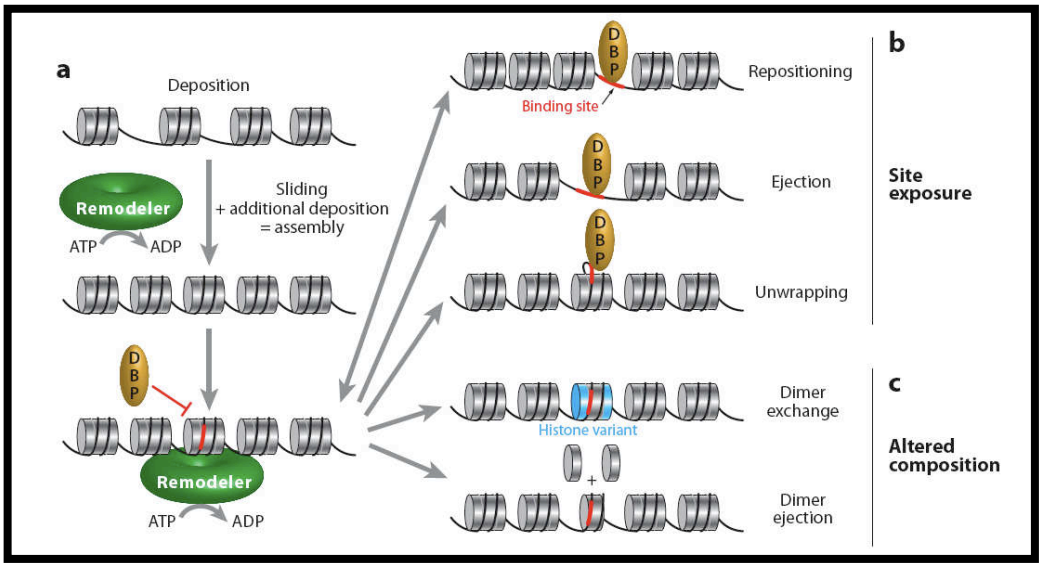

Figure 9: Different outcomes of chromatin remodeling. (*a*) Remodelers (*green*) play a role in chromatin assembly by moving already deposited histone octamers, generating room for additional deposition. The remodeler action on a nucleosome array results in various products that can be classified in two categories: (*b*) site exposure, in which a site [131] for a DNA-binding protein (DBP), initially occluded by the histone octamer, becomes accessible by nucleosomal sliding (repositioning), or nucleosomal eviction (ejection), or localized unwrapping, and (*c*) altered composition, in which the nucleosome content is modified by dimer replacement [exchange of H2A-H2B dimer with an alternative dimer containing a histone variant (*blue*)] or through dimer ejection. Figure adopted from [132]

1.8.3 Chromatin remodeler families

There are four families of chromatin remodelers. All four share some properties (like ATP hydrolysis) but at the same time posses some unique domains in their catalytic ATPases and a unique set of associated proteins [132].

1.8.3.1 SWI/SNF family of remodelers

Remodelers in SWI/SNF (switching defective/sucrose non-fermenting) are composed of 8 to 14 subunits and were initially purified from *S. cerevisiae*. The members of this family include yeast SWI/SNF and RSC complex, the human hBRM and hBRG1 complexes and the *Drosophila* Brahma complex [133, 134]. These remodelers can slide [135] and eject [136] nucleosomes and their functions are correlated with nucleosome disorganization and promoter activation [126, 127, 132, 136]. They have domains that bind acetylated tails **(Figure 10)**, promoting their targeting or activity in promoters undergoing activation [126, 128]. In yeast SWI/SNF remodelers are usually located at the -1 nucleosome [128, 137]. This is consistent with the fact that the binding sites for many condition specific activators reside within the -1 nucleosome in regulated genes.

1.8.3.2 ISWI family of remodelers

The ISWI (imitation Switch) family of remodelers contains 2 to 4 subunits. The members of this family including dNURF, dCHRAC and dACF were initially purified from *Drosophila melanogaster*. Subsequently ISWI members were identified from yeast (ISW1 and ISW2) [138] and eukaryotes, including humans. Most eukaryotes build multiple ISWI family complexes using one or two different catalytic subunits with specialized accessory proteins [132]. The ISWI family of ATPases has characteristic domains at C-terminus: a SANT domain adjacent to a SLIDE domain **(Figure 10)**. Together, these domains form a nucleosome recognition module that binds to an unmodified histone tail and DNA [139]. Except for NURF and Isw1b, ISWI remodelers carry out nucleosome reorganization [140, 141] which often promotes repression. They generally remodel nucleosomes that lack acetylation at H4K16 [142], confining their activity to nucleosomes at transcriptionally inactive regions. They space the nucleosomes by “measuring” the linker DNA between nucleosomes and slide them until nucleosome

array of uniform spacing is created [143]. However, NURF can work antagonistically and can randomize the nucleosome spacing which in turn can assist RNAPII activation [132].

1.8.3.3 CHD family of remodelers

The CHD (Chromodomain, Helicase, DNA binding) family of remodelers contain 1 to 10 subunits and were initially purified from *Xenopus laevis* [144]. These remodelers are distinguished by the presence of two chromo domains on N-terminal of the catalytic subunit that function as interaction surfaces for a variety of chromatin components and SNF2-like ATPase domain located in the central region of the protein structure **(Figure 10)**. The lower eukaryotes have monomeric catalytic subunit while as vertebrates usually have it in large complexes [132]. The accessory proteins of this family of remodelers often bear DNA binding domains and PHD, BRK, CR1-3 and SANT domains. CHD remodelers utilize a number of recruitment mechanisms that include binding to sequence specific transcription factors, histone marks, methylated DNA and poly (ADP-ribose) [145]. These remodelers have been implicated in transcription activation [146] as well as repression [131, 147]. NuRD is the only CHD remodeling complex that has been implicated in transcriptional repression [145].

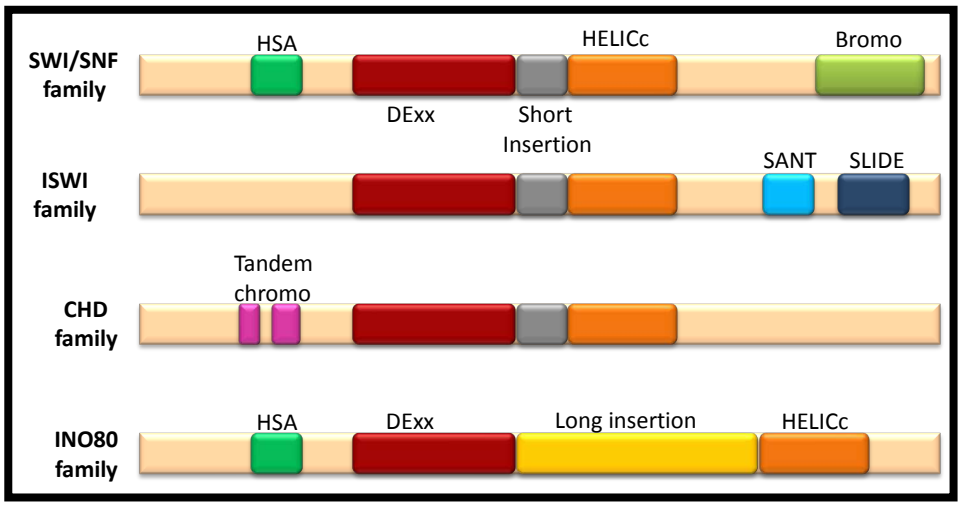

Figure 10: ATPase domain organization of different remodeler families. All remodeler families contain a SWI2/SNF2-family ATPase subunit characterized by an ATPase domain that is split in two parts: DExx [131] and HELICc (*orange*). Unique domains residing within, or adjacent to, the ATPase domain distinguishes each family. Remodelers of the SWI/SNF, ISWI, and CHD families each have a distinctive short insertion (*gray*) within the ATPase domain, whereas remodelers of INO80 family contain a long insertion (*yellow*). Each family is further defined by distinct combinations of flanking domains:

Bromodomain (*light green*) and HSA (helicase-SANT) domain (*dark green*) for SWI/SNF family, SANT-SLIDE module (*blue*) for ISWI family, tandem chromo domains (*magenta*) for the CHD family, and HSA domain (*dark green*) for the INO80 family. Image modified from [132].

1.8.3.4 INO80 family of remodelers

The INO80 (inistol requiring 80) family of remodelers contain 14-15 subunits and includes INO80 remodeling complex (INO80.com) and the SWR1 remodeling complex (SWR1.com) initially purified from *S. cerevisiae* [148]. The distinguishing feature of this family is a "split" ATPase domain with a long insertion present in the middle of the ATPase domain **(Figure 10)**. INO80 has been implicated in transcription regulation and DNA repair [148]. SWR1 restructures the nucleosomes by removing canonical H2A-H2B dimers and replacing them with H2A.Z-H2B dimers [132].

1.8.4 Mechanism of chromatin remodeling

The ATP dependent remodeling complexes have been extensively studied and shown to have the ability to alter and rearrange the nucleosomes in a way that increases the accessibility. However, the mechanistic view of how ATP hydrolysis is coupled to disruption of histone-DNA contacts and subsequent nucleosome re-deposition is still debatable. Several models have been proposed as discussed below.

1.8.4.1 Twist diffusion model

This model was proposed by Van Holde as a possible mechanism for the spontaneous migration of nucleosomes (sliding) on DNA [149]. Basically it involves the diffusion of "twist defects" through the nucleosomal DNA. This model suggested that thermal energy fluctuations would be sufficient to twist the DNA helix at the edge of the nucleosomes, replacing histone-DNA interactions by neighboring DNA base pairs. Propagation of this twist around the histone octamer surface would change the translational position of the nucleosome [110]. This model as such cannot account for unidirectional migration. Richmond and Widom came up with a refined version of this model, in which ATP dependent enzymes attached to one side of the nucleosome, can act either to insert twists of a given sense, or can act as "molecular rachets" to permit only oscillations of a given sense to pass [110, 149]. This model is supported by crystal structures of nucleosome core particle in which the DNA on one side is observed to contain a single base pair "twist

defect" compared to the DNA at the other side of the core [63, 150]. However, this model could not explain why a nick or a gap, which presumably dissipate the twist tension on DNA, had no effect on ISWI or RSC induced nucleosome remodeling [151, 152].

1.8.4.2 Loop recapture model

This model proposed the dissociation of DNA at the edge of the nucleosome with reassociation of DNA inside the nucleosome, forming a DNA bulge or loop on the octamer surface [153]. The DNA loop would then propagate across the surface of the histone octamer in a wave-like manner, resulting in the repositioning of DNA without changes in the total number of histone-DNA contacts [154]. This model was supported by a recent study showing that ACF introduces a DNA loop at the nucleosomal entry site that propagates over the histone octamer surface and leads to nucleosome repositioning [155].

1.8.4.3 Translocation model

A main change in the view of the mechanism of chromatin remodelers came from studies which showed that ATP-dependent chromatin remodelers can translocate on DNA [56, 156-158]. These studies lead to the proposal that remodeling enzymes use a DNA translocase mechanism to induce nucleosome sliding along the DNA **(Figure 11)**. According to this model, the remodeler anchors to the nucleosome at two positions: a DNA binding domain (DBD) contacts the linker DNA, whereas the ATPase domain (translocation domain or Tr domain) binds at the location SHL2 (two turns from the dyad) on the nucleosomal DNA (figure10). The ATP/Translocase domains remain attached at that fixed position on the octamer and DNA is pumped into the nucleosome by coordinated, ATP-dependent conformational changes between the translocation domain and the DNA binding domain of the remodeler. This conformational change would result in a helicase-typical "inch–worm" like movement of the remodeler and it would facilitate the disruption of histone-DNA contacts and the formation of a loop. This may happen from the sequential or concerted action of these two domains: DBD pushes DNA into the nucleosome, creating a DNA loop and Tr domain pumps that DNA towards the nucleosomal dyad. The loop may propagate around the nucleosome by one-dimensional diffusion, breaking histone DNA contacts at the leading edge of the loop and replacing them at the lagging edge [127, 132, 159]. This model is supported by recent single

molecule and biochemical studies demonstrating that both SWI/SNF and RSC are able to translocate on DNA and nucleosomal substrates to produce loops in an ATP dependent manner [56, 160]. A recent study has proposed a modified version of this model, suggesting that the loops do not diffuse about the exterior of the nucleosome but rather feed through specific restriction points by threading past a fixed constriction [150].

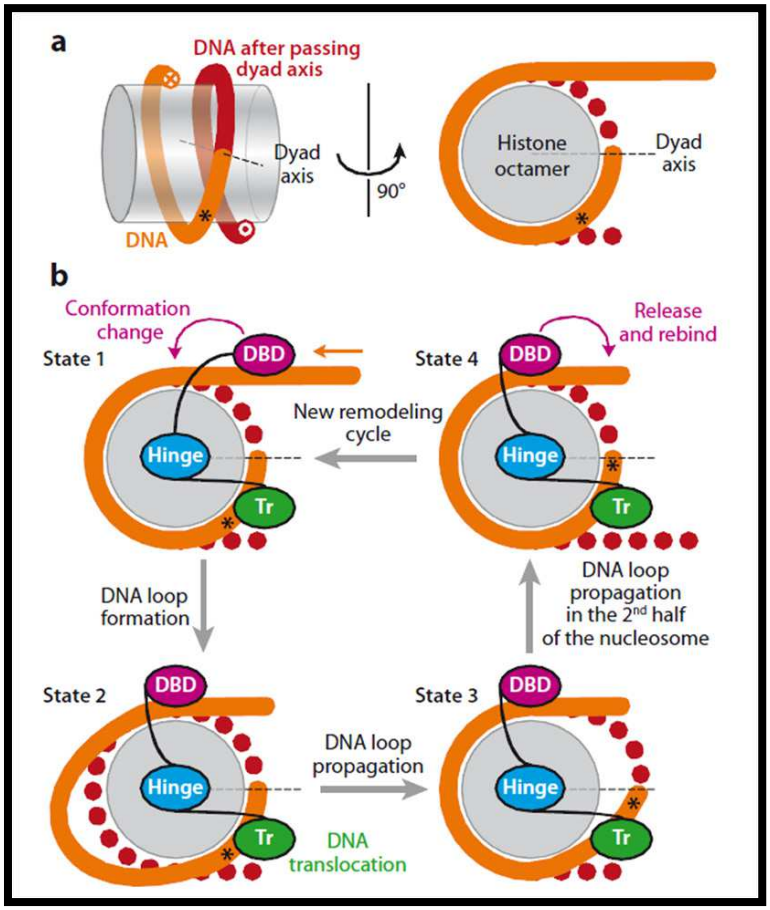

Figure 11: Model of DNA movement during a remodelling event. (a) Shows the side view of nucleosome emphasizing the left-handed wrapping of DNA (orange then red) around the histone octamer (gray transparent cylinder). Note the change in the colour of DNA from orange to red when passing the nucleosomal dyad axis. At right (and also in part b), the nucleosome is rotated 90◦ according to the axis and depicted in two dimensions. An asterisk (∗) provides a reference point on the DNA, useful for following the translocation of DNA along the octamer surface. (b) States 1 to 4 represents the successive steps occurring during a remodeling event. The concerted action of a DNA-binding domain (DBD) located on the linker DNA and a translocation domain (Tr) located near the dyad generates a small DNA loop that propagates on the nucleosome surface. The remodeler undergoes a conformational change in its DBD when DNA loop is generated (State 1 to State 2), followed by the translocation of the DNA through the Tr domain, which passes the DNA loop to the dyad (State 2 to State 3). The DNA loop continues its propagation on the second half of the nucleosome surface by one-dimensional diffusion. Loop propagation then resolves into the distal linker, resulting in nucleosome repositioning (State 3 to State 4). The remodeler resets its conformation with original binding contacts, ready for a new remodeling cycle (State 4 to State 1).

1.8.4.4 Remosomes as the intermediates of remodeling

A recent study from our laboratory has proposed another model for explaining the mechanism of action of RSC. They propose that RSC works in a two step mechanism, first RSC pumps 15-20 bp DNA from each linker into the nucleosome, creating 30-40 bp loops and then dissociates from the nucleosome **(Figure 12)**. Since additional 15-20 bp of each linker is associated with histone octamer, the loop cannot dissipate. As a result, a multitude of stable structures with distinct and irregular DNA path is generated. Such particles were named as "Remosomes". In the second step of the reaction, RSC works as translocase [161].

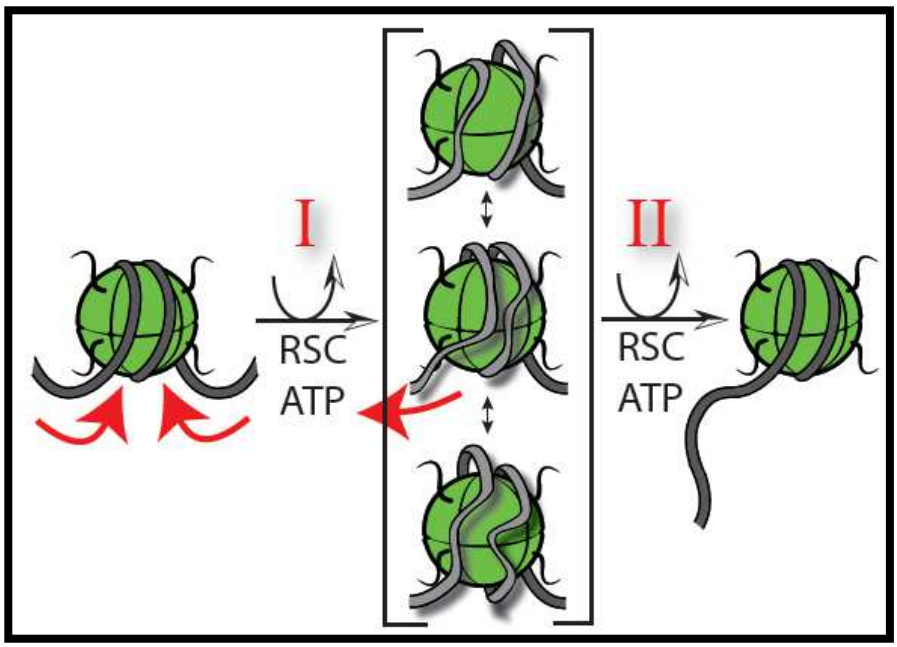

Figure 12: Two step model for remodeling. Nucleosomes are converted first to intermediate species called remosomes. In the second step remosomes are acted upon by remodelers in presence of ATP to lead to final product. Image adopted from [161].

1.8.5 Influence of core histone variants

In addition to core histones, synthesized primarily in S phase and deposited at replication forks, there are numerous histone variants encoded by separate genes, which are often synthesized constitutively at low levels and incorporated differently. Incorporation of the variant histones confers novel structural and functional properties to the nucleosomes. Such compositional changes add to the complexity of chromatin and

can also affect DNA accessibility. There are reported variants for all the canonical histones (except H4), which vary from conventional counterparts from almost no amino acid difference to extremely divergent changes [162]. Variants of histone H2A and H3 have been known for decades, but only recently their functional importance was realized. H2A variants include H2A.Z, H2A.X, H2A-Bbd and macroH2A. Histone H3 variants are H3.3 and CENP-A. Some of these variants are positively correlated with transcriptional activation, including H2A.Z and H3.3. H2A.Z is widespread throughout eukaryotic chromatin. Several studies have highlighted its role in transcription, DNA repair, genome stability and the control of antisense transcription [163, 164]. H2A.Z is highly conserved among eukaryotes and it has 60% amino acid identity with H2A. It differs from H2A and H2X around the L1-α2 and α2-L2 junctions and in the C-terminal docking domain that contacts H3 [162]. The Swr1 remodeling complex exchanges H2A-H2B dimers to create nucleosome containing H2A.Z-H2B dimers near the 5' ends of genes [165]. The deposition of H2A.Z into chromatin is an essential process for many organisms and is important for the proper transcription of many genes [166]. H2A.Z containing nucleosomes are found on either side of the NDRs at transcriptional start sites [163], where they promote efficient RNA polymerase II recruitment in both yeasts and human cells [165, 167, 168]. There is a variation in the placement of H2A.Z within the promoters in different organisms and its precise role. In yeast, H2A.z is found at most genes and mainly occupies the +1 and -1 nucleosomes and it is highly enriched at the open TATA-less promoters [169, 170]. In *Drosophila*, H2A.Z is absent at -1 nucleosome but is highly prevalent at +1 nucleosome [119]. In humans, H2A.Z is found in the promoters, extending from -3 to +3 nucleosomes in genes with low expression [171].

H2A.Z can assemble *in vitro* into either homotypic nucleosomes or hybrid nucleosomes that contain one H2A.Z and one H2A molecule. Both of the nucleosomes protect ~146 bp on 5S rDNA. Homotypic nucleosomes display the highest stability followed by hybrid nucleosomes with intermediate stability and H2A nucleosomes with least stability [172]. The question that arises here is why a histone variant that makes the nucleosomes more stable should facilitate the transcription? The answer comes from the role of another histone variant, H3.3 which is almost identical to the canonical H3 with only four amino acid changes. H3.3 variants are also synthesized outside the S phase of the cell cycle, become incorporated into nucleosomes and are deposited at specific

locations primarily in a replication independent manner by the HIRA and Daxx chaperons [165, 173].

H3.3 is highly enriched for several modifications associated with transcription and is specifically incorporated at transcribed genes and regulatory sequences [106, 174-176]. H2A.Z nucleosomes are more stable than H2A-containg nucleosomes when co-assembled with canonical histone H3 but less stable when co-assembled into nucleosomes with the H3.3 [177]. Interestingly, H2A.Z and H3.3-containing nucleosomes occupy regions surrounding the promoter at the 5' ends of the transcribed genes implying that less stable nucleosomes contribute to generation of 5' NDRs *in vivo* and allow pol II and its regulators access to the underlying DNA to facilitate transcription.

1.8.6 Histone modifications and transcription

The N-terminal core histones tails are less structured than the globular histone fold regions and are not essential for maintaining the integrity of nucleosomes [178]. However, histone tails are thought to play a vital role in dynamicity of the chromatin. Numerous residues within the histone tails and several residues within the histone globular domains are subjected to vast array of posttranslational modifications. These modifications include methylation of arginine (R) residues, methylation, acetylation, ubiquitination, ADP ribosylation and summolation of lysines (K); and phosphorylation of serines and threonines. Histone modification can be categorized into euchromatin modifications when associated with active transcription and heterochromatin modifications when associated with inactive genes or regions. For example, acetylation of H3 and H4 or di- or trimethylation of H3K4 are commonly referred as euchromatin modifications, while as H3K9me and H3K27me are often termed as heterochromatin modifications [46]. All these modifications are reversible and the enzymes transducing these modifications, such as histone acetylases (HATs), deacetylases (HDACs) and methylases are highly specific for particular amino acid positions. Indeed, the location of a modification is tightly regulated and is crucial for its effect on transcription. For example, Set2 mediated methylation of histone H3K36 normally occurs within the open reading frame of actively transcribed gene [124]. But, if Set2 is mistargeted to the promoter region through artificial recruitment, it represses transcription [46, 179, 180].

1.8.6.1 General mode of action of covalent histone modifications

Initial models had suggested that histone modifications may alter chromatin structure by influencing histone-DNA or histone-histone contacts [181]. This could be explained by the fact that with the exception of methylation, histone modifications result in a change in the net charge of the nucleosomes, which could loosen inter or intranucleosomal DNA-histone contacts. For example, acetylation of the histone tails neutralizes the positive charge of lysines and profoundly alters chromatin properties [182, 183]. This idea is further supported by the observation that acetylated histone are easier to displace from DNA both *in vivo* [184, 185] and *in vitro* [186, 187]. *In vitro,* acetylation of H2A-H2B tails weakens the interactions that are present 40 bp on either side of the dyad, and acetylation of H3-H4 greatly reduces the formation of the higher order structures and also reduces the amount of the DNA bound in the nucleosomes [188]. The balance in activity between histone acetyl transferases (HATs) and histone deacetylases (HDACs) governs the acetylation status of a given region of chromatin. In general, hyperacetylation is the hallmark of active chromatin, whereas hypoacetylation is seen in repressed chromatin.

Another mode of action for the covalent modifications is to establish binding sites for recruiting specific regulatory proteins (in a context dependent manner). For example, methylation of H3 at lysine 9 creates a binding site for a domain of HP1 protein [189] leading to the formation of compact chromatin. SWI/SNF and RSC chromatin remodelers both contain subunits that have a bromodomain and can bind to acetylated H3 tails. *In vitro,* acetylation of H3 by SAGA or NuA4 histone acetyltransferase complex greatly stimulates RSC and SWI/SNF chromatin remodeling activities to facilitate Pol II transcript elongation [190, 191]. Given the diversity of the covalent modifications, it has been proposed that individual histone modifications or modification patterns might be read by other proteins that influence chromatin dynamics and function [192, 193]. For example, chromo domains recognize methylations [194], bromodomains recognize acetylations [195] and a domain within 14-3-3 proteins recognizes phosphorylations [196]. Additional modifications have recently been discovered that also affect the intrinsic properties of the chromatin structure to aid the transcription. Ubiquitination of C-terminal tail of H2B interferes with the ability to form the higher order structures by

creating an open accessible fiber. Similarly, modifications such as acetylation of H4K16 inhibit the formation of compact 30 nm fibers [183] and hence directly influence the higher order chromatin structure. It also impairs the efficiency of ATP dependent chromatin assembly and mobilization by the ACF histone chaperone [183], thus suggesting that a single modification can elicit multiple effects on chromatin structure and mechanism discussed above are not mutually exclusive.

1.9 Nucleosomes as transcription barriers

The packaging of DNA into nucleosomes, in general restricts DNA accessibility for regulatory proteins [197] and at the same time also provides an opportunity to regulate DNA based processes through modulating positions and local chromatin structure [198]. Nucleosomes sterically block and strongly distort the DNA except for the terminal segments which are relatively straight [58, 64]. The packaging of promoter DNA in nucleosomes has been shown to inhibits transcription *in vitro* [199] and *in vivo* [107]. Nucleosomes can inhibit initiation of transcription by occupying the key regulatory DNA sequences near the promoter and transcription start sites. One of the well studied promoters with regulatory sites occupied by nucleosome is retroviral MMTV promoter in which an NF1 binding site is localized in the vicinity of four binding sites for glucocorticoid receptor (GR). *In vitro* studies showed that purified glucocorticoid receptor protein could bind to its target sequence in the nucleosome [200, 201] while as NF1 was unable to bind to its nucleosomal target [201, 202]. Later on, it was observed that rotational and translational positioning of the binding site on the nucleosome had no effect on affinity of NF1 for DNA while as GR showed an increased affinity if its binding site was held in certain translational [203] and rotational [204] positions, as only those sites are bound whose major groove points outwards [201, 204]. The difference between the bindings of these two proteins could be explained by their different affinities for the binding sites. NF1 is high affinity protein and is expected to embrace the double helix and contact bases and phosphates at many positions, no matter the rotational orientation of the binding site. On the other hand, hormone receptors such as glucocorticoid receptor bind DNA with relatively low affinity and make fewer contacts with a narrow sector of the double helix, provided their rotational orientation permits access to the relevant major groove [205].

1.9.1 Dynamics of DNA–histone interactions as a mechanism of nucleosome accessibility

The accessibility of nucleosomes to DNA binding regulatory proteins is of prime importance to the life of the cell. Several mechanisms have been proposed to explain how these proteins gain access to nucleosomal DNA. The most predominant view is that accessibility is controlled by histone posttranslational modifications [193, 206] and by the activity of the ATP dependent chromatin remodeling factors. Although both these processes play a vital role in chromatin accessibility, it is not yet clear what determines their targeting to the particular nucleosomes. This suggests that some factors should be able to bind to the nucleosomal DNA and recruit the factors for posttranslational modification and remodeling of the nucleosome. First mechanistic view of how such DNA-binding proteins target nucleosomal DNA was proposed by Pollach and Widom in 1995. They measured the equilibrium constants for spontaneous formation of 'opened' and 'closed' nucleosome conformations by assaying DNA accessibility with restriction enzymes [207]. It was the first study to demonstrate that the inherent dynamics of DNA–histone interactions play a fundamental role in how proteins can bind to target sequences located within nucleosomes. Later on, Widom laboratory determined the rates of spontaneous wrapping/unwrapping of nucleosomal DNA using fluorescently labeled nucleosomes and fluorescence correlation spectroscopy (FCS) measurements and demonstrated that spontaneous unwrapping of DNA facilitates the binding of the LexA transcription factor near the termini of the nucleosomal DNA, and the rewrapping of DNA limits the efficiency of LexA binding [208]. Recently, the same group reported slower dynamics in internal regions of DNA [209].

1.10 NF-κB

Nuclear factor-κB (NF-κB) is a family of transcription factors initially identified in 1986 by Ranjan Sen and David Baltimore [210]. They called it as NF-κB as it was nuclear factor, bound to an enhancer element of immunoglobulin kappa light chain gene in B cells [211]. It was also observed that NF-κB DNA-binding activity and NF-κB-dependent gene transcription were rapidly induced even when new protein synthesis was

blocked with cyclohexamide, demonstrating that the activation of DNA binding activity occurs via a post translational mechanism. There are five members of this family of transcription factors in mammals p50/p105 (NF-κB1), p52/p100 (NF-κB2), RelA (p65), RelB and c-Rel, which are capable of forming homo- and heterodimers in almost any combination [212]. These homo- and heterodimers are associated with specific biological responses that stems from their ability to regulate target gene transcription differentially. For instance, p50 and p52 homodimers function as repressors [213], whereas dimers that contain RelA or c-Rel are transcriptional activators. RelB exhibits a greater regulatory flexibility, and can be both an activator [214] and a repressor [215]. RelB does not homodimerize but it forms stable heterodimers with either p50 or p52 [216].

The main characteristic of these proteins is the presence of a conserved N-terminal 300 amino acid Rel homology domain (RHD) that is responsible for dimerization, interaction with the IκBs and nuclear translocation and binding to DNA [217]. Three members of this family p65, c-Rel and RelB also posses transcription activation domain (TAD) at their C-terminal end while as p50 and p52 lack such a domain as shown in **(Figure 13)**. p50 and p52 are synthesized as large precursors, p105 and p100, that are post-translationally processed to the DNA-binding subunits p50 and p52, respectively. In essentially all unstimulated nucleated cells, NF-κB complexes are retained in inactive form inside the cytoplasm through binding to inhibitory protein called as IκBs [218]. The IκBs physically mask the nuclear localization signal of NF-κB. Upon stimulation, NF-κB induction typically occurs following the activation of the IκB kinase (IKK) pathway, resulting in the phosphorylation and subsequent proteosomal degradation of the inhibitory IκBs [219]. This step represents the cytoplasmic switch of the NF-κB activation and liberates the NF-κB for nuclear translocation and gene activation.

Two major signaling pathways have been described that lead to translocation of NF-κB dimers from the cytoplasm to the nucleus and are shown in the **(Figure 14)**. Inside the nucleus, NF-κB recognizes and binds 9-10 bp specific sequences, called as κB sites (with the consensus sequence GGGRNNYYCC, N is any base, R is purine and Y is pyramidine), in the promoter or enhancer regions of target genes. The critical features of this consensus is the presence of a series of G nucleotides at the 5' ends, while the central portion of the sequence displays greater variation [217] In normal cells, NF-κB mediated

activation is transient and lasts only for less than an hour [220]. Several mechanisms operate to down regulate the activated NF-κB, the most well characterized being the feedback pathway whereby newly synthesized IκBα binds to NF-κB inside the nucleus and shuttles it back to cytoplasm.

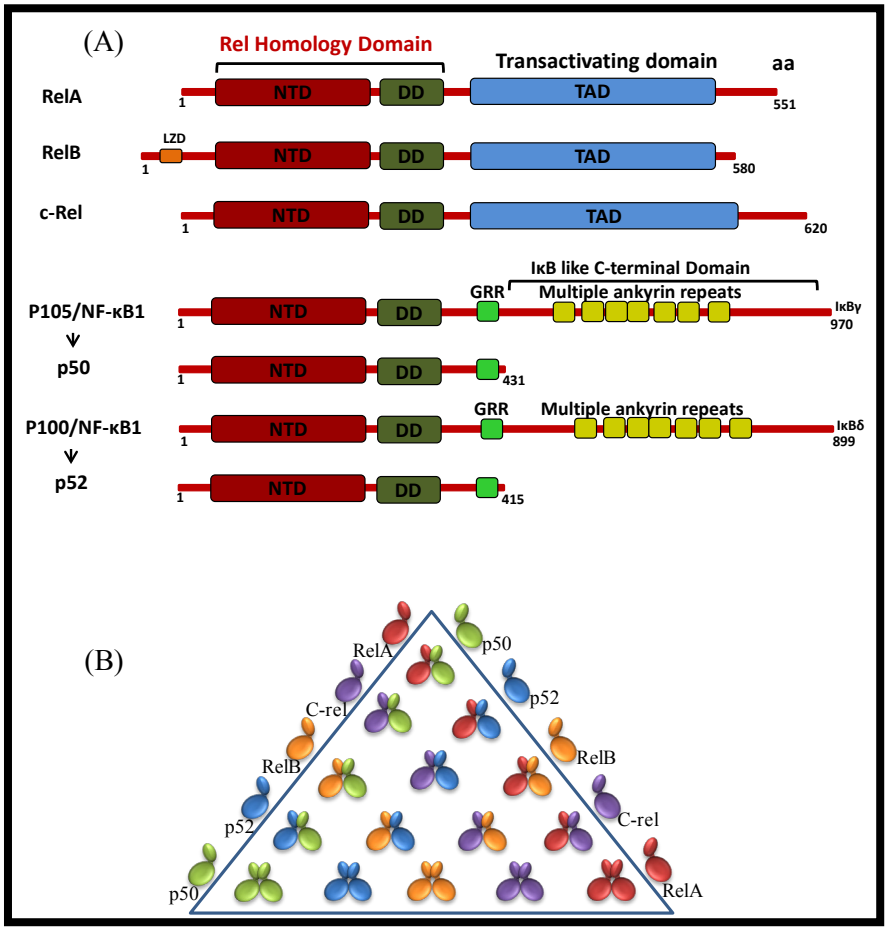

Figure 13: Members of the NF-κB family. (A) Domain organization of the NF-κB monomers showing the characteristic RHD. (B) Different dimer combinations.

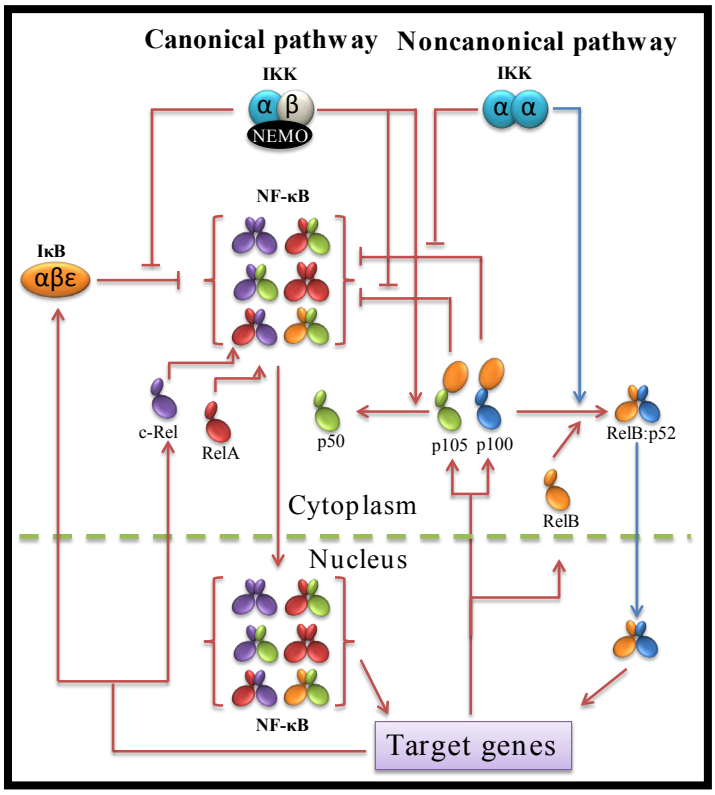

Figure 14: Canonical and non-canonical NF-κB activation pathways. The canonical pathway (left) is induced by most physiological NF-κB stimuli; it involves NEMO-dependent IKKβ-mediated phosphorylation of IκBα, which results in the nuclear translocation of mostly p65-containing heterodimers. In contrast, the noncanonical pathway [188] is induced by certain TNF family cytokines, such as CD40L, BAFF and lymphotoxin-β (LT-β), involves IKKα-mediated phosphorylation of p100 associated with RelB, which leads to partial processing of p100 and the generation of transcriptionally active p52-RelB complexes.

1.10.1 Structures of the NF-κB: DNA complexes

Several three dimentional NF-κB:DNA structures are known and provide important insights into DNA recognition mechanism of NF-κB [217]. In general, the κB DNA is pseudo-symmetric, and each NF-κB monomer binds to one DNA half site. The loops in each NTD (Loop L1 and L2) recognize a flanking region of DNA half site from the major groove side, the linker (Loop L3) and the loops from the dimerization domain then consume the rest of the major groove at the center. Since the minor groove is very narrow in all the NF-κB-DNA complexes, it appears that the residues from the loops encircle the DNA as shown in **(Figure 15C)**. All the DNA base-specific contacts are mediated by amino acid side chains from the immunoglobulin-like NTD of each NF-κB RHR. These complexes exhibit conformational flexibility as NTD is able to translate and/or rotate when it encounters different DNA sequences [217]. This conformation flexibility is

attributed to bi-lobal architecture of the RHR where NTD is linked to the dimerization domain (DD) by a 10 bp linker as shown in **(Figure 15A)**. p50 and p52 subunits optimally contact a 5 bp half site, whereas, RelA, c-Rel and RelB subunits contact a 4 bp half site **(Figure 15B)**. The central bp in majority of κB sites is A:T and serves as a point of reference for studying base-specific interactions between NF-κB subunits and κB sites.

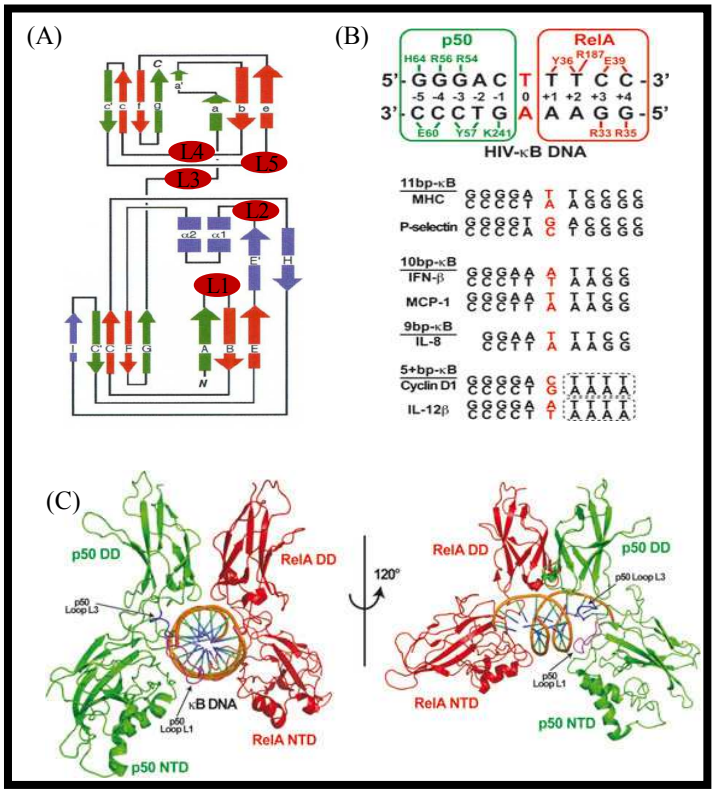

Figure 15: (A) Schematic representation of the immunoglobulin-like folds of NF-KB p50. The strands shown in red correspond to the conserved structural core of the domains (strands b, c, e and f) and those shown in green are also part of the immunoglobulin-like domains but are more variable. The red oval shapes show the loops used to mediate the DNA binding (B) Schematic representation of base-specific contacts mediated by NF-κB p50 (green) and RelA subunits and HIV-κB DNA observed in the X-ray crystal structure. Lower panel in the (B) shows the examples of κB DNAs in the natural target genes with different length and variable half-side. (C) Ribbon structure diagram of the p50:RelA heterodimer in complex with κB DNA. The assembled Rel homology region of the p50 (Green) and RelA subunits viewed orthogonal to their vertical axis of twofold pseudo-symmetry (left) and rotated 120° about the vertical axis to show the interaction of p50 subunit loop L1 (magenta) and L3 (blue) with DNA bases through the major groove.

1.10.2 Selective transactivation by NF-κB

NF-κB is a pleiotropic transcription factor implicated in the regulation of diverse biological phenomena, including apoptosis, cell survival, cell growth, cell division, innate

immunity, cellular differentiation. In addition, these transcription factors are persistently active in a number of disease states, including cancer [221, 222] arthritis [223], chronic inflammation [224], asthma [225], neurodegenerative diseases [226], and heart disease.

How is NF-κB able to regulate so many processes? Although the exact mechanism of how a specific NF-κB dimer is regulating a specific gene under a specific condition is not very clear. Several mechanisms have been proposed to explain the selectivity of the NF-κB response, which operate in a hierarchical manner. The primary source of the selectivity of NF-κB response is the ability of NF-κB to form homo- and heterodimers. This raises the possibility that specific dimers are activated by defined signaling pathways and physiological conditions, with each dimer being involved in the regulation of unique set of target genes. The presence and absence of transactivating domain in a dimer makes a fare contribution towards the selectivity of the NF-κB response. For example, dimers bearing RelA, RelB and c-Rel promote gene activation while as homodimers of p50 and p52 are generally repressive but can confer activation by interacting with some nuclear IκBs like Bcl3, IκBζ [227, 228]. IκBζ was also reported to negatively regulate RelA containing NF-κB complexes [229] suggesting that it may possess the capability to selectively inhibit or activate specific NF-κB species. Selectivity of NF-κB response is also likely to take advantage of differences in transcriptional activation capabilities of dimers that contain activation domains. An NF-κB dimer may be uniquely capable of activating a specific subset of target genes if that dimer is unique in its ability to interact with another transcription factor, co-regulatory protein, chromatin protein or general transcription factor that is required for the activation of that subset of genes. RelA has been reported to interact with multiple components of general transcription machinery and with several co-activators and chromatin complexes [230]. For example, in the enhanceosome of the gene encoding interferon-β, RelA and IRF3 can form a stable complex [231] that can be recruited through an interferon-response element or a κB site, with the indirectly recruited transcription factor acting as a cofactor to facilitate the activation of transcription. Additional transcription factors for which synergistic interaction with NF-κB has been described are Sp1, AP-1, STAT3 and CEBP/β [230]. Furthermore, several post translational modifications (PTMs) of the NF-κB have been identified and suggested to facilitate interactions with co-regulatory proteins. As these modifications have the potential to modulate the interaction of NF-κB with co-activators,

co-repressors, IκB proteins and the binding of NF-κB to heterologous transcription factors, they represent an important means of shaping NF-κB-dependent gene programs. These PTMs are also thought to be critical for the integration of non-NF-κB pathways and context-specific tailoring of the transcriptional response. PTMs of NF-κB subunits have been studied most thoroughly for p65 and have been found to be numerous and distinct in their functional outcomes [232]. Phosphorylation of RelA at Ser276 by the catalytic subunit of protein kinase A (PKAc), which is bound to cytosolic NF-κB-IκB complexes and is activated after IκB degradation, is one of the key RelA modifications [233]. This phosphorylation leads to a conformational change in RelA protein that exposes an interaction surface for transcriptional co-activator, p300/CBP [213, 234].

1.10.3 Selective DNA binding by NF-κB dimers

Similar to dimer specific transactivation, dimer specific DNA binding is likely to make a major contribution to selectivity of NF-κB response. Like other DNA binding modules, NF-κB proteins have highly conserved RHR through which they bind their cognate sites. The extensive conservation of the RHRs through evolution for each family member suggests that there are important DNA binding distinctions between family members [220]. The first study that reported the differences in DNA-binding specificity within the NF-κB family was carried out by Kunsch et al. In this study, p50, cRel and RelA homodimers were allowed to bind to a random pool of oligonucleotides to identify and select the high affinity sequences that bound to each dimer. 18 oligonucleotides that bound with high affinity to each homodimer were reported, allowing the derivation of a consensus recognition sequence for each dimer [235]. An interesting observation of this study was that p50 homodimer consensus sequence (GGGGATYCCC, Y= T or C) was substantially different from the consensus sequences reported for homodimers of RelA (GGGRNTTTCC, where R=A or G, N is any nucleotide) and cRel (NGGNN[A/T]TTCC). The differences in DNA-binding specificity between p50 homodimers versus RelA or c-Rel homodimers suggested that p50 homodimers may bind and regulate different sets of genes than RelA or c-Rel homodimers.

X-ray structures of several NF-κB homo- and heterodimers bound to different κB sites have been determined [236-240]. These structures serve to explain the rules of preferential DNA target recognition by different NF-κB dimers. The NF-κB p50 subunit

recognizes the 5'-GGGRN-3' half site, whereas RelA subunit recognizes specifically 5'-YYCC-3' half site. This specificity partly stems from the fact that both p50 and p52 monomers contact the 5'-G with a histidine side chain unique to these subunits. This histidine residue is replaced by alanine in RelA and c-Rel [241]. Although crystal structures could explain the differences between selective bindings of p50 homodimers, they could not explain the differences in specific binding of Rela and c-Rel homodimers. The c-Rel homodimer consensus appears to be more flexible than RelA consensus as it could bind a few oligonucleotide sequences that were not bound by RelA homodimers in electrophoretic mobility shift assays. In contrast, no sequences were identified that bound RelA homodimers but not c-Rel homodimers [235].

Recently several studies have attempted to decipher the molecular basis for specificity and explain how a given site may be linked to the requirement for a specific NF-κB protein. c-Rel is highly homologous to RelA; yet RelA and c-Rel appear to regulate largely distinct set of genes [242]. In mouse macrophages, only four genes are c-Rel dependent [243]. One of them is Il12b, which encodes for IL-12 p40, one of the two subunits of interleukin 12 (IL-12). Although Il12b expression is slightly reduced in RelA$^{-/-}$ macrophages, its expression is almost completely abrogated in c-Rel-deficient macrophages [244], indicating that no significant redundancy occurs at this specific gene. Smale and coworkers identified a short sequence within the RHR of c-Rel that is responsible for c-Rel requirement for Il12b induction [243]. The RHR contains a 180-amino-acid long amino-terminal domain (N-RHR) responsible for sequence specific DNA binding and a carboxy-terminal dimerization domain (C-RHR) separated by a flexible linker [245]. The N-RHR of RelA and c-Rel are highly homologous and conversely diverge from those of p50 and p52. c-Rel specific induction of IL12b was shown to depend entirely on its N-RHR and in particular on a short sequence stretch (46 amino acids) contained within the region of maximal divergence from RelA (heretofore referred to as specificity determining region, SDR). Conversely, the transcriptional activation domains (TADs) of RelA and c-Rel were largely interchangeable, thus indicating that if c-Rel- and RelA-selective co-activators that directly bind their TADs do exist, they do not critically contribute to specificity. Interestingly, when the most solvent-exposed residues in the c-Rel SDR were simultaneously changed to the corresponding RelA residues, the mutant protein retained its ability to activate IL12b expression: this

finding argues against the possibility that the c-Rel SDR acts by mediating critical protein–protein interactions with co-activators.

To understand the mechanism of selective activation of IL12b by c-Rel, DNA binding properties of wild type c-Rel homodimers, RelA homodimers and homodimers of the functional RelA-c-Rel chimera were compared. Quantitative affinity measurements showed that c-Rel homodimers are capable of binding the IL12b promoters with approximately an order of magnitude higher affinity than RelA homodimers. A key observation was that the c-Rel SDR increases the affinity of c-Rel homodimers (but not c-Rel/p50 heterodimers) not only for canonical κB sites, but also for sites that diverge from the canonical consensus. Two considerations indicate that the c-Rel SDR may affect binding to κB sites only indirectly: first, the N-RHR residues that contact both DNA bases and the sugar–phosphate backbone are conserved between RelA and c-Rel; second, only two of these residues (K100 and K111) are located within the SDR. Therefore, it may be assumed that the c-Rel SDR may promote a selective conformation (maybe a high flexibility) that endows c-Rel with the ability to recognize deviant κB sequences at high affinity [246]. The c-Rel SDR is also required for induction of Il12a in dendritic cells (DCs): remarkably, dependence of this gene on c-Rel is restricted to DCs and is not observed in murine macrophages [244, 247, 248]. If c-Rel dependence reflects exclusively its ability to bind variant κB sites contained in target genes, then it may be inferred that Il12a activation in DCs and macrophages require alternative κB sites and that the Il12a κB site(s) used in macrophages can efficiently and productively bind other NF-κB species than c-Rel homodimers. These observations support the idea that even relatively small differences in the affinity of the various NF-κB species for a specific κB site may be biologically relevant [249]. To understand the effect of nucleotide variations within the binding sites, Udalova *et al*. developed a principal coordinate model that allowed the prediction of the effects of DNA variations within genomic binding sites on DNA-protein interactions with higher accuracy than the traditional profile models [250].

An additional effect of κB site variability is to impart alternative conformations to the bound NF-κB dimer. The X-Ray structures of various NF-κB dimers bound to different κB sites reveal significantly distinct conformations. Moreover, replacement of native κB DNA with other physiological high affinity κB DNA sequence affects NF-κB driven

transcription significantly [251, 252]. These observations suggest that the conformation and flexibility of the κB DNA sequence play a critical role in the recognition of the NF-κB dimers. Baltimore and coworkers have shown that a single base pair change within a κB site is sufficient to alter gene regulation. This mutation does not alter the binding affinity of NF-κB. However, NF-κB binding to mutant site fails to recruit a co-activator protein [253]. These results suggest that the simple occupation of the κB site by NF-κB is not sufficient to drive transcription.

NF-κB dimers are very flexible due to the presence of a short linker connecting the N-RHR to the C-RHR [238, 245]: this linker allows the N-RHR to rotate and translate in order to optimize the alignment with the DNA sequence of the amino acids that make direct contacts with the bases exposed in the major groove. Any nucleotide variation in the κB site implies that NF-κB must bend in an alternative fashion to maximize the contacts with DNA and preserve a high affinity for the site. Similar to the effects observed for other TFs [254], conformational effects induced by alternative recognition sites eventually change the ability of the DNA-bound factor to interact with transcriptional co-regulators, thus causing differences in co-activator requirements at different promoters.

1.10.4 Why to study binding specificity of NF-κB

Studies from ChIP-chip experiments have shown that the *in vitro* affinity of transcription factors binding to DNA sequences often reflect the relative occupancy of these sequences *in vivo* [255, 256]. This observation suggests that, for a given transcription factor, the knowledge of its sequence recognition profile measured *in vitro,* can be highly instructive in characterizing binding sites in genome. Apart from this, there are several other reasons that make it unavoidable to study binding specificity of NF-κB dimers. First, NF-κB binding site is highly degenerate, and several κB sites obviously deviate from the consensus sequence and yet bind some NF-κB species with high affinity. Second, the number of potential κB sites in a genome is estimated to be quite large [246] and it is important to understand why only few of them have a regulatory role. Third, considering the fact that a single base pair change can have a profound effect on gene regulation [249, 253], it becomes imperative to understand the effect of regulatory single nucleotide polymorphisms (SNPs) on gene regulation. Regulatory SNP is the single

nucleotide change taking place within a transcription factor binding site. Such SNPs may either increase the affinity of binding or may abrogate it.

1.10.5 NF-κB and chromatin

Transcription factors of NF-κB family are essential regulators of the inflammatory and immune responses. The main switch in NF-κB activation is cytoplasmic and leads to the release of NF-κB dimers from IκB molecules and their subsequent nuclear translocation. Once in the nucleus, NF-κB dimers must gain access to their cognate sites in target genes. Although some NF-κB binding sites are found in a constitutively accessible state, many others are occluded by nucleosomes. Binding to such occluded sites would need additional regulatory mechanisms at the level of chromatin. Thus NF-κB genes are not only regulated at cytoplasmic level but also at the chromatin level. Regulated recruitment of NF-κB to chromatin generates kinetic complexity in NF-κB dependent gene induction and wires NF-κB regulated gene activity to simultaneously activated pathways and transcription factors [257]. Saccani et al. used chromatin immune precipitation to study the kinetics of recruitment of NF-κB to its target genes. The authors observed that in lipopolysachride stimulated macrophages, recruitment of NF-κB to its target genes occurs in two temporally distinct phases [258]. Some genes (fast genes) recruit NF-κB shortly after its nuclear entry while as others (slow genes) recruit it tens of minutes to hours later, despite the presence of high affinity κB sites in their promoters. The different behavior of the two classes of genes was attributed to the different chromatin configuration at their promoters. Before stimulation, fast genes display a chromatin landscape typical of genes poised for immediate activation, including high levels of H3 and H4 acetylation and H3K4me3. These promoters are also constitutively accessible to nucleases, thus indicating an overall open and accessible organization [259]. Conversely the slow genes showed low to undetectable acetylation levels that were progressively increased in response to stimulation [258]. On the basis of this data, Natoli and coworkers proposed a classification of NF-κB target genes according to which fast genes are those with Constitutive and Immediate Accessibility (CIA) and slow genes are those with Regulated and Late accessibility [258]. Regulated and late accessibility suggests that these genes have an additional level of regulation exerted by the chromatin structure. So, prior to the binding of NF-κB; chromatin needs to be rearranged in a way

that will allow NF-κB to bind its cognate site. This was experimentally shown by Smale's group while studying the mouse IL12b gene, a canonical NF-κB target that specifically requires the cRel subunit for transcriptional induction after LPS treatment of macrophages. The authors used high resolution micrococal nuclease analysis to show that the transcription factor binding sites required for IL12b induction in response to LPS stimulation of mouse macrophages are covered by highly positioned nucleosome that undergoes selective remodeling upon treatment [244, 260]. Nucleosome remodeling was found to be completely independent of cRel, indicating that it could be separated from transcriptional activation. An obvious conclusion from this data is that remodeling of the nucleosome precedes cRel recruitment. Another study that demonstrated the impact of nucleosomal organization on the NF-κB response was carried out by Ramirez-Carrozzi *et al.* The authors used RNA interference to demonstrate that in lipopolysaccharide stimulated macrophages, the catalytic BRG1/BRM subunits of the SWI/SNF class of ATP-dependent nucleosome remodeling complexes are consistently required for the activation of secondary response genes and primary response genes induced with delayed kinetics, but not for rapidly induced primary response genes. Although, both these studies confirmed that remodeling precedes the NF-κB binding to make the promoters accessible to NF-κB, it is still not clear how the remodelers are targeted to the particular nucleosome. It becomes imperative to understand how remodeling complexes are recruited and targeted with a high degree of specificity to a single nucleosome. There has to be some sequence specific factors, which should be able to bind to their cognate sites in nucleosomal templates. These factors, in turn should recruit either remodelers or the histone modifying enzymes to the particular nucleosome. Could NF-κB itself be the factor that's able to bind the nucleosomal κB sites and exert its function?

1.10.6 Binding of NF-κB to nucleosomes

To understand whether NF-κB can bind nucleosomal κB sites, it is imperative to understand how NF-κB binds to these cognate sites in absence of nucleosomes. Five NF-κB/DNA crystal structures have been resolved [237-240, 261]. These three dimensional structures revealed some unique features. The whole Rel Homology Domain (RHD) is involved in contacting the κB site and resembles a butterfly with the 'wings' connected to a cylindrical body of DNA. Each dimer subunit contains two sets of β-sheet

immunoglobulin folds that form an N-terminal domain (NTD) that contacts DNA both base specifically and bacκbone non-specifically, and a C-terminal domain (CTD) that mediates dimerization and non-specific DNA contacts. Unlike most transcription factors which use alpha helices to bind DNA, the Rel/NF-κB proteins use ten flexible loops extending from the secondary structure of these immunoglobulin folds to mediate DNA contacts [237]. Although the DNA molecule is not completely encircled by the dimer, too little space is left in the area delimited by the two N-terminal domains to accommodate the surface of the nucleosome [257]. Thus, it seems quite predictable that if the κB site is wrapped inside the nucleosome, then NF-κB can not bind it because of the steric hindrances.

1.10.7 Linker histones and transcription

The compaction of chromatin by the linker histone in general has a global and repressive impact on transcription. Binding of globular domain of linker histone (H1) at the entry-exit position of the nucleosome allows its carboxy-terminal tail to interact with both the incoming and outgoing linker DNA helices. This way of interaction brings the two helices close to each other and leads to the formation of a so-called 'stem' structure [262-264]. As the DNA termini of nucleosomes have been shown to be accessible to TFs due to spontaneous wrapping and unwrapping, H1 binding would modulate this process and prevent the binding of TFs. Another possibility in which H1 could effect transcription is by occupying the binding sites of those transcription factors whose binding sites are located in the linker region. This suggests that TF will have to compete with H1 to bind their cognate sites. Several studies have provided the evidence that in certain cases linker histone can be directly displaced by transcription factor [79]. Lee et al. have shown that in MMTV promoter, hormone activation of glucocorticoid receptor (GR) binding leads to displacement of phophorylated H1 molecule, which in turn allows the binding of the NF1 and subsequent assembly of the transcription apparatus [265, 266].

1.11 Techniques used

1.11.1 Electrophoretic mobility shift assay (EMSA)

EMSA is a rapid and sensitive technique traditionaly used to study the binding of transcription factor to DNA [267, 268]. The basic concept is that a piece of DNA will migrate through a gel more slowly if it is bound to a protein, such as a transcription factor. A difference, or "shift," in the rate of migration in the presence and absence of transcription factor is thus taken as evidence of binding. This method is mostly used for qualitative purposes but under appropriate conditions can also provide quantitative information about the binding stoichiometries, affinities and kinetics [268, 269]. In a classical assay, the proteins are incubated with radioactively labeled DNA. The resulting mixtures are subjected to electrophoresis under native conditions through polyacrylamide or agarose gel. After electrophoresis, the distribution of species containing nucleic acid is determined, usually by autoradiography of ^{32}P-labeled nucleic acid. Although this technique is simple, inexpensive and robust, it has certain limitations also. The DNA-protein complexes may dissociate during electrophoresis leading to underestimation of the binding constants. Another major limitation of EMSA is that the electrophoretic mobility of a DNA-protein complex depends on many factors other than the size of the protein. Thus, an observed mobility shift does not provide a straightforward measure of the molecular weights or identities of proteins that are present in the complex [269]

1.11.2 DNase footprinting

DNase footprinting is an *in vitro* technique used to examine the binding of proteins to specific regions of DNA [270]. This technique cleverly exploits the fact that when a transcription factor is bound to DNA with a certain affinity, the DNA is protected from degradation by nucleases **(Figure 16A)**. The transcription factor of interest thus leaves its "footprint" on the DNA. A typical footprinting experiment involves radioactive labeling of the DNA containing one or more transcription factor binding sites. This fragment is radioactively labeled on one end and then incubated *in vitro* both with and without the transcription factor of interest. Next, the DNA is treated with DNaseI, which digests only unprotected DNA. Finally, the DNA products resulting from the digestion are separated

on a polyacrylamide gel. Apart from examining where a TF might bind on a DNA sequence, DNase footprinting can also be used to determine the affinity of the TF-DNA interaction [271]. Although this technique gives the information about the specificity of the TF-DNA interaction, it does not resolve the binding site. Rather, it gives the information about the binding region.

1.11.3 Hydroxyl radical footprinting

Hydroxyl radical footprinting is another *in vitro* technique widely used to study the structure of DNA [272], RNA [273] and DNA-protein complexes [274]. The hydroxyl radicals cleave the DNA strands by removing a hydrogen atom from a deoxyribose sugar in the DNA backbone. The lack of base specificity and high reactivity of the hydroxyl radical makes it an efficient probe for high resolution footprinting of DNA-protein complexes **(Figure 16B)**. This technique is very cost effective as it uses commonly available lab equipment and inexpensive reagents. Typically, hydroxyl radicals are generated by Fenton reaction in which $[Fe(II)(EDTA)]^{2-}$ reacts with hydrogen peroxide (H_2O_2) to generate hydroxyl radical ($^{\bullet}OH$) and $[Fe(II)(EDTA)]^{1-}$ as shown below [275, 276].

$$\mathbf{[Fe(II)(EDTA)]^{2-} + H_2O_2 \rightarrow [Fe(II)(EDTA)]^{1-} + OH^- + {}^{\bullet}OH}$$

Sodium ascorbate is added to the reaction mixture to regenerate $[Fe(II)(EDTA)]^{2-}$ from $[Fe(II)(EDTA)]^{1-}$. This technique is based on the same general principle as that of the DNase footprinting i.e the binding of the protein to DNA protects the region of binding from hydroxyl radical cleavage. The hydroxyl radical footprinting experiment can be essentially performed in the same way as that of the DNase footprinting.

1.11.4 The UV laser footprinting

The technique is based on irradiation of free and protein bound DNA and mapping the induced photolesions at one base pair resolution. Cyclobutane pyrimidine dimmers and 8-oxoG are generated by UV laser irradiation and are quantitatively mapped by treatment with Fpg glycosylase (formamidopyrimidine [fapy]-DNA glycosylase or 8-

oxoG glycosylase and AP-lyase) and T4 endo V (pyrimidine dimmers glycosylase and AP-lyase) prior sequencing gel electrophoresis analysis [277-279].

1.11.5 UV laser footprinting of NF-κB-DNA complexes

1.11.5.1 Background

UV footprinting technique was developed by Becker and Wang in 1984 to probe the sequence specific protein-DNA interaction *in vivo* [280]. The UV laser footprinting is based on change in the UV laser induced nucleotide photoreactivity upon protein binding. The photoreactivity of the nucleotide bases is very sensitive to their conformation. Upon protein binding, the conformation of the nucleotide bases in the DNA changes. So, the free DNA and protein bound DNA will react differently to the UV laser. Such differences can be probed by various agents like Fpg which recognizes the 8-OxoG and cleaves the DNA wherever it finds 8-OxoG.

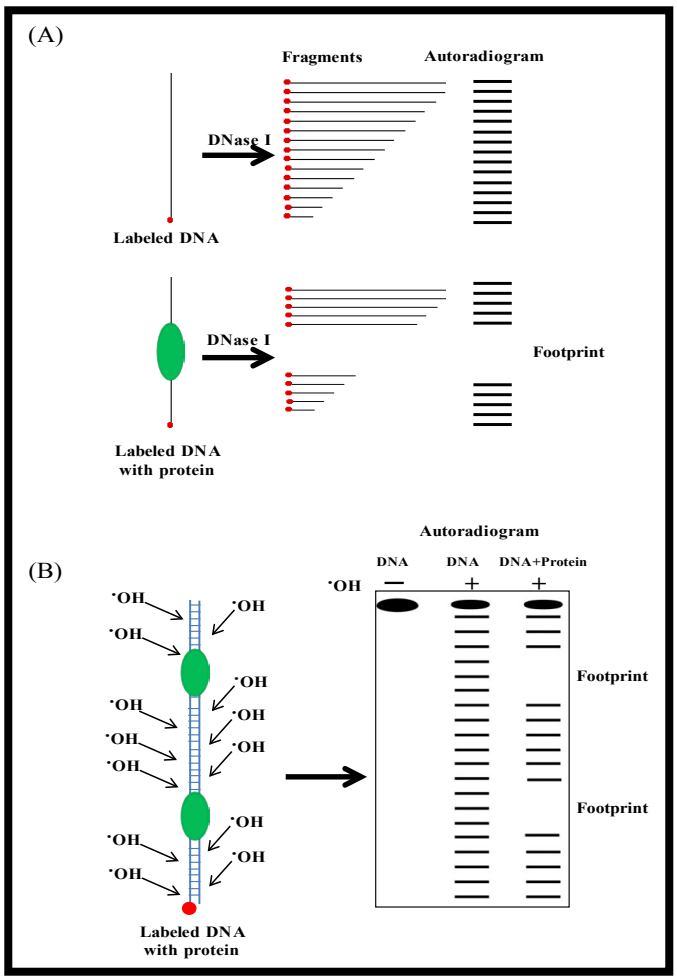

Figure 16: **(A) DNaseI footprinting, (B) Hydroxyl footprinting**

1.11.5.2 Theoretical considerations

Conventional (low-intensity) light at ~260 nm induces DNA pyrimidine dimmers as a result of monophotonic absorption through excited triplet-state [281]. In contrast, at high intensity ($\geq 10^6$ W/cm^2) provided by nanosecond laser pulses, the rate of excitation exceeds the inverse of the lifetime of the excited triplet state **(Figure 17)**. Thus, triplet-state excited molecules become substrates for the absorption of a second photon, leading to nucleobase ionization and selective generation of guanine radical cations due to charge transport phenomena [277, 282]. The latter are rapidly transformed through water addition into the stable oxidative lesion 8-oxoG.

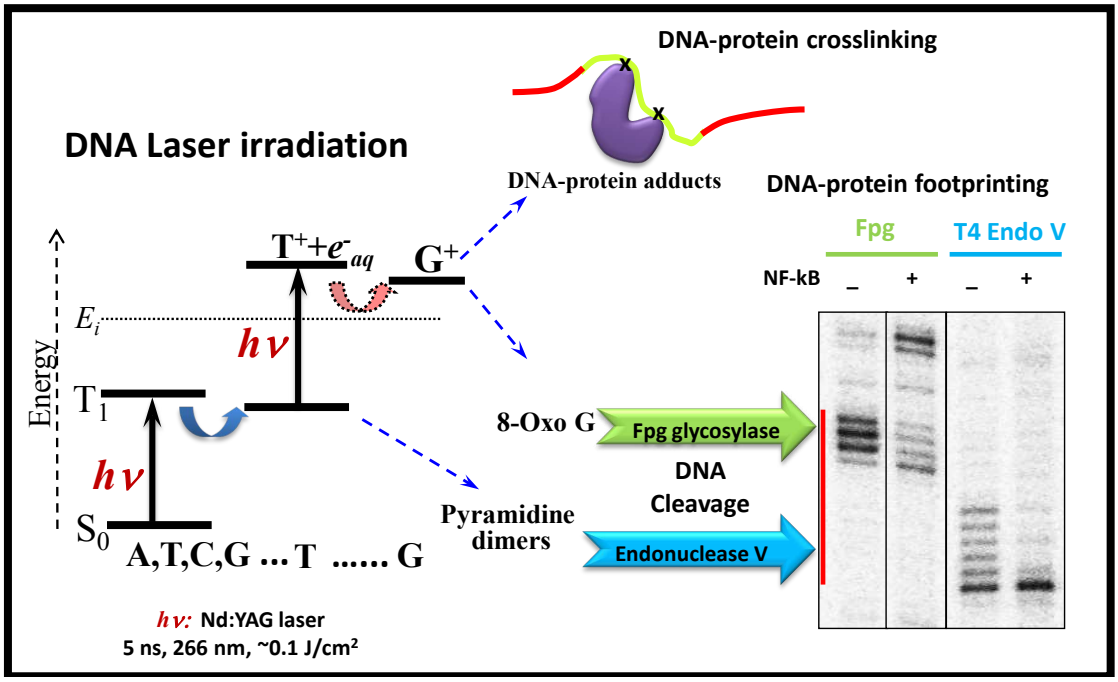

Figure 17: **Simplified principal of UV laser footprinting.** Upon UV laser irradiation nucleotide bases are initially excited via S1 to their lowest triplet state T1 and then they are ionized upon absorption of another photon giving rise to chemically reactive transient radical cation. At high energy, 8-OxoG is the major product formed by biphotonic mechanism while as pyrimidine dimers are mostly formed at low energy by monophotonic mechanism. Each of these lesions is identified and cleaved by Fpg and T4 Endonuclease V respecitively and products analyzed on denaturing gel.

Simultaneously pyrimidine dimers are also generated, although they are mono-photonic lesions, i.e. their quantum yield decrease with the increase of the intensity of the laser pulses (upon increase of the intensity of the pulses a "bleaching" of the triplet state is achieved) [282, 283]. Since DNA laser-induced chemistry involves energy and charge migration, the yield of formation of both mono- and bi- photonic lesions (pyrimidine dimmers and 8-oxoG respectively) are strongly DNA-sequence and DNA-conformation dependent phenomena [282, 283]. Thus, change in conformation and contacts upon protein binding might result in drastic change of photoreactivity of DNA (i.e. in yields of specific photolesions), which is used for UV laser footprinting **(Figure 17)**.

1.11.6 Advantages of the UV laser footprinting technique

The UV laser footrpinting technique has several advantages over conventional footprinting, which is based on physical accessibility of either chemicals or enzymes to DNA. One important advantage is the high-precision in determining specific binding constants by measuring the quantum yield of particular DNA lesions versus the protein concentration. Determination of specific binding constants by means of EMSA or similar low resolution techniques are risky due to interference with unavoidable non-specific binding. By comparing the high-resolution mapping of local photoreactivity change (laser footprinting) with EMSA, correct conclusions on the binding can be made.

RESULTS

MANUSCRIPT: 1

High Resolution study of specificity and dynamics of DNA-NF-κB interactions

1 Objectives:

NF-κB is a family of pleiotropic transcription factors regulating diverse biological phenomena, including apoptosis, cell survival, cell growth, cell division, innate immunity, cellular differentiation. Among the various mechanisms that have been proposed to regulate the NF-κB response, dimer specific DNA binding is likely to make a major contribution to selectivity of NF-κB response. DNA-binding studies [235, 250, 284] and various NF-κB-DNA crystal structures [237, 261, 285] have led to a basic partitioning of NF-κB family members: p50 and p52 recognize a 5-bp 5'-GGGRN-3' half site, whereas c-Rel, RelA and RelB recognizes a 4-bp 5'GGRR-3' half site (where R is A or G and N is any of the four bases). These studies led to a consensus κB site 5'GGGRN(Y)YYCC-3' [286]. However, several studies have reported additional dimer specific DNA binding preferences [287] and non-canonical κB sites [243, 257]. In this study, we attempted to understand the plasticity of DNA-binding of four NF-κB dimers by measuring the affinity and specificity of these dimers for two well known κB sites and five non-traditional κB sites.

Our objectives were:

1. To develop UV laser footprinting approach to study the affinity and specificity of NF-κB dimers at 1-bp resolution
2. To develop a novel approach in which we combined the UV laser footprinting with the stopped flow for studying the kinetics of such interaction at 1-bp spatial and millisecond temporal resolution.

2 Materials and Methods

2.1 Basis of sequence selection for this study

We have used a total of 7 different sequences for this analysis. For positive control, we used two well known canonical κB sequences, a pseudo-symmetric MHC-H2 [236, 240] and non-symmetric HIV kB sites [288]. For both these sites crystal structures with the NF-kB protein have been solved [240, 288]. Other five sequences were received from our collaborator Ionis Ragousis who used high throughput techniques like PBM and EMSA-Seq to study the binding profiles of different NF-kB dimers [289]. The data from these high throughput methods showed that NF-kB transcription factors can recognize sequences which are different from the so called canonical consensus sequence. On the basis of the data achieved from PBM and EMSA-Seq the binding sequences were categorized into canonical binders and non canonical binders owing to their similarity (MATCH score) to a reference binding model (either an established position weight matrix (PWM) or an alternative constructed from quantitative data were used as reference model). Two sets of MATCH scores for 11-mer sequences from microarray and EMSA-Seq datasets were created, one based on the reference binding model and another on the alternative formed using the 300 highest affinity binders from our EMSA-Seq data. Both are highly comparable, with 95% similarity between the two sets (Pearson correlation test). Sequences with MATCH score similarity to NF-kB PWM greater than 0.75 were termed as canonical NF-kB binders while as those with less than 0.75 MATCH score were called as non-canonical binders and they fall outside the known NF-kB consensus. Theoretically, a MATCH score of 1.0 corresponds to the highest degree of similarity possible whilst 0 corresponds to the lowest. Although these high throughput techniques were able to determine the relative binding constants for canonical as well as non canonical kB sites, they could not tell anything about the specificity of the binding. The five sequences that we studied are representative sequences from the data obtained from the high throughput techniques. The main purpose of studying these sequences was to validate if these sequences bind specifically to NF-kB.

2.2 Probe labeling

HPLC purified oligonucleotides containing NF-κB binding sites were purchased from MWG. Typically, 20 pmol from either the top or the bottom strand were 5'end-labeled by T4 polynucleotide kinase with [γ-^{32}P] ATP. The labeled strand was annealed with four-fold excess of its complementary strand and the DNA was treated by Fpg DNA *N*-glycosylase (a kind gift from Serge Boiteux, Commissariat à l'Energie Atomique-Fontenay aux Roses, France) to remove preexisting oxidative guanine lesions [278, 283]. DNA was purified by denaturing gel electrophoresis and reannealed. Duplex formation was checked by native gel electrophoresis. Under the conditions used, 100% of duplexes were obtained.

2.3 Protein expression and purification

Expression constructs for the three human NF-κB dimers RelA/RelA, RelA/p50 and RelA/p52 used in this study were provide by Udalova and were purified as established by Udalova and co-workers [290]. Briefly, His-tagged recombinant proteins in pET vectors were expressed in BL21 (DE3) *Escherichia coli* (Merck). Constructs contained the RHR of each subunit: RelA (1-307), p50 (7-356), p52 (4-332). Proteins were over-expressed through induction with 0.2 mM Isopropyl β-D-1-thiogalactopyranoside (IPTG) at 30 ºC for 5 h. Pellets of cells were harvested in "Ni-NTA" binding buffer with added EDTA-free Protease Inhibitor (Roche), pulse-sonicated for 2 min. The debris was removed via centrifugation at 16,000*g*. A two-step purification procedure was then employed, first with the "Ni-NTA His-Bind Resin" system (Merck 70666) and then a subsequent purification based on DNA-affinity isolation of functional, DNA-binding protein. Ni-NTA purification was carried according to manufacturer's guidelines. For DNA-affinity isolation, a sample derived from 250 ml bacterial culture was processed with 0.128 μM oligonucleotides TNF promoter (biotinylated) and TNF-promoter complementary. Prior to use, oligonucleotides were annealed via incubation in NEB Buffer 3 at 94°C for 1 min, followed by 69 cycles of 1 min incubation with stepwise decrease of 1°C. 712.5 μl of pre-annealed oligo mixture was conjugated with Streptavidina-garose (Sigma) before once-purified material from the preceding step was added to it. NF-kB (p50) was prepared as described in [291]

2.4 DNA-NF-κB binding assays

2.4.1 Electrophoretic Mobility Shift Assay (EMSA)

The binding reactions between transcription factors and DNA were carried out in 1X binding buffer (10mM Tris, pH 7.4, 75 mM NaCl, 1mM EDTA, 1mM DTT, 200µg/ml bovine serum albumin, 5% Glycerol and 0.005% NP40). In a 20 µl reaction, ~10 fmol of labeled DNA were mixed with the indicated amounts of NF-κB (1.6- or 2- fold serial dilution) and the $1/4^{th}$ of the samples were analyzed by electrophoretic mobility shift assay (EMSA) and $3/4^{th}$ of the sample was irradiated and analyzed by UV laser foot-printing as described below. The EMSA was done in a 5% acrylamide gel at room temperature in 0.25X Tris-borate-EDTA (TBE) buffer.

2.4.2 UV Laser footprinting

The NF-κB-DNA complexes along with the free DNA controls were exposed to single high intensity UV pulse (wavelength = 266 nm, pulse duration = 5 ns, fluence = 0.1 J/cm^2) provided by the fourth harmonic generation of a nanosecond Nd:YAG laser (Surelite 1, Continuum USA) The DNA was then supplemented with 0.1 % SDS, purified by phenol-chloroform extraction, ethanol precipitated, dissolved in resuspension buffer (10mM Tris, pH 7.4, 30mM NaCl, 1mM EDTA, 1mM DTT, 200µg/ml BSA, 0.005% NP40) and digested to completeness by Fpg protein and T4 endonuclease V (Trevigen) for 30 minutes at 30°C. Following lyophilization, DNA was re-suspended in formamide loading buffer, and run on 13% polyacrylamide sequencing gel. Dried gels were exposed overnight on a phosphorimager screen, and the images were readout and quantified by using Fuji 5100 Phosphorimege scanner and Multi Gauge 3.0 software (Fujifilm).

2.4.3 DNase I footprinting

The binding reaction was carried out in the same way as that for UV laser foot-printing except that the binding reaction for DNase I was supplemented with 2.5 mM $MgCl_2$ and the products were digested by 0.15 units of DNase I for 2.5 minute at room temperature. Reactions were stopped with 20 mM EDTA, 0.1% SDS, and DNA was extracted with phenol-chloroform and ethanol precipitated prior to analysis on 13%

sequencing gel. Note that our control experiments did not show detectable change of binding constants by the addition of 2.5 mM $MgCl_2$ (1.5 mM above the 1 mM EDTA).

2.5 Determination of the apparent K_d

From EMSA experiments

Integrated radioactivity in the non-shifted DNA band (*y*) was normalized to the total (non-shifted plus total shifted) radioactivity loaded and plotted versus protein concentration represented by x (Figure 1B). Experimental points were connected by smooth curve by least square approximation. The curve fitting was done by using non-linear curve fitting function logistic (OriginLab Corporation). This function was chosen as it provided a good fit of our experimental data as well as for its mathematical simplicity.

$$y = A_2 + (A_1-A_2)/(1 + (x/x_0)^p) \qquad \textbf{(I)}$$

Where, A_1, A_2, x and p are variables constants. A_1 is initial value (left horizontal asymptote), A_2 is final values (right horizontal asymptote), x_o is the point of inflection, and p represents the parameter that affects the slope of the area about the inflection point. For EMSA, A_1 is fixed to 1 and A_2 is fixed to zero. Hence the equation (I) can be written as

$$y = 1/(1 + (x/x_0)^p) \qquad \textbf{(II)}$$

Apparent K_d was determined (manually from the fitted curves) as the concentration of the protein corresponding to ½ (half) of the amplitude change [219].

From laser footprinting experiments

In case of the UV laser footprints, K_d were determined from both bi-photonic as well as mono-photonic lesions. The intensity corresponding to each of the guanine (8-oxoG) and pyrymidine (cyclobutane pyrimidine dimers) cleavage bands within the NF-κB binding site were quantified by integration and normalized to either the total radioactivity loaded or to a reference guanine cleavage band (located outside of the recognition site). The curves representing normalized cleavage band intensities versus protein concentration were plotted (Figure 1 C and D). The curve fitting was done as mentioned

above (Equation I) and K_d values were determined manually as protein concentrations corresponding to the ½ of the amplitude change [219]. The final K_d is the average of the K_d values obtained from mono and bi-photonic lesions. For the sake of simplicity, the final K_d is converted to affinity (Affinity=1/K_d) and is plotted as bar graph for each NF-κB dimer as shown in (Figure 1E).

2.6 Results

2.6.1 Binding affinity of NF-κB p50 homodimer for physiologically known canonical κB sites

We have measured the DNA binding affinity of p50 homodimers using electrophoretic mobility shift assay (EMSA) and UV laser footprinting for two physiologically known κB sites, MHC-H2 κB site and HIV κB site. The 37 mer double stranded oligo containing centrally positioned κB site (either MHC-H2 κB site or HIV κB site) was used as a probe. EMSA shows that the p50 homodimer forms stable complexes with both the canonical κB sites, suggesting that the p50 homodimer is binding to these sites very efficiently **(Figure 1A, upper panel)**. To determine if the binding is specific, we also analyzed the same reactions by UV laser footprinting **(Figure 1A, Lower panel)**. The results show that p50 homodimers not only bind with high affinity **(Figure 1B)** but also with high specificity to these κB sites as is evident by a very specific pattern of footprint. The K_d values were determined both, from EMSA as well as from UV laser footprinting and were quite comparable for this dimer **(Table1)**. We also observed that the UV laser footprints of these canonical sites differ from each other **(compare lane 1 and 9 or 10 and 18 with 19 and 27)**. p50 binding on MHC-H2 leads to the increase in the intensity of the band corresponding to internal G of this κB site while as the same G in HIV site is unaffected. This suggests that p50 homodimers interact with these sites differently. Our results also show that p50 interacts and uses both the half site in these κB sites. The two half sites in HIV κB site are quite different (**GGGGACTTTCC),** one side is rich in purines and another side rich in pyramidines. p50 does not show preference for a particular sequence and both the half sites were footprinted **(Figure 1A, lower panel)**. The footprint shows that p50 homodimer is quite flexible and contributes less for specificity.

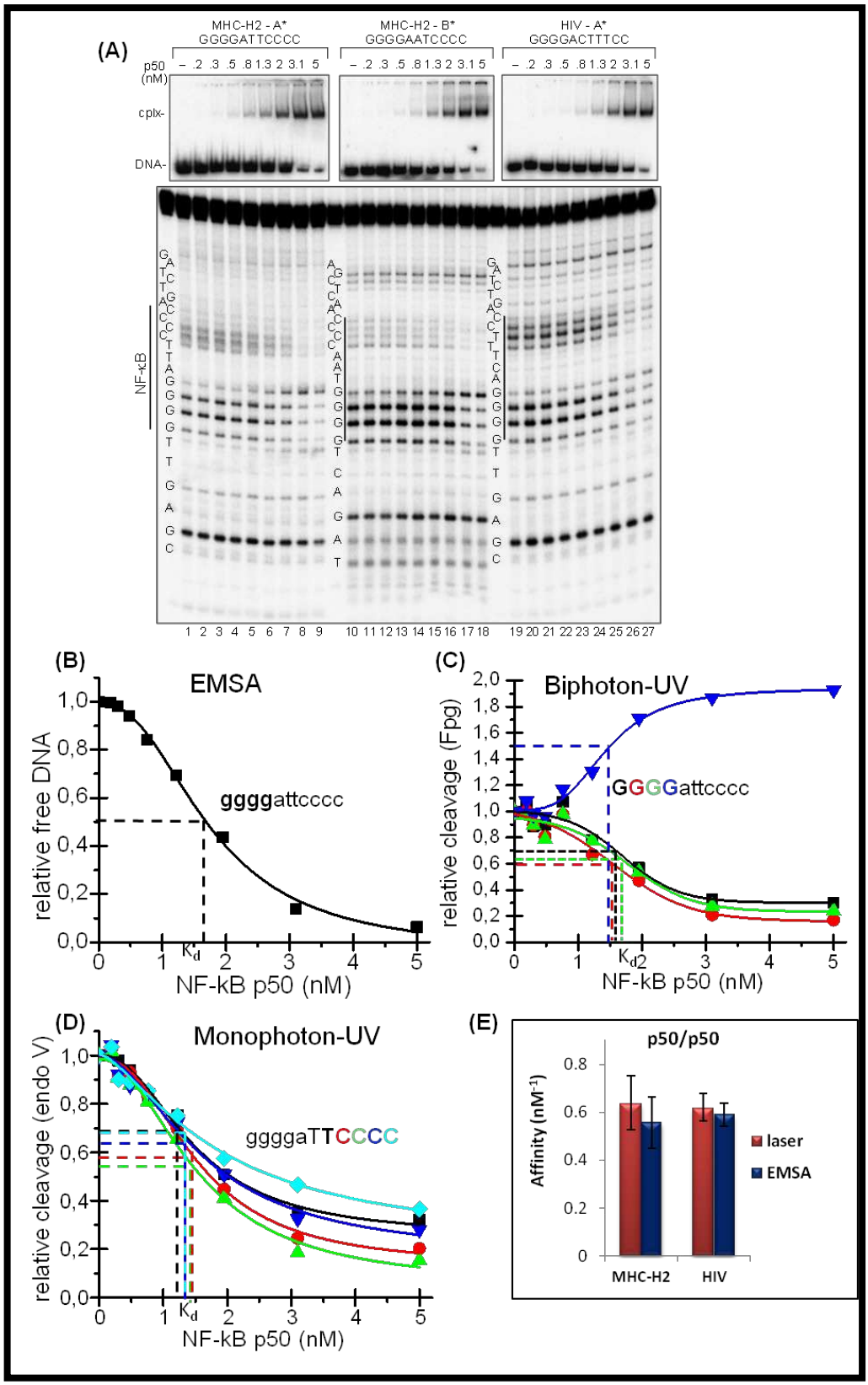

Figure1: EMSA and UV-laser footprinting of p50-homodimer complexed with either MHC-H2 or HIV κB recognition sequences. 37-mer double-stranded oligonucleotide (~0.5 nM) containing either the MHC H-2 or HIV DNA recognition sequence was allowed to interact with increasing concentrations of p50 homodimer (either the top (MHC-H2-A*) or the bottom strand of MHC-H2 (MHC-H2-B*) or the top strand of HIV (HIV-A*) were labeled with ^{32}P). An aliquot of the reaction mixtures was used to carry out EMSA

on a native 5% polyacrylamide gel (upper panels, the positions of free DNA (DNA) and p50-DNA complexes (cplx) are indicated). The remaining reaction mixture was irradiated with a single high intensity UV laser pulse (E_{pulse} = 0.1J/cm^2). Then the different samples were treated with both Fpg and T4 endo V and the digestion products, after purification, were run on a 13 % polyacrylamide sequencing gel (lower panel). The recognition NF-κB sequences are indicated with vertical lines. **(B)** Quantification of the EMSA corresponding to MHC-H2-A*. **(C)** Quantification of the biphotonic lesions from MHC-H2-A* denaturing gel. **(D)** Quantification of the Mono-photonic lesions from MHC-H2-A* denaturing gel. **(E)** Affinity (=1/K_d) of p50 homodimer determined from EMSA and UV laser footprinting for two canonical κB sites.
N.B. Note the change in photo-reactivity pattern for both strands A and B of MHC H-2; in this case GGGG changes from a symmetric (G**GG**G) to an asymmetric (ggg**g**) pattern upon protein binding ("inversion"): compare lane 1 with lane 9, and lane 10 with lane 18). K_d values were determined from EMSA as well as from the UV laser footprinting.

2.6.2 Binding affinity of RelA-RelA, RelA-p50, RelA-p52 for MHC-H2 κB binding site

In this experiment we wanted to see how three different NF-κB dimers will interact with a high affinity κB site. We incubated the NF-κB dimers with a 37 mer double stranded oligos containing centrally positioned MHC-H2 κB site, either top strand **(Figure 2A)** or the bottom strand **(Figure 2B)** was labeled with ^{32}P. We tested the stability of the complexes by EMSA and the binding constants were determined from both EMSA and UV laser footprinting **(Table1)**. Our results show that RelA (or p65) homodimers form relatively less stable complexes compared to RelA-p50 and RelA-p52 dimers as evidenced by the presence of smear in EMSA for RelA homodimer. This suggests that the complex is dissociated during the electrophoresis. However, the binding of RelA homodimer was very specific as a clear footprint could be seen in UV laser footprinting. RelA-p50 and RelA-p52 formed quite stable complexes as we did not observe any dissociation in EMSA. We determined the Kds for each of these dimers from EMSA as well as from UV laser footprinting. We observed that there was a big difference in K_d values determined from EMSA and UV laser footprinting for RelA homodimers **(Table1)**. However, a clear and specific footprint was observed in UV laser footprinting. This suggests that K_d values determined from EMSA could not be reliable. A close look at the UV laser footprint shows that each of these dimers has a characteristic (signature) footprint. It is quite possible to identify the dimer from its signature. The different footprints or signatures also suggest that these three dimers interact differently with MHC-H2 κB site. We again observed that the dimers are interacting with the nucleotide bases in both the half sites.

Name	NF-kB Dimer → / Sequence ↓	p50/p50		RelA/RelA		RelA/p50		RelA/p52	
		K_d_EMSA(nM)	K_d_Laser(nM)	K_d_EMSA(nM)	K_d_Laser(nM)	K_d_EMSA(nM)	K_d_Laser(nM)	K_d_EMSA(nM)	K_d_Laser(nM)
MHC-H2	GGGGATTCCCC	1.8±0.35	1.58 ±0.3	15.9±2*	1.46±0.25	3.8±1.1	3.45±0.45	2.4±0.5	1.61±0.25
HIV	GGGGACTTTCC	1.7± 0.14	1.63 ±0.17	14.5±0.7*	1.36±0.25	2.9±0.4	1.8±0.3	2.1±0.3	1.3±0.2
NF-κB1	GGGGACACCCC	1.8±0.2	1.7 ±0.15	16.2±2*	>60, NB	4.6±0.5	6.7±0.65**	1.3±0.1	1.34±0.15
NF-κB2	CAGATCCCCCT	2.63±0.2	2.45 ±0.24	15.2±2.5*	>60, NB	7.1±0.9	10.5±2**	1.75±0.15	2±0.35
NF-κB3	CGGAATTTCCT	2.9±0.6	4.5 ±1.5	4.4±1*	3.25±0.6	4±0.6	4.6±0.5	1.7±0.2	1.7±0.3
NF-κB4	AGGGGAAGTTA	4.1±0.22	3.6 ±0.25	29±2.5*	>60, NB	23±3	26±5**	18±3	20±2.5**
NF-κB5	CTGGGGATTTA	6.3±0.3	5.96 ±0.25	26±2*	>60, NB	17±1.5	16±3.6**	14±1.5	13.8±1.5**

Table1: Dissociation constants (K_{ds}) determined by EMSA and UV laser footprinting. (*) represents low stability under native gel electrophoresis, (**) represents that binding specificity is low, NB represents no binding

Comparisons of the affinities (1/Kd) of the dimers shows that EMSA based affinities are often misleading **(Figure 2C)**. By looking at the graph, one would conclude that RelA homdimer does not bind to this site. However, this is not the case as UV laser footprint was observed for this dimer and affinity also turned out to be high **(Figure 2C)**. RelA-p50 hetero-dimer displayed lower affinity for this site compared to RelA homo-dimer and RelA-p52 hetero-dimer.

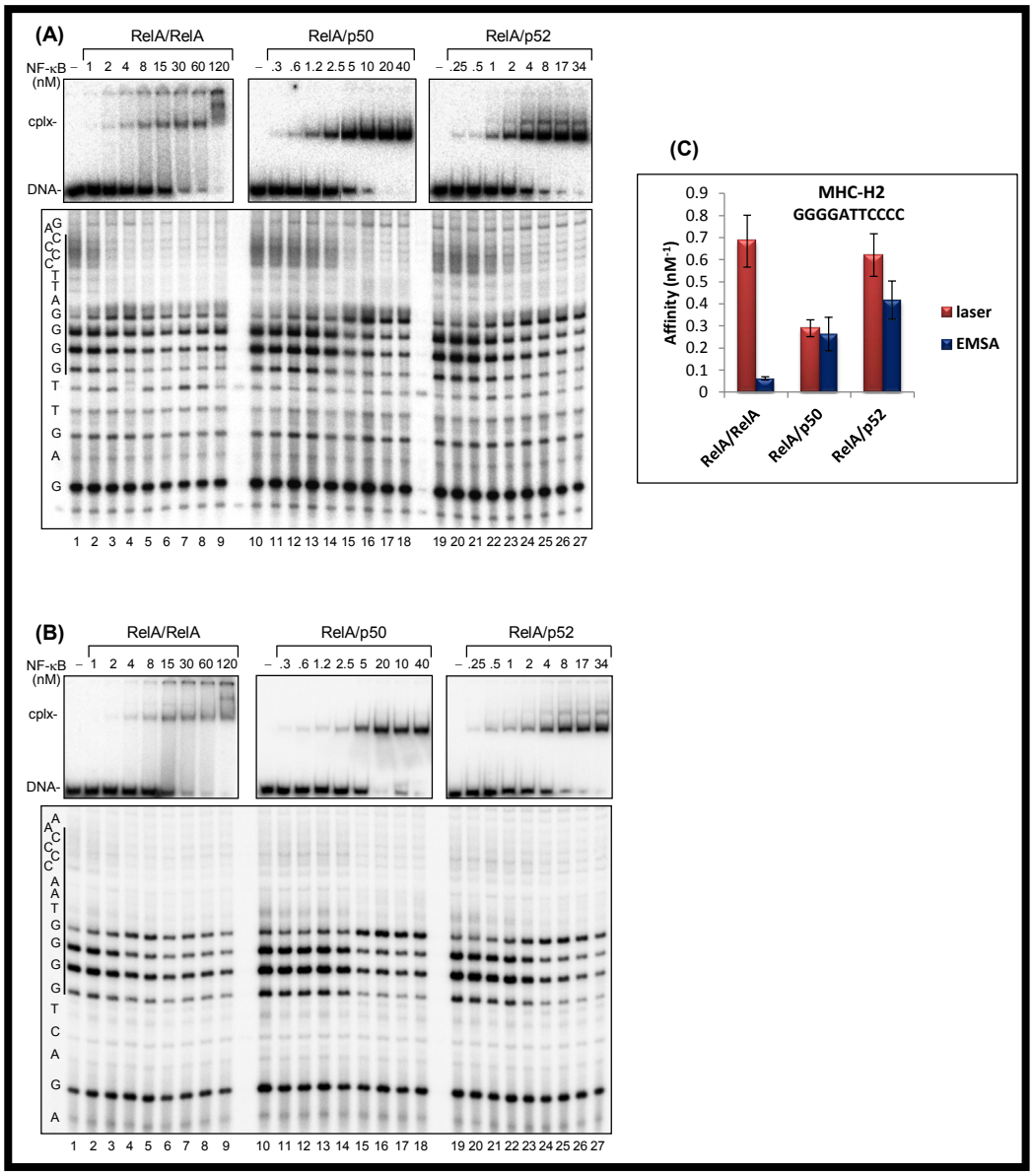

Figure 2: EMSA and UV-laser footprinting of NF-κB dimers RelA-RelA, RelA-p50 and RelA-p52 complexed with MHC-H2 recognition sequence. The upper (A) and lower (B) strands of the 37 oligomer containing the MHC-H2 recognition sequence were labeled with ^{32}P (MHC-H2-A* and MHC-H2-B*) and analyzed separately. The double-stranded oligonucleotide (~0.5 nM) was allowed to interact with increasing concentrations of NF-κB dimers RelA-RelA, RelA-p50 and RelA-p52. An aliquot from each reaction mixtures was used to carry out EMSA on a native 5% polyacrylamide gel (A and B upper panels, the positions of free DNA (DNA) and dimer-DNA complexes (cplx) are indicated). The remaining reaction mixture was irradiated with a single high intensity UV laser pulse (Epulse = 0.1J/cm2). Then the different samples were treated with both Fpg and T4 endo V and the digestion products, after purification, were run on a 13 % polyacrylamide sequencing gel (A and B lower panels). The recognition NF-κB sequences are indicated with vertical lines. **(C)** Affinity of the three NF-κB dimers for MHC-H2 κB site determined from EMSA and UV laser footprinting.
Note: An "inversion" for RelA-p50 & RelA-p52 was observed (compare lane 10 with lane 18, and lane 19 with lane 27). However, no pattern "inversion" for p65-p65 was detected (lanes 1-9); This demonstrates that for the same sequence the three NK-κB complexes p50-p50, RelA-p50 & RelA-p52 exhibit the same "signature" : (G**GG**G) to (ggg**g**), but the "signature of p56-p65 is different: (G**GG**G) to (**g**ggg). Thus, for the same sequence, a specific protein dependent "signature" is observed.

2.6.3 Binding affinities and binding specificity of NF-κB dimers RelA-RelA, RelA-p50 and RelA-p52 to HIV canonical κB site

HIV κB site is asymmetric κB site, with the two half site completely different from each other. We studied the binding affinity and specificity of NF-κB dimers RelA-RelA, RelA-p50 and RelA-p52 to this site. Binding of homodimers RelA-RelA to this site is not stable as the DNA-protein complex dissociates during the EMSA. K_d determined from EMSA is very high and (14.5 nM) suggested that the RelA-RelA has very low affinity for this site **(Figure 3A upper panel)**. The heterodimers RelA-p50 and RelA-p52 formed stable complexes and showed low K_d values 2.9 nM and 2.1 nM respectively. The K_d values determined from EMSA and UV laser footprinting for heterodimers were in the same range **(Table 1)**. UV laser footprinting of the complexes showed that all the NF-κB dimers bind very specifically and with a very high affinity. The most interesting is the binding of RelA-RelA. Although it does not form stable complex, but it binds very specifically **(Figure 3A, Lane 1-9)**. It could be that the turnover is very high and it binds and releases the κB site very quickly. Another interesting observation was that NF-κB dimers seem to bind this sequence in the same manner as shown by the similar footprint at the four G's. This is in contrast to MHC-H2 binding site were these dimers showed different footprints or signatures **(Figure 2A and 2B, lower panels)**.

Affinities ($1/K_d$) determined from EMSA and UV laser footprinting (Figure 3B) again showed significant difference. This was again more prominant in the case of RelA homodimers as shown previously.

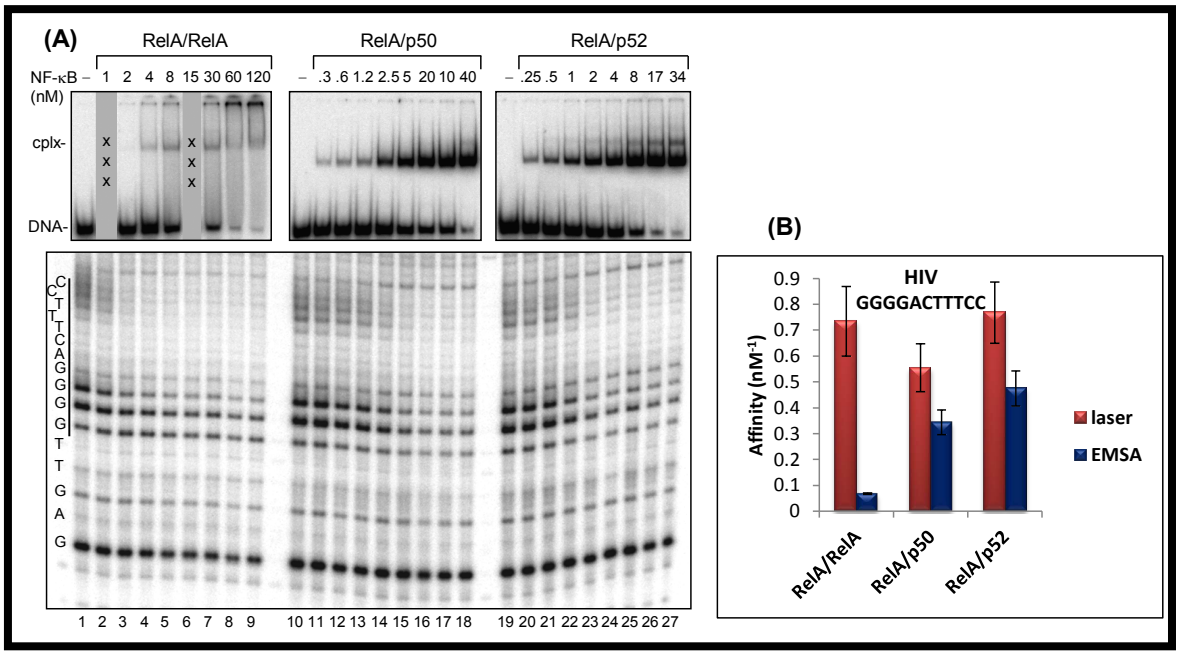

Figure3: EMSA and UV-laser footprinting of NF-κB dimers RelA-RelA, RelA-p50 and RelA-p52 complexed with HIV κB recognition sequence. 37-mer double-stranded oligonucleotide (~0.5 nM) containing HIV κB (upper strand labeled labeled with ^{32}P) recognition sequence was allowed to interact with increasing concentrations of NF-κB dimers RelA-RelA, RelA-p50 and RelA-p52. An aliquot from each reaction mixtures was used to carry out EMSA on a native 5% polyacrylamide gel (upper panels, the positions of free DNA (DNA) and dimer-DNA complexes (cplx) are indicated). The remaining reaction mixture was irradiated with a single high intensity UV laser pulse (Epulse = 0.1J/cm2). Then the different samples were treated with both Fpg and T4 endo V and the digestion products, after purification, were run on a 13 % polyacrylamide sequencing gel (lower panel). The recognition NF-κB sequences are indicated with vertical lines. (B) Affinity of the three dimers for HIV κB site determined from EMSA and UV laser footprinting.
Note: In the case of the HIV sequence, in contrast to the MHC-H2 sequence, the UV laser footprinting (the signature) is the same for all three protein complexes.

2.6.4 Non-traditional κB site exhibit specific binding to some NF-κB dimers and show features of canonical κB sites

After analyzing the binding specificity of four NF-κB dimers to two well know canonical κB site, we started to look if non-traditional sites will exhibit any binding specificity. Non-traditional κB sites are the potential binding site which on the basis of their sequence similarity to κB sites should be bound by some NF-κB dimers. However, these sites have not be reported to have any regulatory role. The extent of similarity is determined on the basis of their MATCH-scores [289], sequences displaying high MATCH-scores (greater than 0.75) behave as canonical κB sites. We tested two high MATCH-score sequences GGGGACACCCC (0.77) and AGGAAATTCCG (0.86) and

three low MATCH-score sequences AGGGGGATCTG (0.49), AGGGGAAGTTA (0.43) and CTGGGGATTTA (0.29) for their ability to bind differernt NF-κB dimers. Our results show that all the NF-κB dimers form stable complxes with these non-traditional sites, **(Figure 4A, upper panel)**. Subsequent study by DNase I footprinting **(Figure 4A, middle panel)** and UV laser footprinting **(Figure 4A, lower panel)** show that non-traditional sequences NF-κB1 **(lane 11-15)** and NF-κB2 **(lane16-20)** bind very specificially and with high affinity to p50 homodimers and p50-p52 heterodimers. RelA-RelA exhibited no binding and Rela-p50 showed very less binding. The sequence NF-κB3 exhibited specific binding to all the NF-κB dimers with p50-p52 showing the strongest affinity **(Figure 4B)**. All these non-traditional canonical sequences have some pecular features. For example, NFκB1 differs from MHC-H2 canonical sequence just at two residues (central TT in MHC-H2 is changed to CA in NF-κB1). This change drastically reduces the affinity of RelA-RelA **(Figure 4A, Lane 13 and Figure B)** for this site to an extent that no binding is observed. The same dinucleotide change also reduces the affinity of RelA-p50 **(Figure 4A, Lane 14 and FigureB)** towords this site. Sequence NF-κB2 (MATCH-score 0.49) contains half site (GGGGA) for p50-p50 and p50-p52 dimers suggesting that these dimers should be able to bind it. Both DNase and UV laser footprinting show that this sequence preferentially binds to p50-p50 **(Figure 4A, Lane17 and FigureB)** and p50-p52 dimers **(Figure 4A, lane20 and FigureB)**. Sequence NF-κB3(MATCH-score 0.86) exhibits features of a canonical κB site. All the dimers formed stable complexes, and showed good affinity for this site and bound very specifically **(Figure 4B)**.

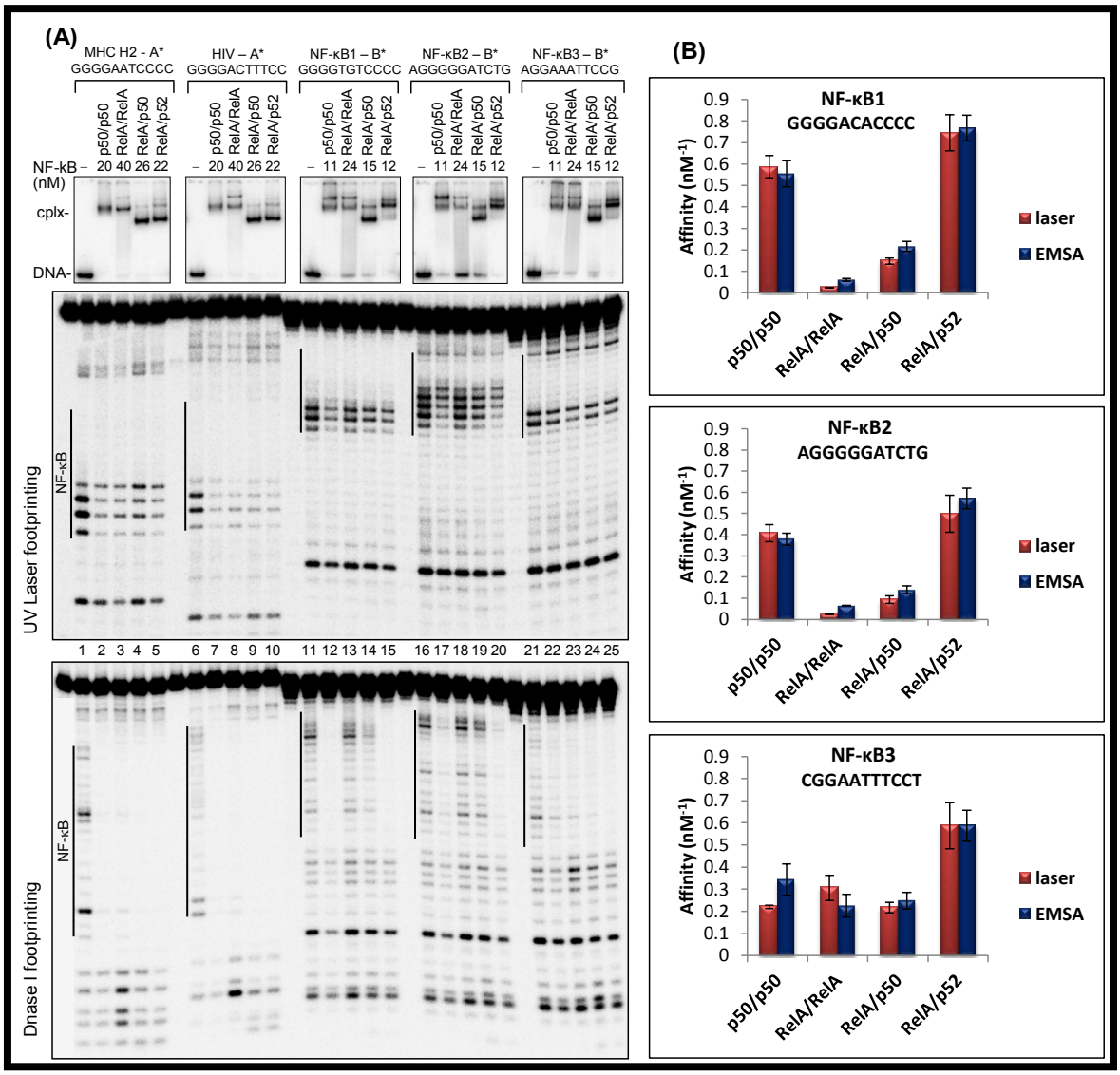

Figure 4: DNase I footprinting (middle panels) and UV laser (lower panels) of the 37-mer oligos containing the MHC H-2 binding site (top-strand labeled - A*), the HIV (top strand) and the oligos 1-3 (bottom-strand labeled – B*) with different NF-κB dimers (p50-p50, p65-p65, RelA-p50 and RelA-p52). The corresponding EMSA (aliquots from the corresponding reaction mixtures) are also shown (upper panels). The NF-κB binding sequence is indicated by a vertical line. Note that in the laser footprinting experiment the treatment by T4 endo V was omitted. (B) Affinity of the four NF-κB dimers for the three non traditional sites.

2.6.5 Non-traditional κB sites with low MATCH-score exhibit specific binding to p50-p50 homodimers only

Here we studied two representative sequuences with low MATCH-score, NF-κB4 (0.43) and NF-κB5 (0.29). These sequences partially resemble to NF-κB sites by the presence of GGGGA sequence within them. EMSA showed the formation of stable

complexes, however, DNase and UV laser footprinting showed that only p50 homodimers could specifically bind to these sequences **(compare lane 1 and 2 in Figure 5B and 5D)** . The affinity of binding was lower then other canonical and non-tradional κB sites studied. Interestingly, 5' half site of NF-κB4 sequence is identical to the 5' half site of NF-κB2 sequence but the binding profiles are very different. NF-κB4 is a very peculiar, an extra "A" infront of the four G's reduces the affinity of p50 homodimer by half and completely abolishes the binding of other dimers **(Figure 5E)**. These two site are catgorized as non canonical sites as almost no binding was observed.

2.6.6 Dimer preferences for traditional and non-traditional κB sites

A comparison of the binding preferences of all four dimers for the seven sequences shows that p50 homodimers are least discriminatory while as RelA homodimers are highly discriminative. RelA/p50 and RelA/p52 bound specifically to traditional and non-traditional canonical κB sites but not to non-canonical sites (NF-κB4 and NF-κB5). RelA/p52 displayed higher affinity towords these sites than RelA/p50 **(Figure 6)**. p50 homodimers bound specifically to all the sequences although with varying affinities. The common feature of all these sequences is the presence of "G" stretches, suggesting that p50 homodimer preffers "G" rich regions. RelA homodimers bound specifically to traditional κB sites. However, the dimer-DNA complexes are not very stable and were dissociated during the EMSA. This dissociation resulted in false high K_d (EMSA). The same dimer formed a quite stable complex with sequence NF-κB3 (CGGAATTTCCT) and showed a specific UV laser footprint. RelA/p52 showed not only high affinity for the canonical κB sites (traditional as well as non-traditional) but also bound specifically to these sequences.

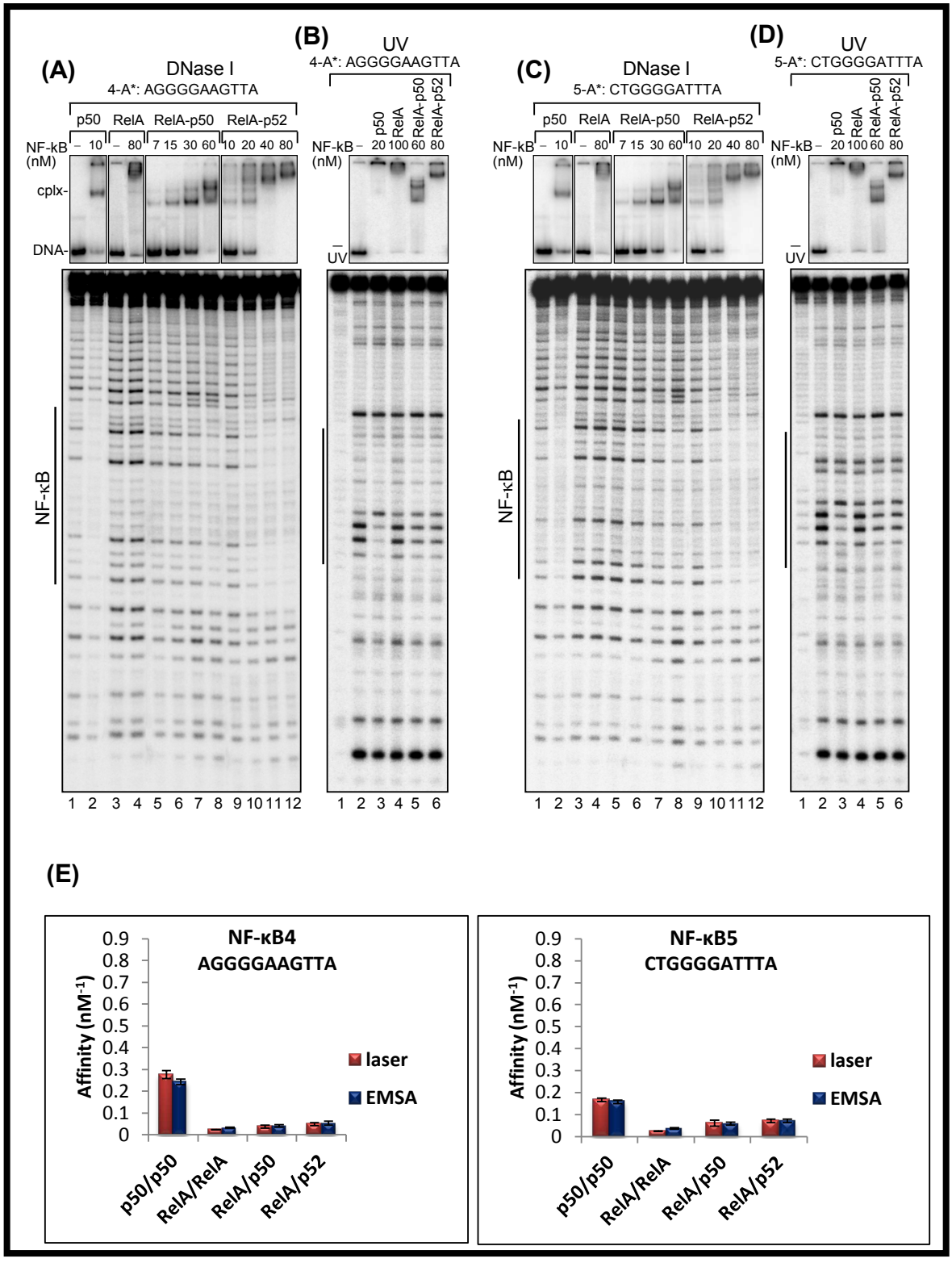

Figure 5: DNase I (A and C) and UV laser (B and D) footprinting analyses (lower panels) of the 60-mer oligos 4 (A, B) and 5 (C, D) containing the "low-affinity" binding sites (top-strand labeled – A*) with different NF-κB dimmers (p50-p50, p65-p65, RelA-p50 and RelA-p52). The corresponding EMSA are also shown (upper panels). The NF-κB binding sequence is indicated by a vertical line. (E) Affinity of the four NF-κB dimers for the three non traditional sites.

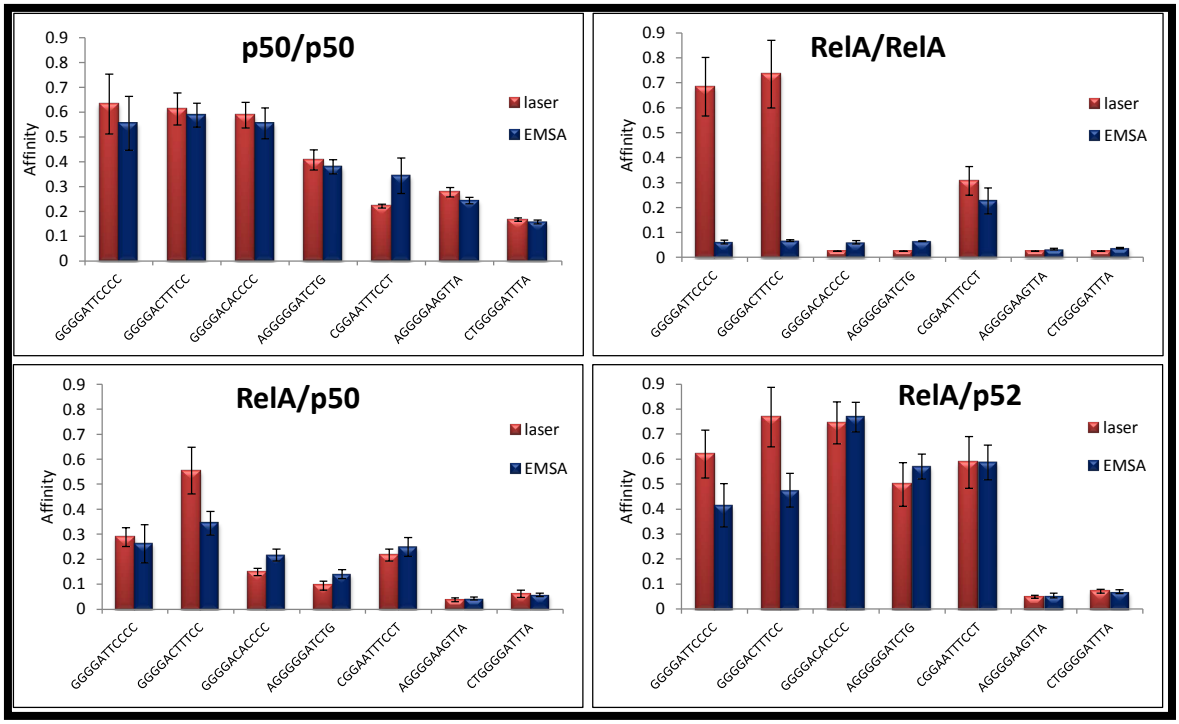

Figure 6: Comparison of binding profiles of all four NF-κB dimers used with all the sequences.

2.7 Dynamics of TF-DNA interactions at milli second time range

The study of rapid conformation changes occurring in nucleic acids during real biological processes is a challenge for molecular biology and physical chemistry. Unfortunately, there are few experimental techniques that are able to address this problem. The highest resolution approaches, such as NMR and X-ray scattering in crystals are restricted to short oligonucleotides due to the low selectivity. Techniques, based on chemical or UV lamp photochemical reactivity (footprinting) have less resolution, but they are more flexible and possess higher selectivity. However, none of these approaches enables conformational dynamic study due to the low time resolution.

After establishing the feasibility of biphotonic UV laser footprinting for studying stationary (at equilibrium) complexes of the transcription factor NF-κB with its DNA target sequence, we carried out dynamic photo-footprinting experiments; in which we

synchronized the laser to the stopped-flow device **(Figure 7)** using a custom designed microprocessor controlled interface, which allows a very rapid mixing and time-delayed photochemical probing of the substrate. Since the volume of the stopped-flow quartz chamber is small (20-40µl), the dead time of the mixing device does not exceed few milliseconds and the mixing time was 10 ms, this allowed us to study the kinetics of protein DNA interactions few milliseconds after mixing.

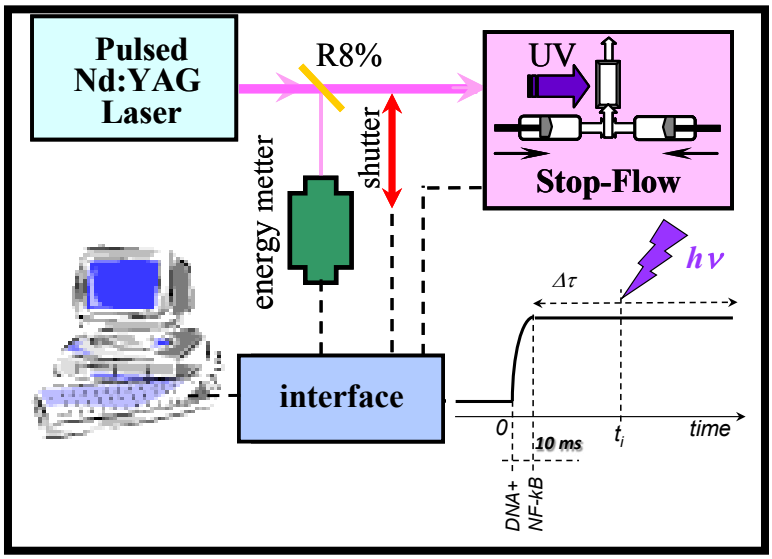

Figure 7: Schematic representation of synchronized UV laser- stopped flow device: The DNA and protein are injected by the syringes into the mixer and then into the quartz microcuvette where they are irradiated by a single UV laser pulse. The interface is a custom designed microprocessor controlled device that allows the synchronization of the UV laser and stopped flow device.

2.7.1 Time-resolved NF-κB-DNA interactions at a millisecond time scale and at one base pair resolution

In order to understand the kinetics of interactions of NF-κB p50 homo-dimer, we used the ^{32}P labeled, 37 bp long oligonucleotide, containing the high affinity MHC-H2 κB site. Saturating amounts of NF-κB were allowed to mix with the DNA for 10 ms and then pushed to the quartz microcuvette for irradiation by UV laser pulse. The time between mixing and irradiation was varied as shown in (**Figure 8A, 8B**). The 10 ms time-resolution kinetics **(Figure 8B)** displays initial fast binding (t~100-120 ms) followed by relatively slow (t~800-900 ms) rearrangement processes before equilibrium is reached. Interestingly, while the interaction with the "inner" guanine G1 shows a single fast one-step character, protein binding

curve with "outer" guanines contains a slow component presumably reflecting the time-dependent stabilization of the NF-κB-DNA complex.

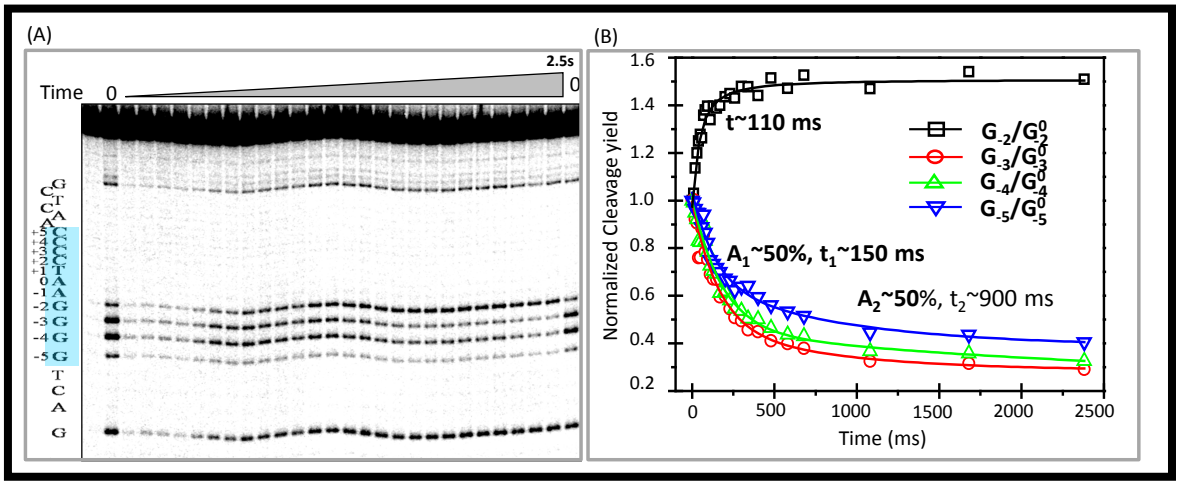

Figure 8: Time resolved UV laser footprinting of the binding of NF-κB to the MHC-H2 sequence. 0.5 nM uniquely 5' labeled DNA fragment were mixed with saturating amounts of NF-κB p50 within 10 ms. The mix was then submitted to a single nanosecond Nd:YAG laser (266 nm, 0.1 J/cm2) at different delay times starting from 10 ms. The irradiated samples were recovered from the irradiation cuvette, and after purification the oligonucleotide DNA was treated with Fpg. The cleaved products were then run on a 13% sequencing gel (A). The position of the binding sequence is indicated at the left. (B) Quantification of the data presented in (A)

Previously we have identified (by using UV laser crosslinking) novel NF-κB–DNA points of contact at the immediate vicinity of the recognition DNA sequence. The data suggested that these contacts are implicated in the transition from non-specific to specific binding of NF-κB via its flexible loop [292]. Some other studies have also highlighted the importance of the flanking sequences in specific recognition through the phosphodiester backbone dynamics [293]. To study the dynamics of generation of these points of contact, we placed the MHC-H2 κB site in a different sequence back ground in which it was flanked by sequence CGC within the 37 mer oligonucleotide sequence, which has allowed to follow the changes in the photoreactivity of this G out side the binding site (designated as *G). The results for the UV laser footprinting for both the top and the bottom strand are shown **(Figure 9)**.

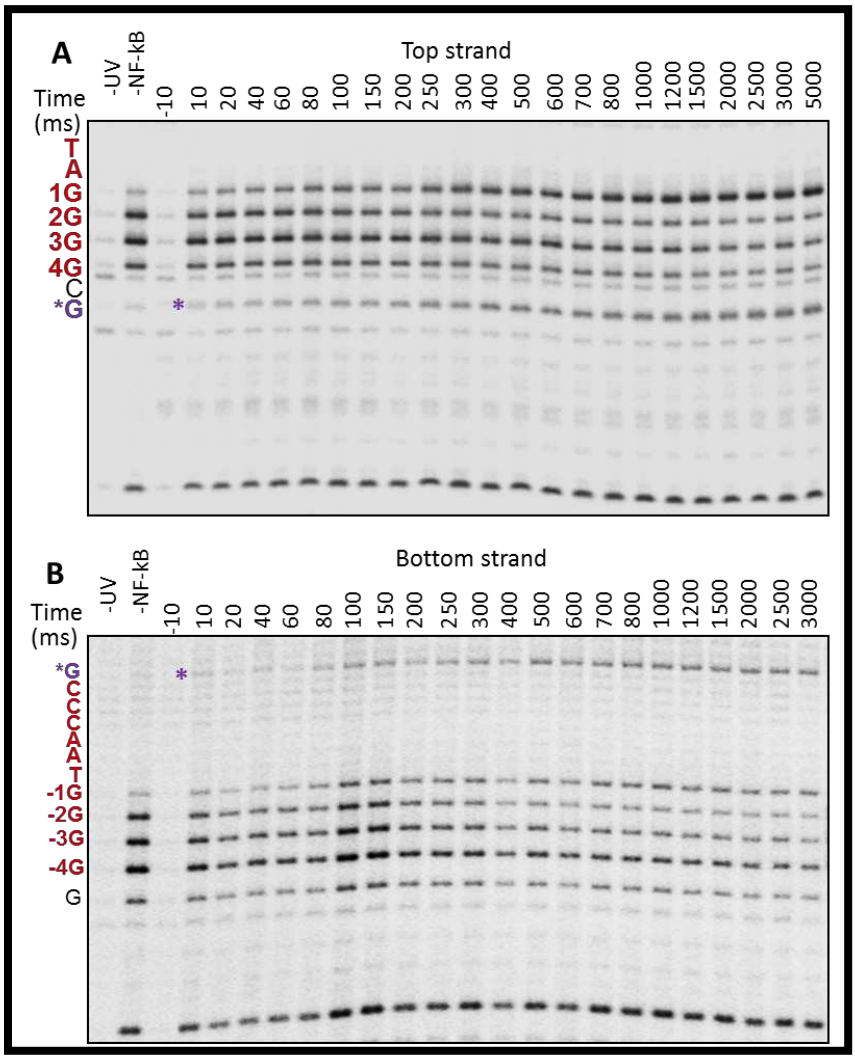

Figure 9: Time resolved UV laser footprinting of the binding of NF-κB to the MHC-H2 sequence with footprintable flanks. 0.5 nM uniquely 5' ^{32}P labeled top DNA fragment (A) or bottom starnd (B) were mixed with saturating amounts of NF-κB p50 within 10 ms. The mix was then submitted to a single nanosecond Nd:YAG laser (266 nm, 0.1 J/cm2) at different delay times starting from 10 ms as shown on top of each gel. The irradiated samples were recovered from the irradiation cuvette, and after purification the oligonucleotide DNA was treated with Fpg. The cleaved products were then run on 13% sequencing gel. The position of the binding sequence is indicated at the left.

As clearly visible, upon stabilization of the NF-κB-DNA binding, the DNA clevage signal for *G as well as that of the "internal" guanine increase in intensity in contrast to the other guanines which exhibit lower signal. In fact, the changes in the intensity of of *G exhibit the same two-exponential profile as these of G2, G3, G4 (see the report for period 2). This testifies that intensity alterations in the *G cleavage reflect indeed the binding of NF-κB. These results are completely novel and illustrate the capacity of the UV laser footpring to study the kinetics of NF-kB binding to its recognition sequences.

2.8 Discussion

Three dimensional X-ray structures of several different complexes of DNA-bound NF-κB dimers have been determined and provided the basic information about how these closely related dimers make contacts with their DNA targets [217]. However, a complete understanding of NF-κB dimer DNA-binding specificities and affinities is still needed in order to understand how NF-κB dimers actually regulate gene expression. This information would provide insight into mechanisms for NF-κB dimer-specific function *in vivo*. Recently non-canonical κB sites have come to focus as several studies have shown that NF-κB dimers can recognize sequences that do not fall under general consensus sequence [289, 294]. These studies used high throughput approaches to investigate the binding profile of the different NF-κB dimers to large number of potential sequences. Surprisingly, they show that NF-κB can recognize sequences that were previously not considered suitable κB sites. Together with computational approaches, these studies highlighted the fact that *in vivo* there could be several not yet identified κB binding sites which may play important role in NF-κB mediated gene expression. Thus, such κB sites need to be identified and studied in detail.

By using EMSA and UV laser footprinting, we studied five such sequences. Three of these sequences, NF-κB1, NF-κB2 and NF-κB3 not only showed a fare degree of specific binding but also high affinity towards p50-p50 homodimers and RelA-p52 heterodimers. Interestingly, RelA-RelA and RelA-p50 did not bind to NF-κB1 and NF-κB2. However, NF-κB3 displayed specific binding to all the dimers. This sequence behaved more like the canonical sequences. RelA-RelA and RelA-p50 dimers seem to be highly discriminative and less tolerant to mutations in the binding site as they displayed higher sequence preferences. Both of these dimers either did not bind to nontraditional-canonical κB sites or bound with very low affinity. The heterodimer, RelA-p52 displayed specific binding to 5 out of 7 sequences studied suggesting that this hetero-dimer can tolerate variations or mutations in its binding site. Such a wide range of binding site preference could imply that this dimer can regulate large number of genes bearing different κB binding sites. It also implies that selective functions of this dimer may not be achieved via dimer-specific recognition of the κB site in target genes but by interaction with other co-regulators.

We have used two different methods to measure binding affinities: traditional gel mobility shift assay (EMSA) and a novel technique called as UV laser footprinting. Our EMSA showed that RelA-RelA binding to high affinity MHC-H2 and HIV κB sites is not stable. However, UV laser footprinting showed that these homodimers not only bind with high affinity but also with high specificity to these physiologically characterized and high affinities κB sites. Moreover, RelA homodimers formed quite stable complexes with one of the nontraditional κB site. This could be explained by the fact that these homodimers are not very stable [20] and the monomers dissociate from the complex during the electrophoresis as shown by the presence of smear in the EMSA gels for RelA-RelA. We hypothesize that *in vivo* this homodimer may interact with other factors that could impart higher stability to this homodimer. On the other hand RelA-p50 and RelA-p52 heterodimers and p50 homodimers form stable complexes with the canonical κB sites and bind with high affinity and specificity. Within the group, RelA-p50 binds with lower affinity than the p50 homodimer and RelA-p52 heterodimer to the physiologically known high affinity canonical κB sites (Figure 9A).

We have also developed a novel approach to study the dynamics of the DNA-protein interactions. Using p50 homodimers as a model transcription factor, we showed that the binding of this factor follows a two step mechanism. First step involves the fast recognition of the sequence and second step follows a slower kinetics most likely for the stabilization of the complex. Our experiments suggest that flanking sequences play a role in the recognition and stabilization process of the complex formation.

Our results also highlight the fact that K_d values determined from EMSA are not always reliable. EMSA interferes with the stability of the complexes and cannot distinguish between specific and non specific binding. UV laser footprinting, on the other hand not only gives correct K_d values but also distinguishes between specific and non specific binding.

2.9 Conclusions and Perspectives

Our results, in general, show that p50 homo-dimers are highly plastic and least discriminative while as RelA homo-dimers are highly discriminative. The hetero-dimers fall in between these extremities. With our approach, we are able to monitor the base specific contacts that NF-kB proteins make while interacting with the DNA. Such an approach is highly applicable to understand the variability of the κB sites [289]. UV laser footprinting can be used to study the regulatory SNPs. By measuring the affinity and specificity of transcription factors for SNP containing binding site, one could understand if such mutations reduce or eliminate the binding. SNPs may not alter the affinity of the TF for its binding site, but they may impose the TF to bind in an alternative conformation and prevent the recruitment of co-regulators [253]. These results suggest that the simple occupation of the binding site by a TF is not sufficient to drive transcription.

Quantitative and selective detection of DNA-protein interactions by UV laser footprinting can be exploited to study the co-operative binding to binding sites located in close vicinity by same or different factors. Such kind of study will shed light on the chain of events taking place at the promoter and also explain why certain combination of binding sites at the promoters is needed.

MANUSCRIPT: 2

Binding of NF-κB to Nucleosomes: Effect of Translational Positioning, Nucleosome Remodeling and Linker Histone H1

Binding of NF-κB to Nucleosomes: Effect of Translational Positioning, Nucleosome Remodeling and Linker Histone H1

Imtiaz Nisar Lone[1], Charles Richard John Lalit[2], Manu Shubhdarshan Shukla[1], Stefan Dimitrov[2]* and Angelov Dimitar[1]*

[1]Université de Lyon, Laboratoire de Biologie Moléculaire de la Cellule, CNRS-UMR 5239, Ecole Normale Supérieure de Lyon, 46 Allée d'Italie, 69364 Lyon cedex 07, [2]Université Joseph Fourier - Grenoble 1, INSERM Institut Albert Bonniot, U823, Site Santé-BP 170, 38042 Grenoble Cedex 9, France

*To whom correspondence should be addressed: Email: Dimitar.Anguelov@ens-lyon.fr, Stefan.Dimitrov@ujf-grenoble.fr

Abstract

NF-kB is a key transcription factor regulating the expression of inflammatory responsive genes. How does NF-kB binds to naked DNA templates is well documented, but how does it interact with chromatin is far from being clear. Here we show that NF-kB p50 homodimer is able to bind to its recognition sequence, when it is localized at the edge of the core particle, but not when the recognition sequence is at the interior of the nucleosome. Remodeling of the nucleosome by the chromatin remodeling machine RSC was not sufficient to allow binding of NF-kB to its recognition sequence located in vicinity of the nucleosome dyad, but RSC-induced histone octamer sliding allowed clearly detectable specific interaction of NF-kB with the slid particle. Importantly, nucleosome dilution driven removal of H2A-H2B dimer led to complete accessibility of the site located close to the dyad to NF-kB. Finally, we found that NF-kB was able to displace histone H1 and prevent its binding to nucleosome. These data provide important insight on the role of chromatin structure in the regulation of transcription of NF-kB dependent genes.

Introduction

In eukaryotes, all DNA-templated reactions occur in the context of chromatin. The repeating structure of chromatin, the nucleosome, consists of a nucleosome core (made up of two copies of each core histone H2A, H2B, H3 and H4 that wraps around 147 bp of DNA [1], a linker histone and a linker DNA [2]. The globular domain of the linker

histone H1 binds to the nucleosomal dyad and contacts a 10 bp region of DNA localized symmetrically with respect to it [3]. Microccocal nuclease digestion of chromatin results in a kinetic cleavage nucleosome intermediate of 168 bp, termed chromatosome, which contains stably bound histone H1 [4].

The packaging of DNA into nucleosomes in general restricts DNA accessibility for regulatory proteins [5] and at the same time also provides an opportunity to regulate DNA based processes through modulating nucleosome positions and local chromatin structure [6]. Nucleosomes sterically block [7] and strongly distort the DNA except for the terminal segments which are relatively straight [1, 8].

Sequence-specific binding of transcription factors is the key event for gene activation. Promoters of repressed genes, however, are usually embedded in nucleosomes. The packaging of promoter DNA in nucleosomes inhibits transcription *in vitro* [7] and *in vivo* [9]. To activate gene expression, transcription factors must access their regulatory sites in chromatin. Nucleosomes act, however, as a barrier for the transcription factor binding [10]. Some transcription factors such as human glucocorticoid receptor [11-13], yeast PHO2/PHO4 proteins [14], and GAL4 [15] have been shown to bind to their recognition sequences in the nucleosomes and the binding of some of them was dependent on the length of the recognition sequence and the recognition sequence distance from the nucleosomal ends and rotational orientation. Other distinct transcription factors, namely Sp1, Lef-1, ETS-1 and USF were also found to be able to invade the nucleosome and to interact with their cognate sequences [16].

The key regulator of gene expression in inflammation is the family of transcription factors NF-κB/Rel [17]. Ways to modulate levels of these transcription factors in inflammation and cancer are considered to be of potential therapeutic importance [18, 19]. In mammalian cells, the NF-κB/Rel family contains five members: RelA (p65), c-Rel, Rel B, NF-κB1 (p50; p105) and NF-κB2 (p52; p100) [20]. p50 and p52 usually form homodimers or heterodimers with one of the other three proteins. Each NF-κB dimer has different DNA-binding affinity for kB sites bearing the consensus sequence GGGRNNYYCC (R, purine : Y, pyrimidine : N, any base), but nonetheless their functions often overlap [21]. How does NF-kB bind to naked DNA is well documented [22-25]. However, whether and how NF-kB interacts with the nucleosome is not well

understood. Indeed, it was reported that NF-kB (p50 homodimer) binding to the nucleosome core particle depends on the localization of the binding site relative to the end of nucleosomal DNA. A severe disruption of DNase1 digestion profile upon binding of NF-kB was also observed [16]. Another study claimed that NF-kB p50 homodimer is able to invade the nucleosome and to bind to its recognition sequence even independent of its localization relative to the end of the nucleosome core particle DNA [26].

However, the studies on the binding of transcription factors in general and of NF-kB in particular have some serious limitations. First, the sequences that were used for nucleosome reconstitution do not give a homogenous population of positioned nucleosomes as these sequences have relatively weak nucleosome positioning potential. Second, the studies were carried out generally at very low nucleosome concentration where the nucleosomes are unstable and H2A-H2B removal might take place. Third, the techniques used to probe the binding of transcription factors were not enough resolutive to make a firm conclusion about the specificity of the binding. In addition, how does the presence of histone H1 and ATP dependents nucleosome remodelers affect the transcription factor binding was essentially not addressed.

In this work we have overcome these limitations by using both strongly centrally positioned nucleosomes and a combination of EMSA and OH radical and UV laser footprinting to analyze how the histone octamer, histone H1 and remodeling and mobilization of the nucleosome impacts the binding of NF-kB to its recognition sequence. Our data sheds light on the *in vivo* mechanism of NF-kB binding and transcriptional regulation of inflammatory NF-kB responsive genes.

Results

Characterization of the nucleosomal templates used to study NF-kB binding

To study the interaction NF-kB (p50 homodimer) with the nucleosome we have used purified (to homogeneity) recombinant proteins **(Figure 1 B-D)**. Centrally positioned nucleosomes were reconstituted on either 601 255 bp DNA fragment or on 152 bp 5S

rDNA. Since NF-kB exhibits clear affinity for continuous G stretches [27], some of the G's within G rich regions of the 601 DNA were substituted with either Ts or As **(See Supplementary Figure 1)**, which allows to diminish the association of NF-kB with "G" rich potential binding sites. The MHC-H2 NF-κB high affinity binding site was inserted either in vicinity of the 601 nucleosome dyad (601-D_0 DNA), or at the core particle edge (601-D_7 DNA) or in the free DNA arm (601-D_8 DNA) **(Figure 1)**. In the case of 5s rDNA the MHC-H2 NF-κB site was inserted close to the dyad **(Figure 1A)**.

EMSA shows that under the experimental conditions, all the DNA was reconstituted into nucleosomes **(Figure 1E)**. The reconstituted 601 particles exhibit clear 10 bp repeat upon cleavage with either •OH **(Figure 1F)** radicals or with DNase I **(Figure 1G)**, thus demonstrating both proper wrapping of DNA around the histone octamer and strong octamer positioning relative to the DNA ends. We conclude that the reconstituted nucleosomes represent a very homogenous population of particles suitable for further NF-kB-nucleosome binding studies.

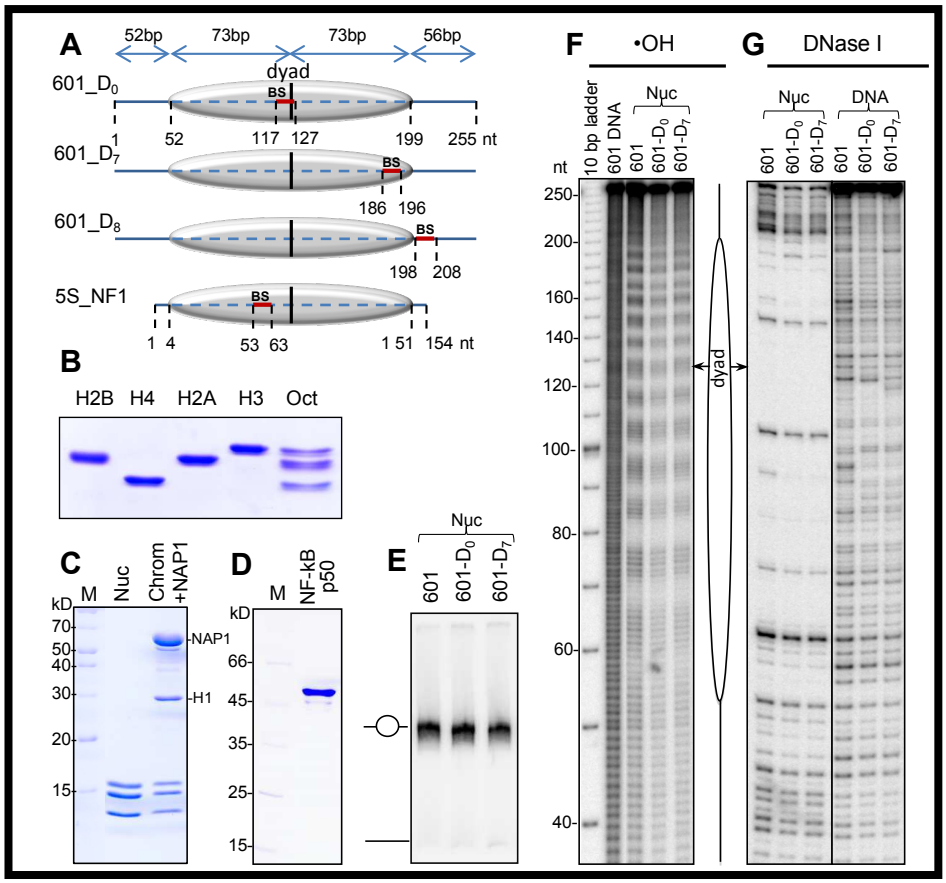

Figure 1 Characterization of the reconstituted nucleosomes. (A) Schematics of the reconstituted nucleosomes. The canonical NF-kB site was inserted in the 255 bp 601 DNA fragment either at the dyad of the nucleosome (601_D_0 DNA) or at the nucleosomal end (601_D_7 DNA) or in the free DNA arm (601_D_8 DNA); bold lines, free DNA arms; dashed line, core particle region. The vertical black line represents the dyad (red C). The NF-κB binding sites (BS) are depicted by the red line. The length of each region is shown on top of the constructs. The very bottom schematics shows the location of the NF-kB binding site inserted in the 5s rDNA *Xenopus borealis* fragment used for nucleosome reconstitution. **(B)** Electrophoretic analysis of the indicated purified recombinant histones and histone octamer. **(C)** SDS gel electrophoresis of indicated reconstituted nucleosomes. **(D)** Electrophoretic analysis of purified recombinant NF-κB (p50); M, molecular marker; p50, the p50 subunit of NF-kB. **(E)** •OH radical and **(G)** DNase I footprinting of free 601 DNA and the indicated reconstituted nucleosomes.

Terminal segments of the nucleosomal DNA, but not sequences in vicinity to the nucleosome dyad, are accessible to NF-κB

We have analyzed the binding of NF-kB by using both EMSA and UV laser footprinting **(Figure 2)**. The UV laser footprinting is based on change in the UV laser induced nucleotide photoreactivity upon protein binding [28, 29]. Irradiation of protein-DNA complexes by a single UV laser pulse results in different nucleotide lesions, whose spatial distribution depends on type of proteins specifically bound with the DNA [29]. Quantitative measurements of the lesions and comparison with those of free DNA allows to analyze at a single base resolution the changes in the structure of DNA upon protein binding. The use of UV lasers has many advantages compared to conventional light sources. With a single UV laser pulse a footprint of the protein is achieved. Additionally, high intensity laser irradiation, contrary to conventional light sources, induces (in addition to monophotonic lesions) specific biphotonic oxidative lesions in DNA [29]. These lesions are extremely sensitive to local DNA structure and can be easily mapped specifically by alkali or enzymatic DNA strand cleavage followed by electrophoresis under denaturing conditions [30, 31]. In our study we have mapped UV laser specific biphotonic lesions 8-OxoG by Fpg glycosylase (formamidopyrimidine [fapy]-DNA glycosylase or 8-oxoG glycosylase and AP-lyase) and cyclobutane pyrimidine dimers (CPDs) by T4 Endonuclease V cleavage, both present in the NF-kB cognate sequence after UV laser irradiation.

EMSA shows that incubation of either free 601-D_7 DNA or 601-D_7 nucleosomes with increasing amount of NF-kB results in the generation of several bands with lower electrophoretic mobility **(Figure 2A)**. These bands reflect the binding of either one or several NF-kB molecules. However, since only one high affinity NF-kB binding sequence

is present within the templates, only one band should reflect the specific NF-kB binding to this site, while the others would reflect the binding to lesser affinity sites (G rich regions) and non-specific interaction of NF-kB with its templates. This is clearly seen in the footprinting pattern of free DNA upon cleavage with Fpg **(Figure 2A, lower left panel)**. Indeed, the disappearance of the 8-oxoG band corresponding to high affinity MHC-H2 κB site (designated by *) reflects the binding of NF-kB to its high affinity cognate sequence. The disappearance of 8-oxoG band corresponding to MHC-H2 site parallels the rise of the first shift in EMSA, suggesting that NF-κB is mostly bound specifically to this site (Figure 2A, upper left panel). The appearance of additional bands in EMSA correlates with the change in the intensity of 8-OxoG specific bands (designated by ♦) in UV laser footprints, reflecting that additional molecules of NF-κB are binding to other low affinity sites. Besides, it is likely that at high concentrations NF-κB interacts non-specifically with the template contributing to super-shifts in EMSA. Therefore, the UV laser footprinting technique allows a clear visualization of specific binding to high and low affinity sites. Indeed, we observed that NF-κB binds specifically at several sites apart from inserted high affinity MHC-H2 κB site in 601-D7 DNA **(Quantified data are shown in supplementary figure 2)**.

In the case of nucleosomes, the behavior of NF-kB binding appears to be somewhat different **(Figure 2A, lower right panel and Figure 2B)**. First, NF-kB binds to its cognate sequence located at the edge of the nucleosome as evidenced by the disappearance of the band originating from the MHC-H2 NF-kB sequence. However, the presence of histone octamer interferes with the binding efficiency since more NF-kB has to be present in the reaction mixture to observe the binding. Histone octamer seems to shield the low affinity binding sites (designated by ♦) located in core particle DNA and prevents binding of NF-κB to these sites. This shielding affect was not observed for the low affinity site near the nucleosome edge **(Figure 2A, lower right panel)**.

Since NF-kB binds with lower affinity to the nucleosomal edge one should expect a completely abolished binding to the NF-kB sequence inserted close to the dyad in the 601_D_0 nucleosome. And this is indeed the case, since in contrast to free 601_D_0, no footprint is observed in the 601_D_0 nucleosome even at the highest NF-κB concentration **(Figure 2C)**.

Binding of NF-κB to remodeled and to slid 601_D_0 nucleosomes

RSC chromatin remodeler is able to both remodel and slide centrally positioned nucleosomes [32]. Note that RSC uses an intriguing two-step mechanism for nucleosome remodeling. During the first step a stable non-mobilized particle, containing ~180 bp DNA associated loosely with the histone octamer, is generated. This particle, termed as "remosome," is then mobilized by RSC. The histone-DNA interactions within the remosome are perturbed and allow accessibility of restriction enzymes all along the remosomal DNA [32]. Remosomes and slid nucleosomes can be isolated by extraction from native gel after remodeling reaction and gel separation of the RSC-remodeled products [32] **(Figure 2A, schematics)**. Does the generation of remosomes or nucleosome mobilization allow binding of NF-kB to the 601_D_0 nucleosome? To test this we have prepared control centrally positioned 601_D_0 nucleosomes and gel purified (after RSC treatment) remodeled nucleosome (remosomes) and slid nucleosome (**see schematics supplementary figure 3 and [32]**) and studied the binding of NF-kB to these templates by using UV laser footprinting. Control EMSA shows that NF-kB is able to associate with all templates at the NF-κB concentrations used **(Figure 3A)**. However, the RSC-induced perturbation in the histone DNA interactions were not sufficient to allow specific binding of NF-kB to the 601-D_0 remosomes, since change in the photoreactivity is very low and no evidence for specificity is observed **(Figure 3C and D, line 3 and 4)**. Although, the NF-kB-slid nucleosome complex exhibits clearly detectable alterations in the footprinting pattern **(Figure 3 C and D, compare line 5 and 6)**. We conclude that nucleosome mobilization which results in the "displacement" of the NF-kB binding site to the edge of the slid nucleosome allows NF-kB to invade the nucleosome and to bind specifically to it **(see figure 1 A for nucleosome and binding site location)**. These data are in agreement with the results described in the previous section for the ability of NF-kB to bind to the edge of the centrally positioned nucleosome.

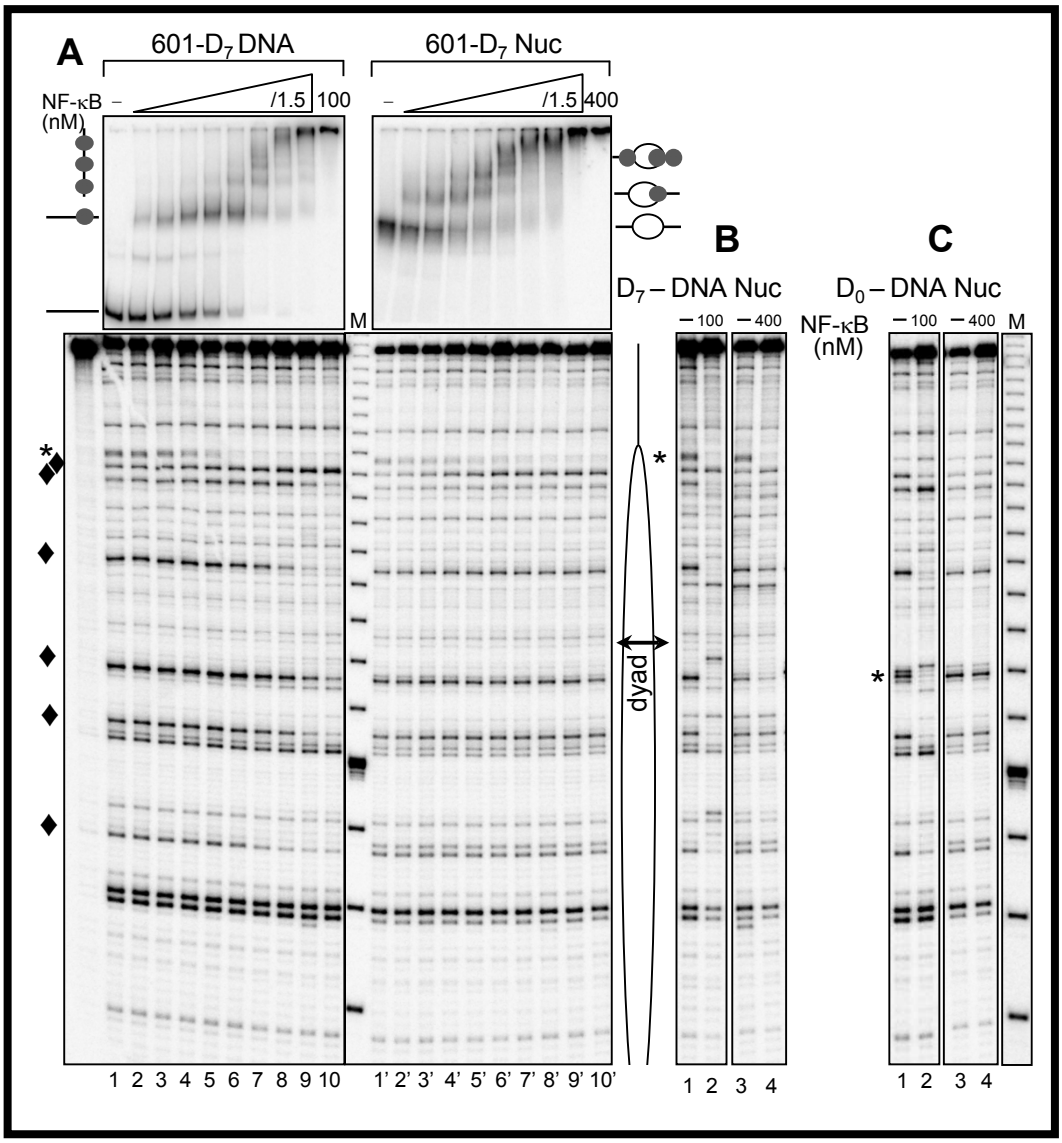

Figure 2 NF-kB is able to specifically bind to the nucleosomal ends, but not to the nucleosomal dyad. (A) Upper panel: EMSA of NF-kB binding to naked 601_D_7 DNA (left) or to 601_D_7 nucleosome (right). Naked ^{32}P-end labeled 601_D_7 DNA or nucleosomes were incubated with increasing amount of NF-kB and aliquots of the reaction mixtures were run on a native PAGE. The positions of free DNA, nucleosomes and their complexes with NF-kB are indicated; **lower panel:** UV laser footprinting patterns of the NF-kB-DNA and NF-kB nucleosomes complexes. The respective remaining mixtures were irradiated with a single 10 nanoseconds UV laser 266 nm pulse (E_{pulse}~0.1 J/cm^2), DNA was purified from the samples and then treated with Fpg glycosylase. The cleaved DNA fragments were separated on 8% sequencing gel and visualized by autoradiography; (*), NF-kB footprint the high-affinity NF-κB binding site; (♦), NF -κB footprints at low-affinity sites. A schematic presentation of the nucleosomes is shown on the right side; the double headed arrow indicates the nucleosomal dyad. **(B)** Footprinting pattern of NF-kB bound to either naked 601 D7_DNA (lanes 1 and 2) or to 601_D7-nucleosome lanes (3, 4); (*) indicates the site of the specifically bound NF-kB. **(C)** Same as (b), but for naked 601_D_0 DNA and 601_D_0 nucleosomes. Note the absence of NF-kB footprint in the case of the nucleosome.

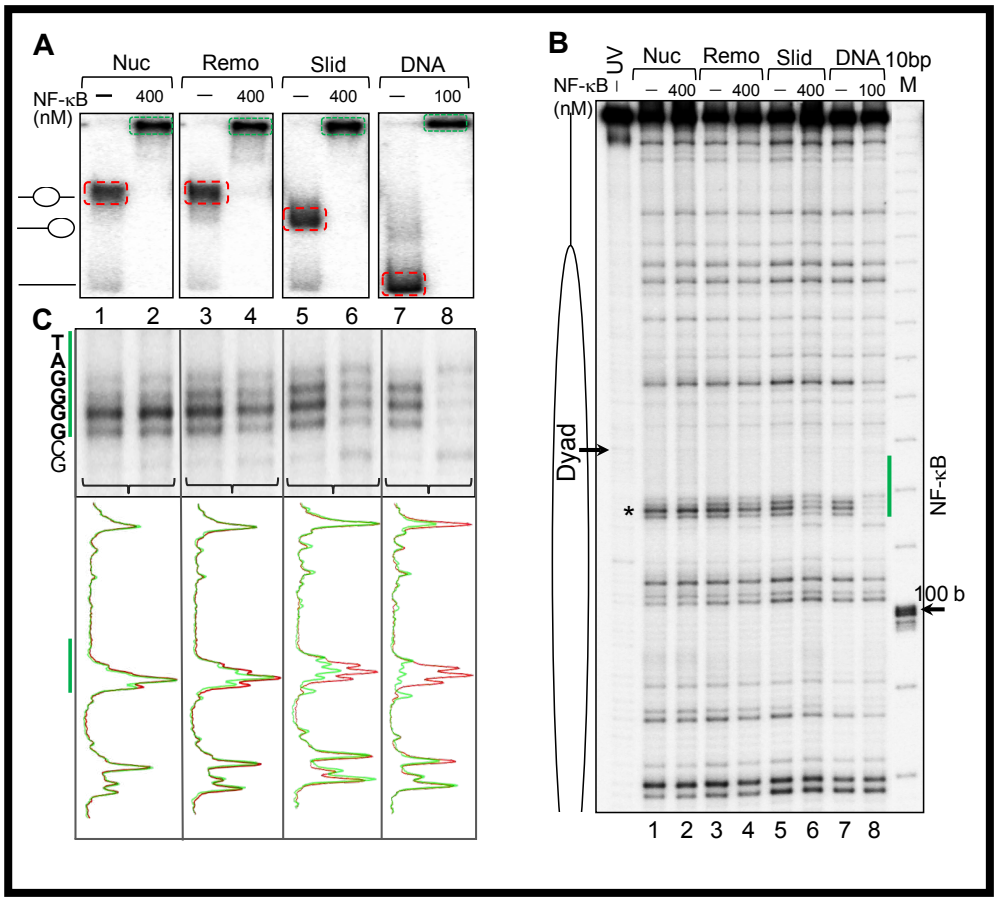

Figure 3 Binding of NF-kB to remodeled and slid nucleosomes. (A) Nucleosomes, RSC-remodeled nucleosomes (remosomes), slid nucleosomes and naked 601_D_0 DNA were incubated with the indicated amount of NF-kB and separated on a native PAGE. The positions of the different particles are shown on the left part of the gel. **(B)** UV laser footprinting of the indicated distinct NF-kB bound particles. The experiment was carried out as described in Figure 2. The NF-κB binding site is shown as vertical green line and the arrow indicated the nucleosomal dyad; M, 10 bp DNA molecular marker **(C)** top, "Zoom" of the NF-kB binding region from the footprints shown in (b); bottom, scan of the footprints; red, scan of the control nucleosomes, remosomes, slid nucleosomes and naked DNA without NF-kB; green, scans of the respective particles in complex with NF-kB.

Removal of H2A-H2B dimer from the nucleosome allows specific NF-kB binding to the dyad in 5S_NF1 nucleosome

The complete histone octamer impedes the binding of NF-kB to its recognition sequence located close to the dyad in the $(H3\text{-}H4)_2$. Surprisingly, ATP dependent remosome generation was not sufficient to overcome this barrier. To understand if nucleosome stability plays any role, we replaced the highest nucleosome affinity 601 sequence by physiologically appropriate and lower affinity 5S positioning sequence. The experiment was done exactly in the same way as for 601-D7 except that each reaction was probed separately by Fpg and T4 EndoV **(Figure 4A)**. Aliquots of the reaction

mixtures were analyzed by EMSA, which shows the formation of complexes **(Figure 4A, upper panels)**. The remaining samples were submitted to UV laser footprinting and treated with either Fpg (to cleave at the sites of generated 8-oxoG) or with Endo V to cleave at the sites of the pyramidine dimers. Although we observed a localized decrease in the intensity of 'G' specific bands (represented by ▶) and no change at pyramidine rich region (represented by ◊), but it does not qualify to be specific binding as the conformational changes in nucleosomal DNA do not match with the specific signature observed in case of naked DNA **(Figure 4A, lower panel)**. Our results show that not only 601 nucleosome but also 5S nucleosomes are not accessible to NF-κB. This suggests that more drastic structural perturbation of the nucleosomes might be required for specific binding. To analyze this possibility, we have prepared nucleosomes lacking H2A-H2B dimmers by simple dilution of 5S_NF1 nucleosomes. Indeed, at about 10 nM nucleosome concentration, H2A-H2B dimers partially dissociate from the nucleosome without affecting the positioning of the remaining $(H3\text{-}H4)_2$ histone tetramer relative to the ends of nucleosomal DNA [33, 34]. With this in mind, we diluted nucleosomes to 7.5 nM concentration and then incubated them with increasing amount of NF-kB at 75 mM Nacl **(Figure 4B)**. The same experiment was carried out with nucleosomes at 40 nM concentration (where no dissociation of the H2A-H2B dimmer is observed, [33] as well as with naked DNA as control **(Figure 4A)**. EMSA shows that NF-kB formed complexes with all the studied samples **(Figure 4 A and B, upper panels)**. In contrast to 5S_NF1 nucleosome complexes at 40nM concentration (H2A-H2B dimers not dissociated), a very well pronounced and specific footprinting pattern of NF-kB was observed in both 5S_NF1 naked DNA and 5S_NF1 nucleosome complexes at 10nM concentration, where H2A-H2B dimmer were removed. This suggests that H2A-H2B dimers eviction is essential for the specific binding of NF-kB to its cognate site located in nucleosome core.

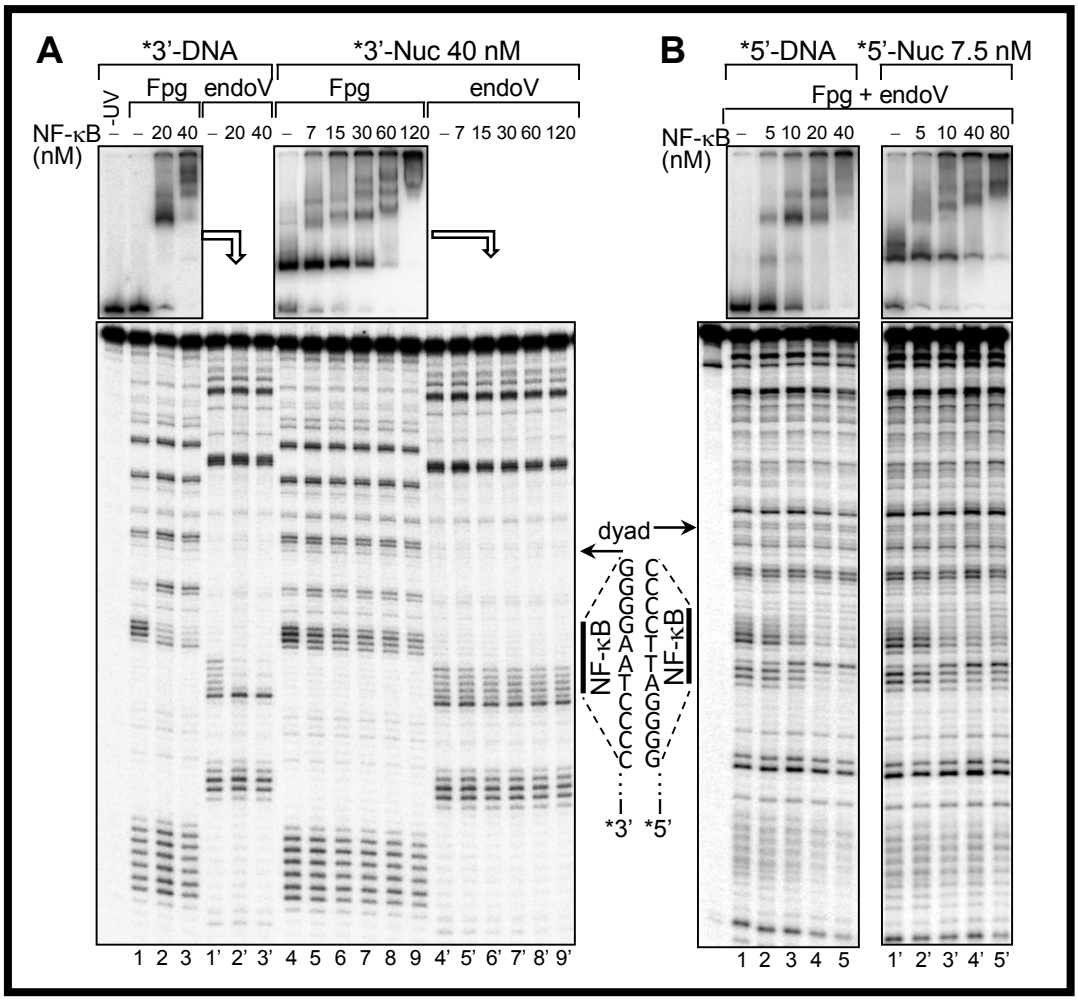

Figure 4 Dilution driven H2A-H2B dimer eviction allows binding of NF-κB to Nucleosome Core Particle: (A) 152 bp DNA fragment derived from *X. borealis* somatic 5 S RNA gene containing single NF-κB site near the dyad NF1 (53-56) was amplified by PCR and 3' end labeled with α-^{32}P by Klenow. Nucleosomes were reconstituted on this labeled fragment as described previously. The DNA and nucleosomes at a concentration 40nM were incubated with increasing amounts of NF-κB as indicated to allow the formation of stable complexes which were subsequently irradiated by a single high intensity UV laser pulse (E_{pulse} ~0.1 J/cm^2). The formation of complexes was checked by EMSA (upper panel, DNA lane 1-3, nucleosomes lane 4-9). The samples were split into two parts, DNA was purified and treated with Fpg to cleave 8-oxoG (represented by►,lower panel, DNA lane 1 -3 and nucleosome lane 4-9) and with T4 endonuclease V to cleave CPDs (represented by◊, DNA lane 1'-3' and nucleosome lane 4'-9'). The cleaved DNA fragments were visualized by 8% sequencing gel. **(B)** The same 152 bp 5S fragment was 5' end labeled with γ-^{32}P by T4 polynucleotide kinase and used for nucleosome reconstitution. DNA and nucleosomes, at 10 nM final concentration, were incubated with increasing amounts of NF-κB as indicated to allow the formation of complexes. The assembly of the complexes was checked by EMSA (upper panel, DNA lane 1-5, nucleosomes lane 1'-5'). The samples were irradiated with a single high intensity UV laser pulse (E_{pulse} ~0.1 J/cm^2), treated with a mix of Fpg glycosylase and T4 endonuclease V to cleave both the 8-oxoG (►) and CPDs (◊). Finally, the cleaved products were visualized by 8% sequencing gel (DNA, lane 1-5; nucleosomes lane 1'-5'). The NF-kB binding sites (vertical bold lines) and the NF-kB recognition sequences are shown. The arrows designated the nucleosomal dyad.

Effect of histone H1 on the NF-kB specific interaction with nucleosomal DNA

Histone H1 is an essential player in modulating and maintaining chromatin architecture [35, 36]. In contrast to core histones, it consists of three domains, a structured ("globular") domain and unstructured and very lysine rich N- and C-termini. The globular domain of histone H1 interacts with the nuclosome dyad and two short (10 bp) sequences at the very beginning of each one of the two linker DNAs. The C-terminus of H1 binds to the remaining linker DNA, brings together the two linkers and form the "stem" linker structure and thus, compact chromatin [3, 37].

To analyze how H1 affects the interaction of NF-kB with the nucleosome we constructed 601_D_8 nucleosome in which the recognition sequence of NF-kB completely overlapped with the binding region of the globular domain of histone H1 on one of the linker DNA **(see Figure 5A and Figure 1A)**. We then used NAP-1 to deposit properly (physiologically relevant conditions) H1 [3] and asked if NF-kB has access to its binding site by using EMSA, •OH and UV-laser footprinting **(Figure 5 and supplementary Figure 4)**. The combination of these three approaches allows in an independent way to judge for the overall association of NF-kB with the nucleosome (EMSA), the presence of H1 on the nucleosome (•OH footprinting) and the specific binding of NF-kB to its cognate sequence (UV laser footprinting) to the nucleosomal DNA. EMSA shows that NF-kB associates with all used naked DNA and nucleosomal templates and that increase of the concentration of NF-kB leads for the formation of particles containing more than one NF-kB molecules **(Figure 5A)**. Interestingly, binding of NF-kB to naked DNA and both nucleosome with and without H1 gives rise to a very clear UV laser footprinting, thus demonstrating that NF-kB is able to invade the H1 containing nucleosome **(Figure 5B, upper panel)**. The •OH radical footprinting shows that the binding of NF-kB paralleled the removal of H1 from the nucleosome **(Figure 5B, lower panel)**. Notably, when NAP1-H1 is added to 601_D_8 nucleosome, no removal of NF-kB by NAP-1-H1 is observed **(Figure 5B**, **lower panel)**. Therefore, in contrast to the core histone, H1 can be displaced by the binding of NF-KB and once NF-kB is bound, adding of H1 does not affect the stability of the 601_D_8 nucleosome complexes.

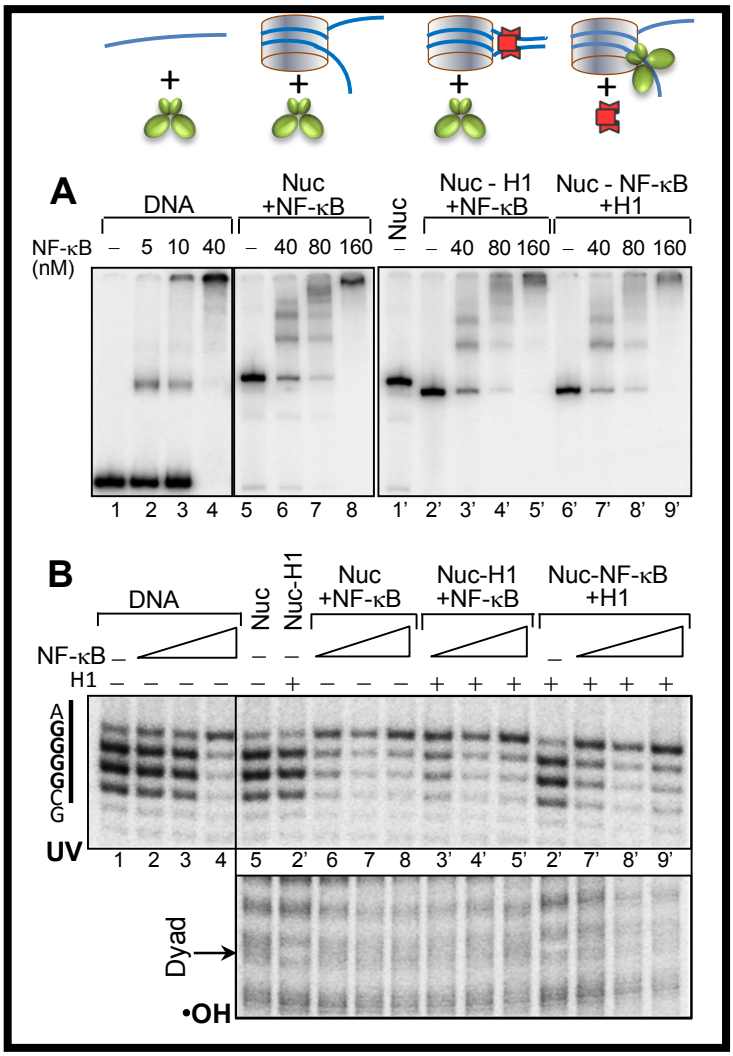

Figure 5 NF-kB displaces H1 from the chromatosome and binds to its recognition sequence. (**A, upper panel**) Schematics of the substrates used in each experiment and binding of histone H1 at the nucleosomal dyad and at the entrance/exit of the DNA arms. (**A, lower panel**) EMSA showing the binding of NF-kB to depicted substrates. 225 bp 601_D_8 DNA was ^{32}P end labeled and used to reconstitute centrally positioned nucleosomes. Chromatosomes were assembled by using the NAP-1/H1 complex to deposit H1 on the nucleosome under "physiological" conditions. The first two panels show the NF-kB-DNA (lanes 1-4) and NF-kB-nucleosome (lanes 5-8) complexes formed upon incubation with increasing amount of NF-kB. The last panel illustrates both the interaction of chromatosomes with the indicated increasing amount of NF-kB (lanes 1'-5') and the deposition of H1 on the already assembled (at increasing NF-kB concentration) NF-kB nucleosome complexes (lanes 6'-9'). (**B**) UV laser (upper panel) and •OH (lower panel) footprinting of the NF-kB binding region of NF-kB-DNA and distinct NF-kB-nucleosome complexes.

Discussion

Studies on the alterations in the chromatin structure required for productive NF-kB binding are essential for understanding the control of expression of inflammatory genes. However, the available data on this important topic are scarce and contradictory [17]. Here we used a combination of EMSA, •OH and UV laser footprinting to analyze how

NF-kB binds to nucleosomes and the effect of histone H1 on the binding. The combination of these methods allows a better understanding of specific and non-specific binding of NF-kB to its templates. The data shows that NF-kB is able to bind specifically to its cognate sequence when binding site is inserted at the end of the nucleosome, but not when it was inserted in vicinity to the nucleosome dyad. The accessibility to the ends of the nucleosome could be explained by the weaker histone-DNA interactions at these sites and their spontaneous unwrapping [38, 39]. At the center (the dyad) of the nucleosome, the histone-DNA interactions are very strong and hence NF-kB is unable to specifically bind to it.

Unexpectedly, remodeling of the nucleosome resulting in strong alterations in the histone-DNA contacts was not sufficient to permit specific binding of NF-kB to the sites located close to the nucleosome dyad. One should stress, however, that nucleosome remodeling allows higher accessibility to dimeric restriction enzymes and permits efficient base excision repair (BER) of sites located at the dyad [40, 41]. Thus, the specific binding of NF-kB requires much higher perturbations in histone-DNA interactions and unpeeling of its cognate sequence from the histone surface allowing it to "embrace" DNA and to productively bind to it. Our experimental results further demonstrate that such specific and productive binding could be efficiently achieved only when the H2A-H2B dimer is removed from the nucleosome or when the histone octamer is slid in a way that the binding site nears the edge.

We also found that the presence of histone H1 does not affect the specific binding of NF-kB to its cognate sequence, when its binding region overlaps with the binding site of NF-kB. In fact, the binding of NF-kB displaces completely histone H1 from the nucleosome. In agreement with this, we observed that H1 cannot bind to the NF-kB nucleosomal complex.

It was reported in the past that several transcription factors, including NF-kB, were able to invade the nucleosome and to bind to its nucleosomally organized recognition sequences even in the center of nucleosomal DNA [16, 26]. However, these studies were usually carried out at low nucleosome concentrations at which H2A-H2B dimer could be released from the nucleosomal DNA [16, 26]. At these very low concentrations, the nucleosome is disassembled and the histone H2A-H2B dimmers are released from the

nucleosomal DNA [33, 34]. This release of H2A-H2B dimmer would then permit the binding of the transcription factors to the disorganized nucleosomal DNA.

Our *in vitro* data sheds light on the *in vivo* requirements for the alterations in chromatin structure necessary for the productive binding of NF-kB. These include either a removal of H2A-H2B dimers from the nucleosome and/or chromatin remodeler induced mobilization of the histone octamer. In mammalian cells the nucleosomes in vicinity to the TSS contain the histone variant H2A.Z [42-44]. A tentative hypothesis is that specific chaperones, recognizing variant H2A.Z nucleosomes, could be involved in the removal of H2A.Z-H2B variant dimer, thus allowing binding of the transcription factors to any site of the disorganized nucleosomal DNA.

Perspectives

Our in vitro study of accessibility of nucleosomes to NF-κB clearly shows that nucleosomes are accessible at edges but not deep inside. The data sheds light on the *in vivo* requirements for the alterations in chromatin structure necessary for the productive binding of NF-kB. These include either a removal of H2A-H2B dimers from the nucleosome and/or chromatin remodeler induced relocation of the histone octamer. Histone eviction is likely the essential and critical for this process [45-47]. However, how nucleosomes are specifically targeted for such disruptions is not clear.

In mammalian cells the nucleosomes in the vicinity of TSS contain the histone variant H2A.Z [42-44]. Our tentative hypothesis is that some factors, recognizing variant H2A.Z nucleosomes, could be involved in the selective removal of H2A.Z-H2B variant dimer, thus allowing binding of the transcription factors to its binding site in the disorganized nucleosomal DNA. In the eukaryotic nucleus, histone eviction is mainly mediated by histone chaperons [47]. It would be highly interesting to investigate the binding of NF-κB to nucleosomes in presence of histone disrupting chaperons. We could try either the chaperons that disrupt the (H3-H4)2 tetramer such as CIA/ASF1 [48] or the chaperons that specifically target H2A-H2B dimers or H2A.Z-H2B.

Another interesting perspective is to look for functional cooperation between NF-κB and transcription factors like PU.1. Recently, while studying the organization of the LPS-induced enhancers in macrophages, Ghisletti et al. observed that in these enhancers,

binding sites for the lineage-restricted and constitutive Ets protein PU.1 coexisted with those for ubiquitous stress-inducible transcription factors such as NF-κB, IRF, and AP-1 [49, 50]. Moreover, PU.1 recognizes just four bases due to which it might be able to bind to nucleosomal templates. Two possibilities arise, either PU.1 recruits the chromatin remodeling/dimer eviction machinery to specific nucleosome or it opens the nucleosomes and clears the ground for other transcription factors.

Acknowledgement: The work was supported by European Community's Seventh Framework Program FP7/2007-2013 under grant agreement number 222008 and "Association pour la Recherche sur le Cancer-ARC" (Grant 1424/2011 to DA)

References:

1. Luger, K., et al., *Crystal structure of the nucleosome core particle at 2.8 A resolution.* Nature, 1997. **389**(6648): p. 251-60.

2. Van Holde, K., *Chromatin : Springer-Verlag, New York*. 1989.

3. Syed, S.H., et al., *Single-base resolution mapping of H1-nucleosome interactions and 3D organization of the nucleosome.* Proc Natl Acad Sci U S A, 2010. **107**(21): p. 9620-5.

4. Simpson, R.T., *Structure of the chromatosome, a chromatin particle containing 160 base pairs of DNA and all the histones.* Biochemistry, 1978. **17**(25): p. 5524-31.

5. Kornberg, R.D. and Y. Lorch, *Twenty-five years of the nucleosome, fundamental particle of the eukaryote chromosome.* Cell, 1999. **98**(3): p. 285-94.

6. Wolffe, A.P. and H. Kurumizaka, *The nucleosome: a powerful regulator of transcription.* Prog Nucleic Acid Res Mol Biol, 1998. **61**: p. 379-422.

7. Imbalzano, A.N., et al., *Facilitated binding of TATA-binding protein to nucleosomal DNA.* Nature, 1994. **370**(6489): p. 481-5.

8. Richmond, T.J. and C.A. Davey, *The structure of DNA in the nucleosome core.* Nature, 2003. **423**(6936): p. 145-50.

9. Han, M. and M. Grunstein, *Nucleosome loss activates yeast downstream promoters in vivo.* Cell, 1988. **55**(6): p. 1137-45.

10. Beato, M. and K. Eisfeld, *Transcription factor access to chromatin.* Nucleic Acids Res, 1997. **25**(18): p. 3559-63.

11. Perlmann, T. and O. Wrange, *Specific glucocorticoid receptor binding to DNA reconstituted in a nucleosome.* EMBO J, 1988. **7**(10): p. 3073-9.

12. Pina, B., U. Bruggemeier, and M. Beato, *Nucleosome positioning modulates accessibility of regulatory proteins to the mouse mammary tumor virus promoter.* Cell, 1990. **60**(5): p. 719-31.

13. Archer, T.K., et al., *Transcription factor access is mediated by accurately positioned nucleosomes on the mouse mammary tumor virus promoter.* Mol Cell Biol, 1991. **11**(2): p. 688-98.

14. Fascher, K.D., J. Schmitz, and W. Horz, *Role of trans-activating proteins in the generation of active chromatin at the PHO5 promoter in S. cerevisiae.* EMBO J, 1990. **9**(8): p. 2523-8.

15. Taylor, I.C., et al., *Facilitated binding of GAL4 and heat shock factor to nucleosomal templates: differential function of DNA-binding domains.* Genes Dev, 1991. **5**(7): p.

1285-98.

16. Steger, D.J. and J.L. Workman, *Stable co-occupancy of transcription factors and histones at the HIV-1 enhancer.* EMBO J, 1997. **16**(9): p. 2463-72.

17. Natoli, G., *Tuning up inflammation: how DNA sequence and chromatin organization control the induction of inflammatory genes by NF-kappaB.* FEBS Lett, 2006. **580**(12): p. 2843-9.

18. Feldmann, M., et al., *Is NF-kappaB a useful therapeutic target in rheumatoid arthritis?* Ann Rheum Dis, 2002. **61 Suppl 2**: p. ii13-8.

19. Karin, M. and F.R. Greten, *NF-kappaB: linking inflammation and immunity to cancer development and progression.* Nat Rev Immunol, 2005. **5**(10): p. 749-59.

20. Ghosh, G., et al., *NF-kappaB regulation: lessons from structures.* Immunol Rev, 2012. **246**(1): p. 36-58.

21. Hayden, M.S. and S. Ghosh, *Signaling to NF-kappaB.* Genes Dev, 2004. **18**(18): p. 2195-224.

22. Chen, F.E., et al., *Crystal structure of p50/p65 heterodimer of transcription factor NF-kappaB bound to DNA.* Nature, 1998. **391**(6665): p. 410-3.

23. Cramer, P., et al., *Structure of the human NF-kappaB p52 homodimer-DNA complex at 2.1 A resolution.* EMBO J, 1997. **16**(23): p. 7078-90.

24. Ghosh, G., et al., *Structure of NF-kappa B p50 homodimer bound to a kappa B site.* Nature, 1995. **373**(6512): p. 303-10.

25. Muller, C.W., et al., *Structure of the NF-kappa B p50 homodimer bound to DNA.* Nature, 1995. **373**(6512): p. 311-7.

26. Angelov, D., et al., *The histone octamer is invisible when NF-kappaB binds to the nucleosome.* J Biol Chem, 2004. **279**(41): p. 42374-82.

27. Wong, D., et al., *Extensive characterization of NF-kappaB binding uncovers non-canonical motifs and advances the interpretation of genetic functional traits.* Genome Biol, 2011. **12**(7): p. R70.

28. Angelov, D., S. Khochbin, and S. Dimitrov, *UV laser footprinting and protein-DNA crosslinking. Application to chromatin.* Methods Mol Biol, 1999. **119**: p. 481-95.

29. Angelov, D., et al., *Ultraviolet laser footprinting of histone H1(0)-four-way junction DNA complexes.* Biochemistry, 1999. **38**(35): p. 11333-9.

30. Spassky, A. and D. Angelov, *Influence of the local helical conformation on the guanine modifications generated from one-electron DNA oxidation.* Biochemistry, 1997. **36**(22): p. 6571-6.

31. Angelov, D., B. Beylot, and A. Spassky, *Origin of the heterogeneous distribution of the yield of guanyl radical in UV laser photolyzed DNA.* Biophys J, 2005. **88**(4): p.

2766-78.

32. Shukla, M.S., et al., *Remosomes: RSC generated non-mobilized particles with approximately 180 bp DNA loosely associated with the histone octamer.* Proc Natl Acad Sci U S A, 2010. **107**(5): p. 1936-41.

33. Claudet, C., et al., *Histone octamer instability under single molecule experiment conditions.* J Biol Chem, 2005. **280**(20): p. 19958-65.

34. Kelbauskas, L., et al., *Nucleosomal stability and dynamics vary significantly when viewed by internal versus terminal labels.* Biochemistry, 2008. **47**(36): p. 9627-35.

35. Zlatanova, J., P. Caiafa, and K. Van Holde, *Linker histone binding and displacement: versatile mechanism for transcriptional regulation.* FASEB J, 2000. **14**(12): p. 1697-704.

36. Catez, F., T. Ueda, and M. Bustin, *Determinants of histone H1 mobility and chromatin binding in living cells.* Nat Struct Mol Biol, 2006. **13**(4): p. 305-10.

37. Hamiche, A., et al., *Linker histone-dependent DNA structure in linear mononucleosomes.* J Mol Biol, 1996. **257**(1): p. 30-42.

38. Anderson, J.D. and J. Widom, *Sequence and position-dependence of the equilibrium accessibility of nucleosomal DNA target sites.* J Mol Biol, 2000. **296**(4): p. 979-87.

39. Li, G., et al., *Rapid spontaneous accessibility of nucleosomal DNA.* Nat Struct Mol Biol, 2005. **12**(1): p. 46-53.

40. Menoni, H., et al., *ATP-dependent chromatin remodeling is required for base excision repair in conventional but not in variant H2A.Bbd nucleosomes.* Mol Cell Biol, 2007. **27**(17): p. 5949-56.

41. Menoni, H., et al., *Base excision repair of 8-oxoG in dinucleosomes.* Nucleic Acids Res, 2012. **40**(2): p. 692-700.

42. Barski, A., et al., *High-resolution profiling of histone methylations in the human genome.* Cell, 2007. **129**(4): p. 823-37.

43. Kelly, T.K., et al., *H2A.Z maintenance during mitosis reveals nucleosome shifting on mitotically silenced genes.* Mol Cell, 2010. **39**(6): p. 901-11.

44. Jin, C., et al., *H3.3/H2A.Z double variant-containing nucleosomes mark 'nucleosome-free regions' of active promoters and other regulatory regions.* Nat Genet, 2009. **41**(8): p. 941-5.

45. De Koning, L., et al., *Histone chaperones: an escort network regulating histone traffic.* Nat Struct Mol Biol, 2007. **14**(11): p. 997-1007.

46. Eitoku, M., et al., *Histone chaperones: 30 years from isolation to elucidation of the mechanisms of nucleosome assembly and disassembly.* Cell Mol Life Sci, 2008. **65**(3): p. 414-44.

47. Park, Y.J. and K. Luger, *Histone chaperones in nucleosome eviction and histone exchange.* Curr Opin Struct Biol, 2008. **18**(3): p. 282-9.

48. Akai, Y., et al., *Structure of the histone chaperone CIA/ASF1-double bromodomain complex linking histone modifications and site-specific histone eviction.* Proc Natl Acad Sci U S A, 2010. **107**(18): p. 8153-8.

49. Natoli, G., S. Ghisletti, and I. Barozzi, *The genomic landscapes of inflammation.* Genes Dev, 2011. **25**(2): p. 101-6.

50. Ghisletti, S., et al., *Identification and characterization of enhancers controlling the inflammatory gene expression program in macrophages.* Immunity, 2010. **32**(3): p. 317-28.

Supplimentary figures and information

(A) 601 original sequence

Gctcggaaca ctatccgact ggcaccggca aggtcgctgt tcaatacatg ca**caggatgt**
atatatctga cacgtgcctg gagactaggg agtaatcccc ttggcggtta aaacgcgggg
gacagCgcgt acgtgcgttt aagcggtgct agagcttgct acgaccaatt gagcggcctc
ggcaccggga ttctccaggg cggccgcgta tagggtccat cacataaggg atgaactcgg
tgtgaagaat catg**C**

(B) 601_D0

gctcggaatt ctatccgact ggcaccggca aggtcgctgt tcaatacatg ca**CAGGATGT**
ATATATCTGA CACGTGCCTG GAGACTAGGT AGTAATTCTC TTGGCGGTTA AAACGCGGGG
ATTCCCCCGT ACGTGCGTTT AAGCGGTGCT AGAGCTTGCT ACGACCAATT GAGCGGCCTC
GGCACCTTGA TTCTCAAGGt cggccgcgta tagtgtccat cacataagtg atgaactcgg
tgtgaagaat catgc

(C) 601_D7

gctcggaatt ctatccgact ggcaccggca aggtcgctgt tcaatacatg ca**CAGGATGT**
ATATATCTGA CACGTGCCTG GAGACTAGGT AGTAATTCTC TTGGCGGTTA AAACGCGGTG
TACAGCGCGT ACGTGCGTTT AAGCGGTGCT AGAGCTTGCT ACGACCAATT GAGCGGCCTC
GGCACGGGGA TTCCCCAGGt cggccgcgta tagtgtccat cacataagtg atgaactcgg
tgtgaagaat catgc

(D) 601_D8

Gctcggaatt ctatccgact ggcaccggca aggtcgctgt tcaatacatg ca**CAGGATGT**
ATATATCTGA CACGTGCCTG GAGACTAGGT AGTAATTCTC TTGGCGGTTA AAACGCGGTG
TACAGCGCGT ACGTGCGTTT AAGCGGTGCT AGAGCTTGCT ACGACCAATT GAGCGGCCTC
GGCACCTTGA TTCTCAAGGg gattcccta tagtgtccat cacataagtg atgaactcgg
tgtgaagaat catgc

(E) 5S_NF1

aaTTCGAGCT CGCCCGGGGA TCCGGCTGGG CCCCCCCCAG AAGGCAGCAC AAGGGGATTC
CCCGTCAGCC TTGTGCTCGC CTACGGCCAT ACCACCCTGA AAGTGCCCGA TATCGTCTGA
TCTCGGAAGC CAAGCAGGGT CGGGCCTGGT TAGT

Supplementary Figure 1 Sequences of the different 255 bp 601 DNA fragments and 152 bp 5S rDNA used for nucleosome reconstitution. The substituted Gs (Cs) in either T or A are in blue. The MHC-H2 NF-κB binding site is in bold and highlighted. The dyade nucleotide is in red.

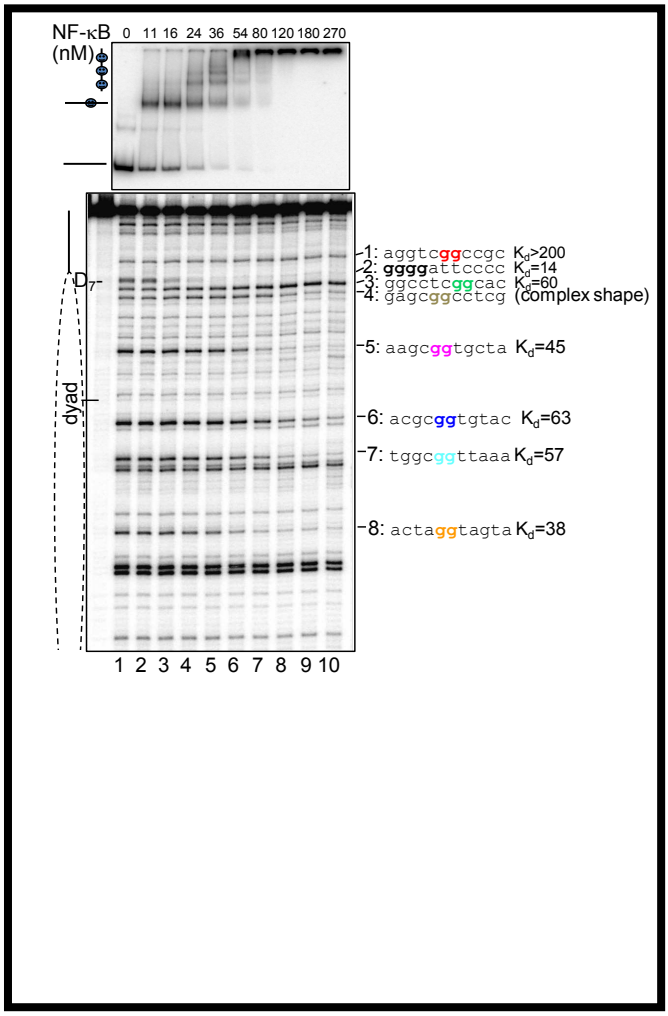

Supplementary Figure 2 601_D7 DNA containing the MHC-H2 binding site was analyzed for NF-κB binding. Apparent binding constants for MHC-H2 site (K_d=14 nM) and other region displaying the specific binding of NF-κB were determined and are plotted as shown in the lower panel.

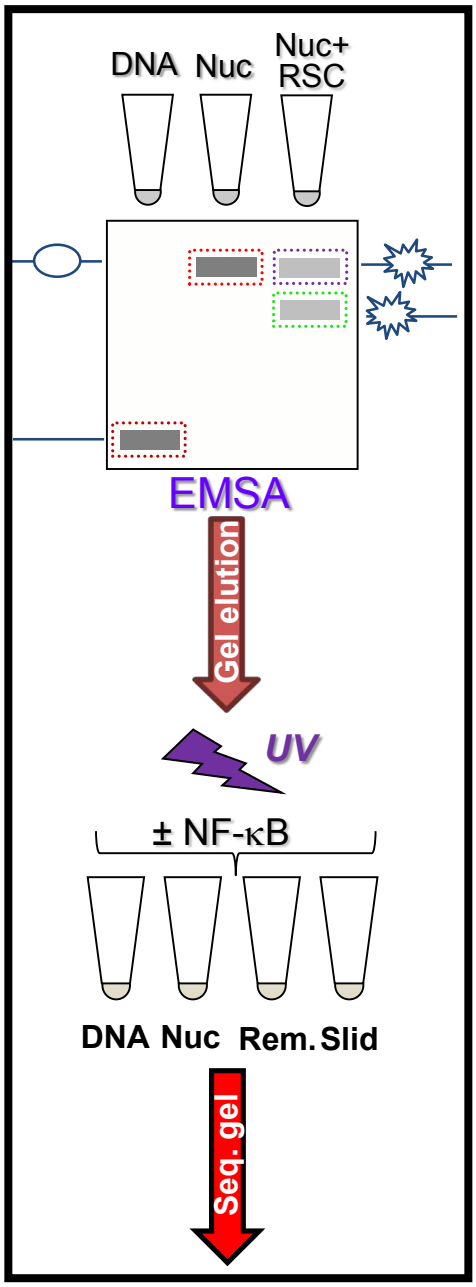

Supplementary Figure 3: Schematic representation of the remodeling assay. Naked DNA, nuclesomes and the remodeling products (Remosomes and slid nucleosomes) were gel purified. The purified substrates are then allowed to bind saturating amount of NF-kB followed by irradiation by a single pulse UV laser. The formation of complexes with NF-kB is analyzed by EMSA.

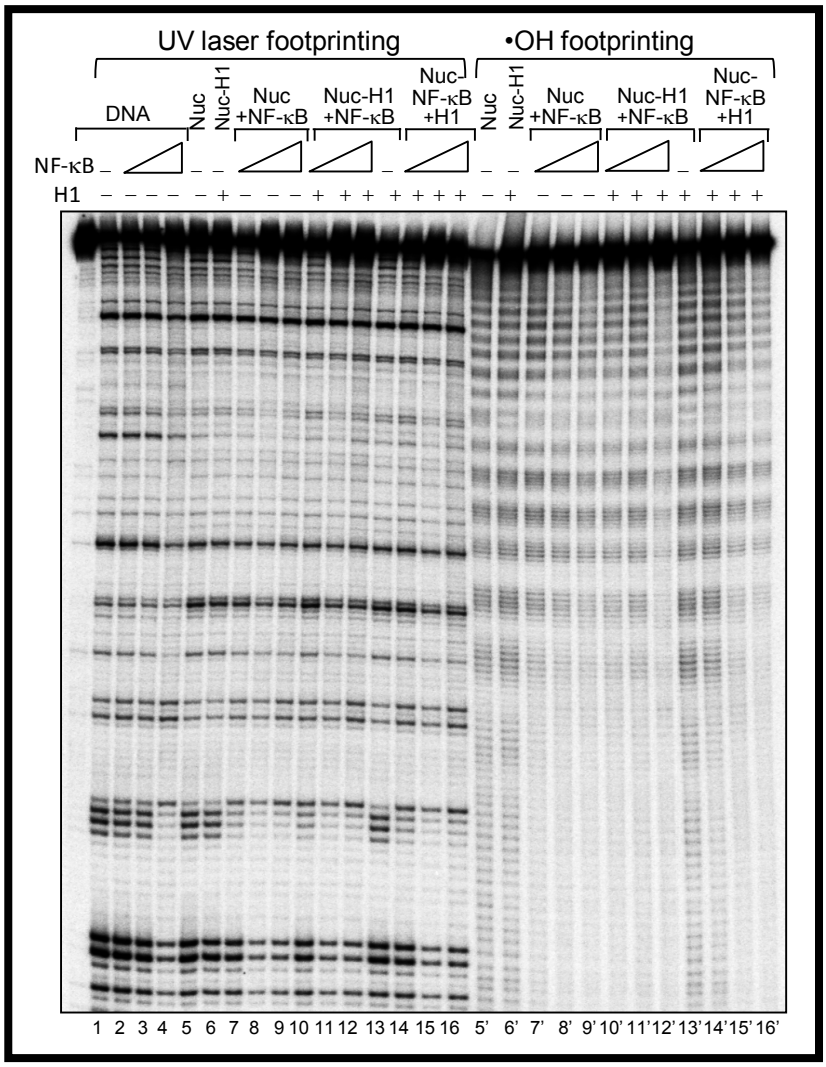

Supplementary Figure 4 Hydroxyl radical and UV laser footprinting of NF-kB-DNA and NF-kB nucleosome and NF-kB chromatosome complexes. 255 bp 601_D_8 DNA was ^{32}-P end labeled and used to reconstitute centrally positioned nucleosomes. Chromatosomes were assembled by using the NAP-1/H1 complex to deposit H1 on the nucleosome under "physiological" conditions. NF-kB-naked DNA and the indicated NF-kB nucleosome and NF-kB chromatosome complexes were incubated with increasing amount of NF-kB and used for UV laser (lanes 1-16) and •OH (lanes 5'-16') footprinting analysis (for details see figure 5).

References

1. Rhodes, D., et al., *Towards an understanding of protein-DNA recognition.* Philos Trans R Soc Lond B Biol Sci, 1996. **351**(1339): p. 501-9.

2. Rohs, R., et al., *Origins of specificity in protein-DNA recognition.* Annu Rev Biochem, 2010. **79**: p. 233-69.

3. Kissinger, C.R., et al., *Crystal structure of an engrailed homeodomain-DNA complex at 2.8 A resolution: a framework for understanding homeodomain-DNA interactions.* Cell, 1990. **63**(3): p. 579-90.

4. Wolberger, C., et al., *Crystal structure of a MAT alpha 2 homeodomain-operator complex suggests a general model for homeodomain-DNA interactions.* Cell, 1991. **67**(3): p. 517-28.

5. Schwabe, J.W., et al., *The crystal structure of the estrogen receptor DNA-binding domain bound to DNA: how receptors discriminate between their response elements.* Cell, 1993. **75**(3): p. 567-78.

6. Glover, J.N. and S.C. Harrison, *Crystal structure of the heterodimeric bZIP transcription factor c-Fos-c-Jun bound to DNA.* Nature, 1995. **373**(6511): p. 257-61.

7. Schwabe, J.W. and A. Klug, *Zinc mining for protein domains.* Nat Struct Biol, 1994. **1**(6): p. 345-9.

8. Klemm, J.D., et al., *Crystal structure of the Oct-1 POU domain bound to an octamer site: DNA recognition with tethered DNA-binding modules.* Cell, 1994. **77**(1): p. 21-32.

9. Shakked, Z. and D. Rabinovich, *The effect of the base sequence on the fine structure of the DNA double helix.* Prog Biophys Mol Biol, 1986. **47**(3): p. 159-95.

10. Jolma, A., et al., *Multiplexed massively parallel SELEX for characterization of human transcription factor binding specificities.* Genome Res, 2010. **20**(6): p. 861-73.

11. Farnham, P.J., *Insights from genomic profiling of transcription factors.* Nat Rev Genet, 2009. **10**(9): p. 605-16.

12. Li, X.Y., et al., *Transcription factors bind thousands of active and inactive regions in the Drosophila blastoderm.* PLoS Biol, 2008. **6**(2): p. e27.

13. Gordan, R., A.J. Hartemink, and M.L. Bulyk, *Distinguishing direct versus indirect transcription factor-DNA interactions.* Genome Res, 2009. **19**(11): p. 2090-100.

14. Kharchenko, P.V., M.Y. Tolstorukov, and P.J. Park, *Design and analysis of ChIP-seq experiments for DNA-binding proteins.* Nat Biotechnol, 2008. **26**(12): p. 1351-9.

15. Park, P.J., *ChIP-seq: advantages and challenges of a maturing technology.* Nat Rev Genet, 2009. **10**(10): p. 669-80.

16. Meng, X., M.H. Brodsky, and S.A. Wolfe, *A bacterial one-hybrid system for determining the DNA-binding specificity of transcription factors.* Nat Biotechnol, 2005. **23**(8): p. 988-94.

17. Riggs, A.D., S. Bourgeois, and M. Cohn, *The lac repressor-operator interaction. 3. Kinetic studies.* J Mol Biol, 1970. **53**(3): p. 401-17.

18. Berg, O.G., R.B. Winter, and P.H. von Hippel, *Diffusion-driven mechanisms of protein translocation on nucleic acids. 1. Models and theory.* Biochemistry, 1981. **20**(24): p. 6929-48.

19. Hammar, P., et al., *The lac repressor displays facilitated diffusion in living cells.* Science, 2012. **336**(6088): p. 1595-8.

20. Marcovitz, A. and Y. Levy, *Frustration in protein-DNA binding influences conformational switching and target search kinetics.* Proc Natl Acad Sci U S A, 2011. **108**(44): p. 17957-62.

21. Winkler, F.K., et al., *The crystal structure of EcoRV endonuclease and of its complexes with cognate and non-cognate DNA fragments.* EMBO J, 1993. **12**(5): p. 1781-95.

22. Viadiu, H. and A.K. Aggarwal, *Structure of BamHI bound to nonspecific DNA: a model for DNA sliding.* Mol Cell, 2000. **5**(5): p. 889-95.

23. Kalodimos, C.G., et al., *Structure and flexibility adaptation in nonspecific and specific protein-DNA complexes.* Science, 2004. **305**(5682): p. 386-9.

24. Misra, V.K., et al., *Electrostatic contributions to the binding free energy of the lambdacI repressor to DNA.* Biophys J, 1998. **75**(5): p. 2262-73.

25. Record, M.T., Jr., J.H. Ha, and M.A. Fisher, *Analysis of equilibrium and kinetic measurements to determine thermodynamic origins of stability and specificity and mechanism of formation of site-specific complexes between proteins and helical DNA.* Methods Enzymol, 1991. **208**: p. 291-343.

26. von Hippel, P.H., *From "simple" DNA-protein interactions to the macromolecular machines of gene expression.* Annu Rev Biophys Biomol Struct, 2007. **36**: p. 79-105.

27. Lundback, T. and T. Hard, *Sequence-specific DNA-binding dominated by dehydration.* Proc Natl Acad Sci U S A, 1996. **93**(10): p. 4754-9.

28. Schechter, A.N., *Measurement of fast biochemical reactions.* Science, 1970. **170**(3955): p. 273-80.

29. Nesmelov, Y.E., et al., *Structural kinetics of myosin by transient time-resolved FRET.* Proc Natl Acad Sci U S A, 2011. **108**(5): p. 1891-6.

30. Kuehn, F., K. Fischer, and M. Schmidt, *Kinetics of Complex Formation between DNA and Cationically Charged Cylindrical Brush Polymers Observed by Stopped Flow Light Scattering.* Macromol Rapid Commun, 2009. **30**(17): p. 1470-6.

31. Defais, M., E. Phez, and N.P. Johnson, *Kinetic mechanism for the formation of the presynaptic complex of the bacterial recombinase RecA.* J Biol Chem, 2003. **278**(6): p. 3545-51.

32. Sclavi, B., *Time-resolved footprinting for the study of the structural dynamics of DNA-protein interactions.* Biochem Soc Trans, 2008. **36**(Pt 4): p. 745-8.

33. Shcherbakova, I., et al., *Following molecular transitions with single residue spatial and millisecond time resolution.* Methods Cell Biol, 2008. **84**: p. 589-615.

34. Petri, V. and M. Brenowitz, *Quantitative nucleic acids footprinting: thermodynamic and kinetic approaches.* Curr Opin Biotechnol, 1997. **8**(1): p. 36-44.

35. Sclavi, B., et al., *Real-time characterization of intermediates in the pathway to open complex formation by Escherichia coli RNA polymerase at the T7A1 promoter.* Proc Natl Acad Sci U S A, 2005. **102**(13): p. 4706-11.

36. Paweletz, N., *Walther Flemming: pioneer of mitosis research.* Nat Rev Mol Cell Biol, 2001. **2**(1): p. 72-5.

37. Olins, D.E. and A.L. Olins, *Chromatin history: our view from the bridge.* Nat Rev Mol Cell Biol, 2003. **4**(10): p. 809-14.

38. Grewal, S.I. and S.C. Elgin, *Heterochromatin: new possibilities for the inheritance of structure.* Curr Opin Genet Dev, 2002. **12**(2): p. 178-87.

39. Sun, F.L., M.H. Cuaycong, and S.C. Elgin, *Long-range nucleosome ordering is associated with gene silencing in Drosophila melanogaster pericentric heterochromatin.* Mol Cell Biol, 2001. **21**(8): p. 2867-79.

40. Filion, G.J., et al., *Systematic protein location mapping reveals five principal chromatin types in Drosophila cells.* Cell, 2010. **143**(2): p. 212-24.

41. Schubeler, D., *Chromatin in multicolor.* Cell, 2010. **143**(2): p. 183-4.

42. Felsenfeld, G. and M. Groudine, *Controlling the double helix.* Nature, 2003. **421**(6921): p. 448-53.

43. Cremer, T. and C. Cremer, *Chromosome territories, nuclear architecture and gene regulation in mammalian cells.* Nat Rev Genet, 2001. **2**(4): p. 292-301.

44. Varga-Weisz, P., K. van Holde, and J. Zlatanova, *Preferential binding of histone H1 to four-way helical junction DNA.* J Biol Chem, 1993. **268**(28): p. 20699-700.

45. van Steensel, B., *Chromatin: constructing the big picture.* EMBO J, 2011. **30**(10): p. 1885-95.

46. Li, B., M. Carey, and J.L. Workman, *The role of chromatin during transcription.* Cell, 2007. **128**(4): p. 707-19.

47. Duan, Z., et al., *A three-dimensional model of the yeast genome.* Nature, 2010. **465**(7296): p. 363-7.
48. Williamson, R., *Properties of rapidly labelled deoxyribonucleic acid fragments isolated from the cytoplasm of primary cultures of embryonic mouse liver cells.* J Mol Biol, 1970. **51**(1): p. 157-68.

49. Hewish, D.R. and L.A. Burgoyne, *Chromatin sub-structure. The digestion of chromatin DNA at regularly spaced sites by a nuclear deoxyribonuclease.* Biochem Biophys Res Commun, 1973. **52**(2): p. 504-10.

50. Olins, A.L. and D.E. Olins, *Spheroid chromatin units (v bodies).* Science, 1974. **183**(4122): p. 330-2.

51. Oudet, P., M. Gross-Bellard, and P. Chambon, *Electron microscopic and biochemical evidence that chromatin structure is a repeating unit.* Cell, 1975. **4**(4): p. 281-300.

52. Kornberg, R.D. and J.O. Thomas, *Chromatin structure; oligomers of the histones.* Science, 1974. **184**(4139): p. 865-8.

53. Johns, E.W., *The electrophoresis of histones in polyacrylamide gel and their quantitative determination.* Biochem J, 1967. **104**(1): p. 78-82.

54. Franklin, S.G. and A. Zweidler, *Non-allelic variants of histones 2a, 2b and 3 in mammals.* Nature, 1977. **266**(5599): p. 273-5.

55. Travers, A.A., *Why bend DNA?* Cell, 1990. **60**(2): p. 177-80.

56. Lia, G., et al., *Direct observation of DNA distortion by the RSC complex.* Mol Cell, 2006. **21**(3): p. 417-25.

57. Harp, J.M., et al., *Asymmetries in the nucleosome core particle at 2.5 A resolution.* Acta Crystallogr D Biol Crystallogr, 2000. **56**(Pt 12): p. 1513-34.

58. Luger, K., et al., *Crystal structure of the nucleosome core particle at 2.8 A resolution.* Nature, 1997. **389**(6648): p. 251-60.

59. Arents, G., et al., *The nucleosomal core histone octamer at 3.1 A resolution: a tripartite protein assembly and a left-handed superhelix.* Proc Natl Acad Sci U S A, 1991. **88**(22): p. 10148-52.

60. Becker, P.B. and W. Horz, *ATP-dependent nucleosome remodeling.* Annu Rev Biochem, 2002. **71**: p. 247-73.

61. Suto, R.K., et al., *Crystal structure of a nucleosome core particle containing the variant histone H2A.Z.* Nat Struct Biol, 2000. **7**(12): p. 1121-4.

62. White, C.L., R.K. Suto, and K. Luger, *Structure of the yeast nucleosome core particle reveals fundamental changes in internucleosome interactions.* EMBO J, 2001. **20**(18): p. 5207-18.

63. Davey, C.A., et al., *Solvent mediated interactions in the structure of the nucleosome core particle at 1.9 a resolution.* J Mol Biol, 2002. **319**(5): p. 1097-113.
64. Richmond, T.J. and C.A. Davey, *The structure of DNA in the nucleosome core.* Nature, 2003. **423**(6936): p. 145-50.

65. Allan, J., D.Z. Staynov, and H. Gould, *Reversible dissociation of linker histone from chromatin with preservation of internucleosomal repeat.* Proc Natl Acad Sci U S A, 1980. **77**(2): p. 885-9.

66. Lennox, R.W. and L.H. Cohen, *The histone H1 complements of dividing and nondividing cells of the mouse.* J Biol Chem, 1983. **258**(1): p. 262-8.

67. Lennox, R.W. and L.H. Cohen, *The alterations in H1 histone complement during mouse spermatogenesis and their significance for H1 subtype function.* Dev Biol, 1984. **103**(1): p. 80-4.

68. Tanaka, M., et al., *A mammalian oocyte-specific linker histone gene H1oo: homology with the genes for the oocyte-specific cleavage stage histone (cs-H1) of sea urchin and the B4/H1M histone of the frog.* Development, 2001. **128**(5): p. 655-64.

69. Cole, R.D., *Microheterogeneity in H1 histones and its consequences.* Int J Pept Protein Res, 1987. **30**(4): p. 433-49.

70. Clore, G.M., et al., *The polypeptide fold of the globular domain of histone H5 in solution. A study using nuclear magnetic resonance, distance geometry and restrained molecular dynamics.* EMBO J, 1987. **6**(6): p. 1833-42.

71. Ramakrishnan, V., et al., *Crystal structure of globular domain of histone H5 and its implications for nucleosome binding.* Nature, 1993. **362**(6417): p. 219-23.

72. Thomas, J.O., C. Rees, and J.T. Finch, *Cooperative binding of the globular domains of histones H1 and H5 to DNA.* Nucleic Acids Res, 1992. **20**(2): p. 187-94.

73. Krylov, D., et al., *Histones H1 and H5 interact preferentially with crossovers of double-helical DNA.* Proc Natl Acad Sci U S A, 1993. **90**(11): p. 5052-6.

74. Allan, J., et al., *Roles of H1 domains in determining higher order chromatin structure and H1 location.* J Mol Biol, 1986. **187**(4): p. 591-601.

75. Lu, X. and J.C. Hansen, *Revisiting the structure and functions of the linker histone C-terminal tail domain.* Biochem Cell Biol, 2003. **81**(3): p. 173-6.

76. Lu, X. and J.C. Hansen, *Identification of specific functional subdomains within the linker histone H10 C-terminal domain.* J Biol Chem, 2004. **279**(10): p. 8701-7.

77. Misteli, T., et al., *Dynamic binding of histone H1 to chromatin in living cells.* Nature, 2000. **408**(6814): p. 877-81.

78. Woodcock, C.L., A.I. Skoultchi, and Y. Fan, *Role of linker histone in chromatin structure and function: H1 stoichiometry and nucleosome repeat length.* Chromosome Res, 2006. **14**(1): p. 17-25.

79. Zlatanova, J., P. Caiafa, and K. Van Holde, *Linker histone binding and displacement: versatile mechanism for transcriptional regulation.* FASEB J, 2000. **14**(12): p. 1697-704.

80. Catez, F., T. Ueda, and M. Bustin, *Determinants of histone H1 mobility and chromatin binding in living cells.* Nat Struct Mol Biol, 2006. **13**(4): p. 305-10.

81. Hayes, J.J. and A.P. Wolffe, *Preferential and asymmetric interaction of linker histones with 5S DNA in the nucleosome.* Proc Natl Acad Sci U S A, 1993. **90**(14): p. 6415-9.

82. An, W., et al., *Linker histone protects linker DNA on only one side of the core particle and in a sequence-dependent manner.* Proc Natl Acad Sci U S A, 1998. **95**(7): p. 3396-401.

83. An, W., K. van Holde, and J. Zlatanova, *Linker histone protection of chromatosomes reconstituted on 5S rDNA from Xenopus borealis:a reinvestigation.* Nucleic Acids Res, 1998. **26**(17): p. 4042-6.

84. Noll, M. and R.D. Kornberg, *Action of micrococcal nuclease on chromatin and the location of histone H1.* J Mol Biol, 1977. **109**(3): p. 393-404.

85. Staynov, D.Z. and C. Crane-Robinson, *Footprinting of linker histones H5 and H1 on the nucleosome.* EMBO J, 1988. **7**(12): p. 3685-91.

86. Brown, D.T., T. Izard, and T. Misteli, *Mapping the interaction surface of linker histone H1(0) with the nucleosome of native chromatin in vivo.* Nat Struct Mol Biol, 2006. **13**(3): p. 250-5.

87. Fan, L. and V.A. Roberts, *Complex of linker histone H5 with the nucleosome and its implications for chromatin packing.* Proc Natl Acad Sci U S A, 2006. **103**(22): p. 8384-9.

88. Shintomi, K., et al., *Nucleosome assembly protein-1 is a linker histone chaperone in Xenopus eggs.* Proc Natl Acad Sci U S A, 2005. **102**(23): p. 8210-5.

89. Howe, L. and J. Ausio, *Nucleosome translational position, not histone acetylation, determines TFIIIA binding to nucleosomal Xenopus laevis 5S rRNA genes.* Mol Cell Biol, 1998. **18**(3): p. 1156-62.

90. Noll, M., *Internal structure of the chromatin subunit.* Nucleic Acids Res, 1974. **1**(11): p. 1573-8.

91. Kornberg, R.D., *Chromatin structure: a repeating unit of histones and DNA.* Science, 1974. **184**(4139): p. 868-71.

92. Van Holde, K.E., C.G. Sahasrabuddhe, and B.R. Shaw, *A model for particulate structure in chromatin.* Nucleic Acids Res, 1974. **1**(11): p. 1579-86.

93. Woodcock, C.L. and S. Dimitrov, *Higher-order structure of chromatin and chromosomes.* Curr Opin Genet Dev, 2001. **11**(2): p. 130-5.

94. Grigoryev, S.A. and C.L. Woodcock, *Chromatin organization - the 30 nm fiber.* Exp Cell Res, 2012. **318**(12): p. 1448-55.

95. Tremethick, D.J., *Higher-order structures of chromatin: the elusive 30 nm fiber.* Cell, 2007. **128**(4): p. 651-4.

96. Finch, J.T. and A. Klug, *Solenoidal model for superstructure in chromatin.* Proc Natl Acad Sci U S A, 1976. **73**(6): p. 1897-901.

97. Worcel, A., S. Strogatz, and D. Riley, *Structure of chromatin and the linking number of DNA.* Proc Natl Acad Sci U S A, 1981. **78**(3): p. 1461-5.

98. Woodcock, C.L., L.L. Frado, and J.B. Rattner, *The higher-order structure of chromatin: evidence for a helical ribbon arrangement.* J Cell Biol, 1984. **99**(1 Pt 1): p. 42-52.

99. Daban, J.R. and A. Bermudez, *Interdigitated solenoid model for compact chromatin fibers.* Biochemistry, 1998. **37**(13): p. 4299-304.

100. Robinson, P.J., et al., *EM measurements define the dimensions of the "30-nm" chromatin fiber: evidence for a compact, interdigitated structure.* Proc Natl Acad Sci U S A, 2006. **103**(17): p. 6506-11.

101. Paulson, J.R. and U.K. Laemmli, *The structure of histone-depleted metaphase chromosomes.* Cell, 1977. **12**(3): p. 817-28.

102. Belmont, A.S. and K. Bruce, *Visualization of G1 chromosomes: a folded, twisted, supercoiled chromonema model of interphase chromatid structure.* J Cell Biol, 1994. **127**(2): p. 287-302.

103. Hayes, J.J. and A.P. Wolffe, *Histones H2A/H2B inhibit the interaction of transcription factor IIIA with the Xenopus borealis somatic 5S RNA gene in a nucleosome.* Proc Natl Acad Sci U S A, 1992. **89**(4): p. 1229-33.

104. Lieb, J.D. and N.D. Clarke, *Control of transcription through intragenic patterns of nucleosome composition.* Cell, 2005. **123**(7): p. 1187-90.

105. Rando, O.J. and K. Ahmad, *Rules and regulation in the primary structure of chromatin.* Curr Opin Cell Biol, 2007. **19**(3): p. 250-6.

106. Bell, O., et al., *Determinants and dynamics of genome accessibility.* Nat Rev Genet, 2011. **12**(8): p. 554-64.

107. Han, M. and M. Grunstein, *Nucleosome loss activates yeast downstream promoters in vivo.* Cell, 1988. **55**(6): p. 1137-45.

108. Knezetic, J.A. and D.S. Luse, *The presence of nucleosomes on a DNA template prevents initiation by RNA polymerase II in vitro.* Cell, 1986. **45**(1): p. 95-104.

109. Satchwell, S.C., H.R. Drew, and A.A. Travers, *Sequence periodicities in chicken nucleosome core DNA.* J Mol Biol, 1986. **191**(4): p. 659-75.

110. Widom, J., *Role of DNA sequence in nucleosome stability and dynamics.* Q Rev Biophys, 2001. **34**(3): p. 269-324.

111. Segal, E., et al., *A genomic code for nucleosome positioning.* Nature, 2006. **442**(7104): p. 772-8.

112. Trifonov, E.N., *Sequence-dependent deformational anisotropy of chromatin DNA.* Nucleic Acids Res, 1980. **8**(17): p. 4041-53.

113. Thastrom, A., et al., *Sequence motifs and free energies of selected natural and non-natural nucleosome positioning DNA sequences.* J Mol Biol, 1999. **288**(2): p. 213-29.

114. Ghaemmaghami, S., et al., *Global analysis of protein expression in yeast.* Nature, 2003. **425**(6959): p. 737-41.

115. Cairns, B.R., *Chromatin remodeling complexes: strength in diversity, precision through specialization.* Curr Opin Genet Dev, 2005. **15**(2): p. 185-90.

116. Bernstein, B.E., et al., *Global nucleosome occupancy in yeast.* Genome Biol, 2004. **5**(9): p. R62.

117. Lee, C.K., et al., *Evidence for nucleosome depletion at active regulatory regions genome-wide.* Nat Genet, 2004. **36**(8): p. 900-5.

118. Yuan, G.C., et al., *Genome-scale identification of nucleosome positions in S. cerevisiae.* Science, 2005. **309**(5734): p. 626-30.

119. Mavrich, T.N., et al., *Nucleosome organization in the Drosophila genome.* Nature, 2008. **453**(7193): p. 358-62.

120. Johnson, S.M., et al., *Flexibility and constraint in the nucleosome core landscape of Caenorhabditis elegans chromatin.* Genome Res, 2006. **16**(12): p. 1505-16.

121. Valouev, A., et al., *A high-resolution, nucleosome position map of C. elegans reveals a lack of universal sequence-dictated positioning.* Genome Res, 2008. **18**(7): p. 1051-63.

122. Ozsolak, F., et al., *High-throughput mapping of the chromatin structure of human promoters.* Nat Biotechnol, 2007. **25**(2): p. 244-8.

123. Mavrich, T.N., et al., *A barrier nucleosome model for statistical positioning of nucleosomes throughout the yeast genome.* Genome Res, 2008. **18**(7): p. 1073-83.

124. Kaplan, N., et al., *The DNA-encoded nucleosome organization of a eukaryotic genome.* Nature, 2009. **458**(7236): p. 362-6.

125. Zhang, Y., et al., *Intrinsic histone-DNA interactions are not the major determinant of nucleosome positions in vivo.* Nat Struct Mol Biol, 2009. **16**(8): p. 847-52.

126. Narlikar, G.J., H.Y. Fan, and R.E. Kingston, *Cooperation between complexes that regulate chromatin structure and transcription.* Cell, 2002. **108**(4): p. 475-87.
127. Saha, A., J. Wittmeyer, and B.R. Cairns, *Chromatin remodelling: the industrial revolution of DNA around histones.* Nat Rev Mol Cell Biol, 2006. **7**(6): p. 437-47.

128. Cairns, B.R., *The logic of chromatin architecture and remodelling at promoters.* Nature, 2009. **461**(7261): p. 193-8.

129. Jiang, C. and B.F. Pugh, *Nucleosome positioning and gene regulation: advances through genomics.* Nat Rev Genet, 2009. **10**(3): p. 161-72.

130. Gaillard, H., et al., *Chromatin remodeling activities act on UV-damaged nucleosomes and modulate DNA damage accessibility to photolyase.* J Biol Chem, 2003. **278**(20): p. 17655-63.

131. Reddy, B.A., et al., *Drosophila transcription factor Tramtrack69 binds MEP1 to recruit the chromatin remodeler NuRD.* Mol Cell Biol, 2010. **30**(21): p. 5234-44.

132. Clapier, C.R. and B.R. Cairns, *The biology of chromatin remodeling complexes.* Annu Rev Biochem, 2009. **78**: p. 273-304.

133. Wang, W., et al., *Diversity and specialization of mammalian SWI/SNF complexes.* Genes Dev, 1996. **10**(17): p. 2117-30.

134. Dingwall, A.K., et al., *The Drosophila snr1 and brm proteins are related to yeast SWI/SNF proteins and are components of a large protein complex.* Mol Biol Cell, 1995. **6**(7): p. 777-91.

135. Whitehouse, I., et al., *Nucleosome mobilization catalysed by the yeast SWI/SNF complex.* Nature, 1999. **400**(6746): p. 784-7.

136. Lorch, Y., M. Zhang, and R.D. Kornberg, *Histone octamer transfer by a chromatin-remodeling complex.* Cell, 1999. **96**(3): p. 389-92.

137. Venters, B.J. and B.F. Pugh, *A canonical promoter organization of the transcription machinery and its regulators in the Saccharomyces genome.* Genome Res, 2009. **19**(3): p. 360-71.

138. Tsukiyama, T., et al., *Characterization of the imitation switch subfamily of ATP-dependent chromatin-remodeling factors in Saccharomyces cerevisiae.* Genes Dev, 1999. **13**(6): p. 686-97.

139. Boyer, L.A., R.R. Latek, and C.L. Peterson, *The SANT domain: a unique histone-tail-binding module?* Nat Rev Mol Cell Biol, 2004. **5**(2): p. 158-63.

140. Langst, G., et al., *Nucleosome movement by CHRAC and ISWI without disruption or trans-displacement of the histone octamer.* Cell, 1999. **97**(7): p. 843-52.

141. Ito, T., et al., *ACF, an ISWI-containing and ATP-utilizing chromatin assembly and remodeling factor.* Cell, 1997. **90**(1): p. 145-55.

142. Corona, D.F., et al., *Modulation of ISWI function by site-specific histone acetylation.* EMBO Rep, 2002. **3**(3): p. 242-7.
143. Kagalwala, M.N., et al., *Topography of the ISW2-nucleosome complex: insights into nucleosome spacing and chromatin remodeling.* EMBO J, 2004. **23**(10): p. 2092-104.

144. Marfella, C.G. and A.N. Imbalzano, *The Chd family of chromatin remodelers.* Mutat Res, 2007. **618**(1-2): p. 30-40.

145. Murawska, M. and A. Brehm, *CHD chromatin remodelers and the transcription cycle.* Transcription, 2011. **2**(6): p. 244-53.

146. Schnetz, M.P., et al., *Genomic distribution of CHD7 on chromatin tracks H3K4 methylation patterns.* Genome Res, 2009. **19**(4): p. 590-601.

147. Ramirez, J. and J. Hagman, *The Mi-2/NuRD complex: a critical epigenetic regulator of hematopoietic development, differentiation and cancer.* Epigenetics, 2009. **4**(8): p. 532-6.

148. Bao, Y. and X. Shen, *INO80 subfamily of chromatin remodeling complexes.* Mutat Res, 2007. **618**(1-2): p. 18-29.

149. van Holde, K. and T. Yager, *Models for chromatin remodeling: a critical comparison.* Biochem Cell Biol, 2003. **81**(3): p. 169-72.

150. Liu, N., C.L. Peterson, and J.J. Hayes, *SWI/SNF- and RSC-catalyzed nucleosome mobilization requires internal DNA loop translocation within nucleosomes.* Mol Cell Biol, 2011. **31**(20): p. 4165-75.

151. Langst, G. and P.B. Becker, *ISWI induces nucleosome sliding on nicked DNA.* Mol Cell, 2001. **8**(5): p. 1085-92.

152. Lorch, Y., B. Davis, and R.D. Kornberg, *Chromatin remodeling by DNA bending, not twisting.* Proc Natl Acad Sci U S A, 2005. **102**(5): p. 1329-32.

153. Studitsky, V.M., D.J. Clark, and G. Felsenfeld, *A histone octamer can step around a transcribing polymerase without leaving the template.* Cell, 1994. **76**(2): p. 371-82.

154. Flaus, A. and T. Owen-Hughes, *Mechanisms for nucleosome mobilization.* Biopolymers, 2003. **68**(4): p. 563-78.

155. Strohner, R., et al., *A 'loop recapture' mechanism for ACF-dependent nucleosome remodeling.* Nat Struct Mol Biol, 2005. **12**(8): p. 683-90.

156. Ristic, D., et al., *The architecture of the human Rad54-DNA complex provides evidence for protein translocation along DNA.* Proc Natl Acad Sci U S A, 2001. **98**(15): p. 8454-60.

157. Saha, A., J. Wittmeyer, and B.R. Cairns, *Chromatin remodeling by RSC involves ATP-dependent DNA translocation.* Genes Dev, 2002. **16**(16): p. 2120-34.

158. Whitehouse, I., et al., *Evidence for DNA translocation by the ISWI chromatin-remodeling enzyme.* Mol Cell Biol, 2003. **23**(6): p. 1935-45.
159. Zofall, M., et al., *Chromatin remodeling by ISW2 and SWI/SNF requires DNA translocation inside the nucleosome.* Nat Struct Mol Biol, 2006. **13**(4): p. 339-46.

160. Zhang, Y., et al., *DNA translocation and loop formation mechanism of chromatin remodeling by SWI/SNF and RSC.* Mol Cell, 2006. **24**(4): p. 559-68.

161. Shukla, M.S., et al., *Remosomes: RSC generated non-mobilized particles with approximately 180 bp DNA loosely associated with the histone octamer.* Proc Natl Acad Sci U S A, 2010. **107**(5): p. 1936-41.

162. Malik, H.S. and S. Henikoff, *Phylogenomics of the nucleosome.* Nat Struct Biol, 2003. **10**(11): p. 882-91.

163. Zlatanova, J. and A. Thakar, *H2A.Z: view from the top.* Structure, 2008. **16**(2): p. 166-79.

164. Marques, M., et al., *Reconciling the positive and negative roles of histone H2A.Z in gene transcription.* Epigenetics, 2010. **5**(4): p. 267-72.

165. Talbert, P.B. and S. Henikoff, *Histone variants--ancient wrap artists of the epigenome.* Nat Rev Mol Cell Biol, 2010. **11**(4): p. 264-75.

166. Petesch, S.J. and J.T. Lis, *Overcoming the nucleosome barrier during transcript elongation.* Trends Genet, 2012. **28**(6): p. 285-94.

167. Hardy, S., et al., *The euchromatic and heterochromatic landscapes are shaped by antagonizing effects of transcription on H2A.Z deposition.* PLoS Genet, 2009. **5**(10): p. e1000687.

168. Zofall, M., et al., *Histone H2A.Z cooperates with RNAi and heterochromatin factors to suppress antisense RNAs.* Nature, 2009. **461**(7262): p. 419-22.

169. Raisner, R.M., et al., *Histone variant H2A.Z marks the 5' ends of both active and inactive genes in euchromatin.* Cell, 2005. **123**(2): p. 233-48.

170. Zhang, H., D.N. Roberts, and B.R. Cairns, *Genome-wide dynamics of Htz1, a histone H2A variant that poises repressed/basal promoters for activation through histone loss.* Cell, 2005. **123**(2): p. 219-31.

171. Schones, D.E., et al., *Dynamic regulation of nucleosome positioning in the human genome.* Cell, 2008. **132**(5): p. 887-98.

172. Ishibashi, T., et al., *Acetylation of vertebrate H2A.Z and its effect on the structure of the nucleosome.* Biochemistry, 2009. **48**(22): p. 5007-17.

173. Goldberg, A.D., et al., *Distinct factors control histone variant H3.3 localization at specific genomic regions.* Cell, 2010. **140**(5): p. 678-91.

174. Mito, Y., J.G. Henikoff, and S. Henikoff, *Histone replacement marks the boundaries of cis-regulatory domains.* Science, 2007. **315**(5817): p. 1408-11.

175. McKittrick, E., et al., *Histone H3.3 is enriched in covalent modifications associated with active chromatin.* Proc Natl Acad Sci U S A, 2004. **101**(6): p. 1525-30.

176. Schwartz, B.E. and K. Ahmad, *Transcriptional activation triggers deposition and removal of the histone variant H3.3.* Genes Dev, 2005. **19**(7): p. 804-14.

177. Jin, C. and G. Felsenfeld, *Nucleosome stability mediated by histone variants H3.3 and H2A.Z.* Genes Dev, 2007. **21**(12): p. 1519-29.

178. Luger, K. and T.J. Richmond, *The histone tails of the nucleosome.* Curr Opin Genet Dev, 1998. **8**(2): p. 140-6.

179. Landry, J., et al., *Set2-catalyzed methylation of histone H3 represses basal expression of GAL4 in Saccharomyces cerevisiae.* Mol Cell Biol, 2003. **23**(17): p. 5972-8.

180. Strahl, B.D., et al., *Set2 is a nucleosomal histone H3-selective methyltransferase that mediates transcriptional repression.* Mol Cell Biol, 2002. **22**(5): p. 1298-306.

181. Wolffe, A.P. and J.J. Hayes, *Chromatin disruption and modification.* Nucleic Acids Res, 1999. **27**(3): p. 711-20.

182. Waterborg, J.H., *Dynamics of histone acetylation in vivo. A function for acetylation turnover?* Biochem Cell Biol, 2002. **80**(3): p. 363-78.

183. Shogren-Knaak, M., et al., *Histone H4-K16 acetylation controls chromatin structure and protein interactions.* Science, 2006. **311**(5762): p. 844-7.

184. Reinke, H. and W. Horz, *Histones are first hyperacetylated and then lose contact with the activated PHO5 promoter.* Mol Cell, 2003. **11**(6): p. 1599-607.

185. Zhao, J., J. Herrera-Diaz, and D.S. Gross, *Domain-wide displacement of histones by activated heat shock factor occurs independently of Swi/Snf and is not correlated with RNA polymerase II density.* Mol Cell Biol, 2005. **25**(20): p. 8985-99.

186. Chandy, M., et al., *SWI/SNF displaces SAGA-acetylated nucleosomes.* Eukaryot Cell, 2006. **5**(10): p. 1738-47.

187. Hassan, A.H., S. Awad, and P. Prochasson, *The Swi2/Snf2 bromodomain is required for the displacement of SAGA and the octamer transfer of SAGA-acetylated nucleosomes.* J Biol Chem, 2006. **281**(26): p. 18126-34.

188. Brower-Toland, B., et al., *Specific contributions of histone tails and their acetylation to the mechanical stability of nucleosomes.* J Mol Biol, 2005. **346**(1): p. 135-46.

189. Jacobs, S.A. and S. Khorasanizadeh, *Structure of HP1 chromodomain bound to a lysine 9-methylated histone H3 tail.* Science, 2002. **295**(5562): p. 2080-3.

190. Chatterjee, N., et al., *Histone H3 tail acetylation modulates ATP-dependent remodeling through multiple mechanisms.* Nucleic Acids Res, 2011. **39**(19): p. 8378-91.

191. Carey, M., B. Li, and J.L. Workman, *RSC exploits histone acetylation to abrogate the nucleosomal block to RNA polymerase II elongation.* Mol Cell, 2006. **24**(3): p. 481-7.

192. Jenuwein, T. and C.D. Allis, *Translating the histone code.* Science, 2001. **293**(5532): p. 1074-80.

193. Strahl, B.D. and C.D. Allis, *The language of covalent histone modifications.* Nature, 2000. **403**(6765): p. 41-5.

194. Bannister, A.J., et al., *Selective recognition of methylated lysine 9 on histone H3 by the HP1 chromo domain.* Nature, 2001. **410**(6824): p. 120-4.

195. Bottomley, M.J., *Structures of protein domains that create or recognize histone modifications.* EMBO Rep, 2004. **5**(5): p. 464-9.

196. Morrison, D.K., *The 14-3-3 proteins: integrators of diverse signaling cues that impact cell fate and cancer development.* Trends Cell Biol, 2009. **19**(1): p. 16-23.

197. Kornberg, R.D. and Y. Lorch, *Twenty-five years of the nucleosome, fundamental particle of the eukaryote chromosome.* Cell, 1999. **98**(3): p. 285-94.

198. Wolffe, A.P. and H. Kurumizaka, *The nucleosome: a powerful regulator of transcription.* Prog Nucleic Acid Res Mol Biol, 1998. **61**: p. 379-422.

199. Imbalzano, A.N., et al., *Facilitated binding of TATA-binding protein to nucleosomal DNA.* Nature, 1994. **370**(6489): p. 481-5.

200. Perlmann, T. and O. Wrange, *Specific glucocorticoid receptor binding to DNA reconstituted in a nucleosome.* EMBO J, 1988. **7**(10): p. 3073-9.

201. Pina, B., U. Bruggemeier, and M. Beato, *Nucleosome positioning modulates accessibility of regulatory proteins to the mouse mammary tumor virus promoter.* Cell, 1990. **60**(5): p. 719-31.

202. Archer, T.K., et al., *Transcription factor access is mediated by accurately positioned nucleosomes on the mouse mammary tumor virus promoter.* Mol Cell Biol, 1991. **11**(2): p. 688-98.

203. Li, Q. and O. Wrange, *Translational positioning of a nucleosomal glucocorticoid response element modulates glucocorticoid receptor affinity.* Genes Dev, 1993. **7**(12A): p. 2471-82.

204. Li, Q. and O. Wrange, *Accessibility of a glucocorticoid response element in a nucleosome depends on its rotational positioning.* Mol Cell Biol, 1995. **15**(8): p. 4375-84.

205. Eisfeld, K., et al., *Binding of NF1 to the MMTV promoter in nucleosomes: influence of rotational phasing, translational positioning and histone H1.* Nucleic Acids Res, 1997. **25**(18): p. 3733-42.

206. Turner, B.M., *Decoding the nucleosome.* Cell, 1993. **75**(1): p. 5-8.

207. Polach, K.J. and J. Widom, *Mechanism of protein access to specific DNA sequences in chromatin: a dynamic equilibrium model for gene regulation.* J Mol Biol, 1995. **254**(2): p. 130-49.

208. Li, G., et al., *Rapid spontaneous accessibility of nucleosomal DNA.* Nat Struct Mol Biol, 2005. **12**(1): p. 46-53.

209. Tims, H.S., et al., *Dynamics of nucleosome invasion by DNA binding proteins.* J Mol Biol, 2011. **411**(2): p. 430-48.

210. Sen, R. and D. Baltimore, *Multiple nuclear factors interact with the immunoglobulin enhancer sequences.* Cell, 1986. **46**(5): p. 705-16.

211. Lenardo, M., J.W. Pierce, and D. Baltimore, *Protein-binding sites in Ig gene enhancers determine transcriptional activity and inducibility.* Science, 1987. **236**(4808): p. 1573-7.

212. Hayden, M.S. and S. Ghosh, *Signaling to NF-kappaB.* Genes Dev, 2004. **18**(18): p. 2195-224.

213. Zhong, H., et al., *The phosphorylation status of nuclear NF-kappa B determines its association with CBP/p300 or HDAC-1.* Mol Cell, 2002. **9**(3): p. 625-36.

214. Ryseck, R.P., et al., *RelB, a new Rel family transcription activator that can interact with p50-NF-kappa B.* Mol Cell Biol, 1992. **12**(2): p. 674-84.

215. Ruben, S.M., et al., *I-Rel: a novel rel-related protein that inhibits NF-kappa B transcriptional activity.* Genes Dev, 1992. **6**(5): p. 745-60.

216. Bonizzi, G. and M. Karin, *The two NF-kappaB activation pathways and their role in innate and adaptive immunity.* Trends Immunol, 2004. **25**(6): p. 280-8.

217. Ghosh, G., et al., *NF-kappaB regulation: lessons from structures.* Immunol Rev, 2012. **246**(1): p. 36-58.

218. Lenardo, M.J. and D. Baltimore, *NF-kappa B: a pleiotropic mediator of inducible and tissue-specific gene control.* Cell, 1989. **58**(2): p. 227-9.

219. Hacker, H. and M. Karin, *Regulation and function of IKK and IKK-related kinases.* Sci STKE, 2006. **2006**(357): p. re13.

220. Smale, S.T., *Dimer-specific regulatory mechanisms within the NF-kappaB family of transcription factors.* Immunol Rev, 2012. **246**(1): p. 193-204.

221. Gilmore, T., et al., *Rel/NF-kappa B/I kappa B signal transduction in the generation and treatment of human cancer.* Cancer Lett, 2002. **181**(1): p. 1-9.

222. Karin, M., et al., *NF-kappaB in cancer: from innocent bystander to major culprit.* Nat Rev Cancer, 2002. **2**(4): p. 301-10.

223. Roshak, A.K., J.F. Callahan, and S.M. Blake, *Small-molecule inhibitors of NF-kappaB for the treatment of inflammatory joint disease.* Curr Opin Pharmacol, 2002. **2**(3): p. 316-21.

224. Jackson, L. and B.M. Evers, *Chronic inflammation and pathogenesis of GI and pancreatic cancers.* Cancer Treat Res, 2006. **130**: p. 39-65.

225. Charokopos, N., et al., *Bronchial asthma, chronic obstructive pulmonary disease and NF-kappaB.* Curr Med Chem, 2009. **16**(7): p. 867-83.

226. Mattson, M.P. and S. Camandola, *NF-kappaB in neuronal plasticity and neurodegenerative disorders.* J Clin Invest, 2001. **107**(3): p. 247-54.

227. Fujita, T., et al., *The candidate proto-oncogene bcl-3 encodes a transcriptional coactivator that activates through NF-kappa B p50 homodimers.* Genes Dev, 1993. **7**(7B): p. 1354-63.

228. Yamamoto, M. and K. Takeda, *Role of nuclear IkappaB proteins in the regulation of host immune responses.* J Infect Chemother, 2008. **14**(4): p. 265-9.

229. Kang, S.M., et al., *NF-kappa B subunit regulation in nontransformed CD4+ T lymphocytes.* Science, 1992. **256**(5062): p. 1452-6.

230. Oeckinghaus, A., M.S. Hayden, and S. Ghosh, *Crosstalk in NF-kappaB signaling pathways.* Nat Immunol, 2011. **12**(8): p. 695-708.

231. Wietek, C., et al., *Interferon regulatory factor-3-mediated activation of the interferon-sensitive response element by Toll-like receptor (TLR) 4 but not TLR3 requires the p65 subunit of NF-kappa.* J Biol Chem, 2003. **278**(51): p. 50923-31.

232. Chen, L.F. and W.C. Greene, *Shaping the nuclear action of NF-kappaB.* Nat Rev Mol Cell Biol, 2004. **5**(5): p. 392-401.

233. Dong, J., et al., *Repression of gene expression by unphosphorylated NF-kappaB p65 through epigenetic mechanisms.* Genes Dev, 2008. **22**(9): p. 1159-73.

234. Zhong, H., R.E. Voll, and S. Ghosh, *Phosphorylation of NF-kappa B p65 by PKA stimulates transcriptional activity by promoting a novel bivalent interaction with the coactivator CBP/p300.* Mol Cell, 1998. **1**(5): p. 661-71.

235. Kunsch, C., S.M. Ruben, and C.A. Rosen, *Selection of optimal kappa B/Rel DNA-binding motifs: interaction of both subunits of NF-kappa B with DNA is required for transcriptional activation.* Mol Cell Biol, 1992. **12**(10): p. 4412-21.

236. Muller, C.W. and S.C. Harrison, *The structure of the NF-kappa B p50:DNA-complex: a starting point for analyzing the Rel family.* FEBS Lett, 1995. **369**(1): p. 113-7.

237. Ghosh, G., et al., *Structure of NF-kappa B p50 homodimer bound to a kappa B site.* Nature, 1995. **373**(6512): p. 303-10.

238. Chen, F.E., et al., *Crystal structure of p50/p65 heterodimer of transcription factor NF-kappaB bound to DNA.* Nature, 1998. **391**(6665): p. 410-3.

239. Chen, Y.Q., S. Ghosh, and G. Ghosh, *A novel DNA recognition mode by the NF-kappa B p65 homodimer.* Nat Struct Biol, 1998. **5**(1): p. 67-73.

240. Cramer, P., et al., *Structure of the human NF-kappaB p52 homodimer-DNA complex at 2.1 A resolution.* EMBO J, 1997. **16**(23): p. 7078-90.

241. Huang, D.B., et al., *Crystal structure of a free kappaB DNA: insights into DNA recognition by transcription factor NF-kappaB.* J Mol Biol, 2005. **346**(1): p. 147-60.

242. Hoffmann, A., T.H. Leung, and D. Baltimore, *Genetic analysis of NF-kappaB/Rel transcription factors defines functional specificities.* EMBO J, 2003. **22**(20): p. 5530-9.

243. Sanjabi, S., et al., *A c-Rel subdomain responsible for enhanced DNA-binding affinity and selective gene activation.* Genes Dev, 2005. **19**(18): p. 2138-51.

244. Sanjabi, S., et al., *Selective requirement for c-Rel during IL-12 P40 gene induction in macrophages.* Proc Natl Acad Sci U S A, 2000. **97**(23): p. 12705-10.

245. Huxford, T., S. Malek, and G. Ghosh, *Structure and mechanism in NF-kappa B/I kappa B signaling.* Cold Spring Harb Symp Quant Biol, 1999. **64**: p. 533-40.

246. Natoli, G., *Tuning up inflammation: how DNA sequence and chromatin organization control the induction of inflammatory genes by NF-kappaB.* FEBS Lett, 2006. **580**(12): p. 2843-9.

247. Grumont, R., et al., *c-Rel regulates interleukin 12 p70 expression in CD8(+) dendritic cells by specifically inducing p35 gene transcription.* J Exp Med, 2001. **194**(8): p. 1021-32.

248. Ouaaz, F., et al., *Dendritic cell development and survival require distinct NF-kappaB subunits.* Immunity, 2002. **16**(2): p. 257-70.

249. Udalova, I.A., et al., *Functional consequences of a polymorphism affecting NF-kappaB p50-p50 binding to the TNF promoter region.* Mol Cell Biol, 2000. **20**(24): p. 9113-9.

250. Udalova, I.A., et al., *Quantitative prediction of NF-kappa B DNA-protein interactions.* Proc Natl Acad Sci U S A, 2002. **99**(12): p. 8167-72.

251. Toledano, M.B., et al., *N-terminal DNA-binding domains contribute to differential DNA-binding specificities of NF-kappa B p50 and p65.* Mol Cell Biol, 1993. **13**(2): p. 852-60.

252. Chen-Park, F.E., et al., *The kappa B DNA sequence from the HIV long terminal repeat functions as an allosteric regulator of HIV transcription.* J Biol Chem, 2002. **277**(27): p. 24701-8.

253. Leung, T.H., A. Hoffmann, and D. Baltimore, *One nucleotide in a kappaB site can determine cofactor specificity for NF-kappaB dimers.* Cell, 2004. **118**(4): p. 453-64.

254. Walker, S., S. Hayes, and P. O'Hare, *Site-specific conformational alteration of the Oct-1 POU domain-DNA complex as the basis for differential recognition by Vmw65 (VP16).* Cell, 1994. **79**(5): p. 841-52.

255. Horak, C.E., et al., *GATA-1 binding sites mapped in the beta-globin locus by using mammalian chIp-chip analysis.* Proc Natl Acad Sci U S A, 2002. **99**(5): p. 2924-9.

256. Harbison, C.T., et al., *Transcriptional regulatory code of a eukaryotic genome.* Nature, 2004. **431**(7004): p. 99-104.

257. Natoli, G., et al., *Interactions of NF-kappaB with chromatin: the art of being at the right place at the right time.* Nat Immunol, 2005. **6**(5): p. 439-45.

258. Saccani, S., S. Pantano, and G. Natoli, *Two waves of nuclear factor kappaB recruitment to target promoters.* J Exp Med, 2001. **193**(12): p. 1351-9.

259. Ramirez-Carrozzi, V.R., et al., *Selective and antagonistic functions of SWI/SNF and Mi-2beta nucleosome remodeling complexes during an inflammatory response.* Genes Dev, 2006. **20**(3): p. 282-96.

260. Weinmann, A.S., S.E. Plevy, and S.T. Smale, *Rapid and selective remodeling of a positioned nucleosome during the induction of IL-12 p40 transcription.* Immunity, 1999. **11**(6): p. 665-75.

261. Muller, C.W., et al., *Structure of the NF-kappa B p50 homodimer bound to DNA.* Nature, 1995. **373**(6512): p. 311-7.

262. Hamiche, A., et al., *Linker histone-dependent DNA structure in linear mononucleosomes.* J Mol Biol, 1996. **257**(1): p. 30-42.

263. Bednar, J., et al., *Nucleosomes, linker DNA, and linker histone form a unique structural motif that directs the higher-order folding and compaction of chromatin.* Proc Natl Acad Sci U S A, 1998. **95**(24): p. 14173-8.

264. Syed, S.H., et al., *Single-base resolution mapping of H1-nucleosome interactions and 3D organization of the nucleosome.* Proc Natl Acad Sci U S A, 2010. **107**(21): p. 9620-5.

265. Lee, H.L. and T.K. Archer, *Prolonged glucocorticoid exposure dephosphorylates histone H1 and inactivates the MMTV promoter.* EMBO J, 1998. **17**(5): p. 1454-66.

266. Bresnick, E.H., C. Rories, and G.L. Hager, *Evidence that nucleosomes on the mouse mammary tumor virus promoter adopt specific translational positions.* Nucleic Acids Res, 1992. **20**(4): p. 865-70.

267. Garner, M.M. and A. Revzin, *A gel electrophoresis method for quantifying the binding of proteins to specific DNA regions: application to components of the Escherichia coli lactose operon regulatory system.* Nucleic Acids Res, 1981. **9**(13): p. 3047-60.

268. Fried, M.G., *Measurement of protein-DNA interaction parameters by electrophoresis mobility shift assay.* Electrophoresis, 1989. **10**(5-6): p. 366-76.

269. Hellman, L.M. and M.G. Fried, *Electrophoretic mobility shift assay (EMSA) for detecting protein-nucleic acid interactions.* Nat Protoc, 2007. **2**(8): p. 1849-61.

270. Galas, D.J. and A. Schmitz, *DNAse footprinting: a simple method for the detection of protein-DNA binding specificity.* Nucleic Acids Res, 1978. **5**(9): p. 3157-70.

271. Johnson, A.D., B.J. Meyer, and M. Ptashne, *Interactions between DNA-bound repressors govern regulation by the lambda phage repressor.* Proc Natl Acad Sci U S A, 1979. **76**(10): p. 5061-5.

272. Price, M.A. and T.D. Tullius, *Using hydroxyl radical to probe DNA structure.* Methods Enzymol, 1992. **212**: p. 194-219.

273. Tullius, T.D. and J.A. Greenbaum, *Mapping nucleic acid structure by hydroxyl radical cleavage.* Curr Opin Chem Biol, 2005. **9**(2): p. 127-34.

274. Tullius, T.D. and B.A. Dombroski, *Hydroxyl radical "footprinting": high-resolution information about DNA-protein contacts and application to lambda repressor and Cro protein.* Proc Natl Acad Sci U S A, 1986. **83**(15): p. 5469-73.

275. Udenfriend, S., et al., *Ascorbic acid in aromatic hydroxylation. I. A model system for aromatic hydroxylation.* J Biol Chem, 1954. **208**(2): p. 731-9.

276. Jain, S.S. and T.D. Tullius, *Footprinting protein-DNA complexes using the hydroxyl radical.* Nat Protoc, 2008. **3**(6): p. 1092-1100.

277. Angelov, D., et al., *The histone octamer is invisible when NF-kappaB binds to the nucleosome.* J Biol Chem, 2004. **279**(41): p. 42374-82.

278. Angelov, D., et al., *Ultraviolet laser footprinting of histone H1(0)-four-way junction DNA complexes.* Biochemistry, 1999. **38**(35): p. 11333-9.

279. Spassky, A. and D. Angelov, *Influence of the local helical conformation on the guanine modifications generated from one-electron DNA oxidation.* Biochemistry, 1997. **36**(22): p. 6571-6.

280. Becker, M.M. and J.C. Wang, *Use of light for footprinting DNA in vivo.* Nature, 1984. **309**(5970): p. 682-7.

281. Geiselmann, J. and F. Boccard, *Ultraviolet-laser footprinting.* Methods Mol Biol, 2001. **148**: p. 161-73.

282. Douki, T., D. Angelov, and J. Cadet, *UV laser photolysis of DNA: effect of duplex stability on charge-transfer efficiency.* J Am Chem Soc, 2001. **123**(46): p. 11360-6.
283. Angelov, D., B. Beylot, and A. Spassky, *Origin of the heterogeneous distribution of the yield of guanyl radical in UV laser photolyzed DNA.* Biophys J, 2005. **88**(4): p. 2766-78.

284. Chen, F.E. and G. Ghosh, *Regulation of DNA binding by Rel/NF-kappaB transcription factors: structural views.* Oncogene, 1999. **18**(49): p. 6845-52.

285. Hoffmann, A., G. Natoli, and G. Ghosh, *Transcriptional regulation via the NF-kappaB signaling module.* Oncogene, 2006. **25**(51): p. 6706-16.

286. Hoffmann, A. and D. Baltimore, *Circuitry of nuclear factor kappaB signaling.* Immunol Rev, 2006. **210**: p. 171-86.

287. Bonizzi, G., et al., *Activation of IKKalpha target genes depends on recognition of specific kappaB binding sites by RelB:p52 dimers.* EMBO J, 2004. **23**(21): p. 4202-10.

288. Stroud, J.C., et al., *Structural basis of HIV-1 activation by NF-kappaB--a higher-order complex of p50:RelA bound to the HIV-1 LTR.* J Mol Biol, 2009. **393**(1): p. 98-112.

289. Wong, D., et al., *Extensive characterization of NF-kappaB binding uncovers non-canonical motifs and advances the interpretation of genetic functional traits.* Genome Biol, 2011. **12**(7): p. R70.

290. Field, S., I. Udalova, and J. Ragoussis, *Accuracy and reproducibility of protein-DNA microarray technology.* Adv Biochem Eng Biotechnol, 2007. **104**: p. 87-110.

291. Kretzschmar, M., et al., *Transcriptional regulation of the HIV-1 promoter by NF-kappa B in vitro.* Genes Dev, 1992. **6**(5): p. 761-74.

292. Angelov, D., et al., *Solution study of the NF-kappaB p50-DNA complex by UV laser protein-DNA cross-linking.* Photochem Photobiol, 2003. **77**(6): p. 592-6.

293. Tisne, C., M. Delepierre, and B. Hartmann, *How NF-kappaB can be attracted by its cognate DNA.* J Mol Biol, 1999. **293**(1): p. 139-50.

294. Siggers, T., et al., *Principles of dimer-specific gene regulation revealed by a comprehensive characterization of NF-kappaB family DNA binding.* Nat Immunol, 2012. **13**(1): p. 95-102.